1996

The Effect of Membrane Structure on Lipid Peroxidation and Its Inhibition.

Tammy Renee Dugas
Louisiana State University and Agricultural & Mechanical College

THE EFFECT OF MEMBRANE STRUCTURE ON LIPID PEROXIDATION AND ITS INHIBITION

A Dissertation

Submitted to the Graduate Faculty of the
Louisiana State University and
Agricultural and Mechanical College
in partial fulfillment of the
requirements for the degree of
Doctor of Philosophy

in

The Department of Chemistry

by
Tammy R. Dugas
B. S., Louisiana State University, 1992
August 1996

ACKNOWLEDGMENTS

First of all, I thank my advisor, Dr. Daniel Church, for his encouragement and advice, even in matters other than my research. I also extend my appreciation to Dr. Mark McLaughlin and Dr. Robert Hammer for additional guidance along the way. I thank Anna Shanklin, my group member, for her friendship and thoughtfulness. I extend my appreciation to three undergraduates, April Erwin, Gina Pineda, and Jherie Blazier, whose research in our laboratory was a great benefit to the research endeavors of our group and to my own research.

I express my gratitude to Pharmacia & Upjohn and Louisiana State University for their financial support in this combined project.

Most importantly, I thank my family. I thank my parents, Ivy and Patsy Dugas, for their continual love and encouragement . They taught me never to give up on anything worthwhile. I thank my husband, Robert Gaudet, for his unmitigated support throughout my graduate career. Many times he stayed up all night with me when deadlines were near and he sacrificed his own personal goals, including his career, for my education. Most of all, I thank my one-year-old son Jordan. Though he won't remember how many nights Mommy spent away from home, I hope he knows how much I wanted to be there.

TABLE OF CONTENTS

LIST OF TABLES

LIST OF FIGURES

LIST OF ABBREVIATIONS

α-T = α-tocopherol

FFA = free fatty acid

ULV = unilamellar vesicle liposomes

MLV = multilamellar vesicle liposomes

DTPA = diethylenetriamine penta-acidic acid

LOOH = lipid hydroperoxide

$LOO^{\cdot}$ = lipid peroxyl radical

$L^{\cdot}$ = lipid alkyl radical

LH = lipid

SDS = sodium dodecyl sulfate

PC = phosphatidylcholine

ABAP = 2,2'-azobis-2-amidinopropane

ESR = electron spin resonance

FAB-MS = fast-atom bombardment mass spectrometry

HPLC = high performance liquid chromatography

ABSTRACT

Lipid peroxidation is the process by which lipids in the cell membrane undergo free radical-initiated oxidation. The resulting cell damage has been implicated in the onset of many diseases, including as cancer, aging, and stroke. Lipid oxidation has been studied in a variety of membrane models, including homogeneous solution, micelles, liposomes, and microsomes. The kinetics for free radical reactions proven to occur during lipid oxidation in homogeneous solution have been thoroughly elucidated. These kinetics were also shown to apply to oxidation in micelles. This dissertation presents evidence that the kinetics of more biologically realistic membrane models such as liposomes may be quite different. Antioxidants such as α-tocopherol (α-T) have been shown to inhibit lipid oxidation. Work presented here suggests that the efficiency with which antioxidants inhibit oxidation is dependent on the structure of the membrane model. It was observed that the antioxidant efficiency of α-T decreases dramatically from homogeneous to heterogeneous systems of lipid, including micelles, liposomes, and microsomes. This could be due to a decrease in fluidity in the membrane model, limiting the diffusion of α-T. A less mobile antioxidant may have fewer opportunities for encountering and trapping free radicals. Addition of free fatty acids (FFA) to the membrane model to mimic damaged tissue enhanced α-T's efficiency. Differential Scanning Calorimetry data show there is an increase in fluidity when FFA are present, indicating α-T should then diffuse more readily through the

membrane. This work thus demonstrates that while α-T appears effective in homogeneous solution, micelles, and liposome models of damaged membranes, its antioxidant efficiency is much smaller in biologically relevant models for normal tissues. Furthermore, the concentration of α-T required to inhibit oxidation in liposomes is greater than that which exists in tissues *in vivo*. Finally, the antioxidant effectiveness of several synthetic antioxidant drugs called 21-aminosteroids was compared with that of α-T. It is shown here that α-T is much more effective than any of the 21-aminosteroids. In addition, the 21-aminosteroids were shown to be much less effective below pH 7.0. This may be important in damaged tissue, where the pH reportedly falls to as low as 5.9.

CHAPTER 1: INTRODUCTION

1.1. Autoxidation and its biological initiation

It is generally well understood that oxygen is critical to life. Naturally occurring oxygen exists as a diradical, shown below. [1] When this oxygen species

undergoes one-electron reduction, for example by NADPH to form $NADP^+$, the result is an oxygen species with a highly reactive unpaired electron called a free radical. [2] This oxygen species, $O_2^{\bullet -}$, is termed superoxide. Superoxide is involved in and is essential to many important biological processes, including the detoxifying reaction of cytochrome P450, phagocytosis, and prostaglandin biosynthesis. [3-5]

The reduction of hydrogen peroxide can lead to the formation of hydroxyl radical ($^{\bullet}OH$). [6] Low levels of hydroxyl radical normally exist in the body. [7] This highly reactive free radical can attack and oxidize almost any component of human cells, eventually resulting in cell death. [8,9] Fortunately, nature provides the body with its own defense - antioxidants - to protect against this oxidative damage. Typical antioxidants react with free radicals to produce non-radical products and prevent further oxidative damage to tissues. [10] Natural antioxidants, discussed in length in a later section, include α-tocopherol, β-carotene, ascorbic acid, and enzymes such as superoxide dismutase and catalase, to name a few. [11]

As long as there is a balance in the body between the formation of free radicals and antioxidation, tissues remain healthy. When tissues become stressed by any one of a number of factors including ionizing radiation, traumatic injury, or inflammation, the production of free radicals exceeds antioxidation. [12] When this occurs, wide-scale lipid peroxidation results in tissue damage.

Lipid peroxidation is a free-radical process in which lipids in cell membranes become oxidized and are thus damaged. This cell damage has been implicated in cancer, aging, traumatic head injury, atherosclerosis and stroke, to name a few. [13-15] Figure 1.1 illustrates the reactions for oxidative damage to cell membrane lipids that occur during peroxidation. In this figure LH represents oxidizable lipid and LOO•, the highly reactive lipid peroxyl radical resulting from

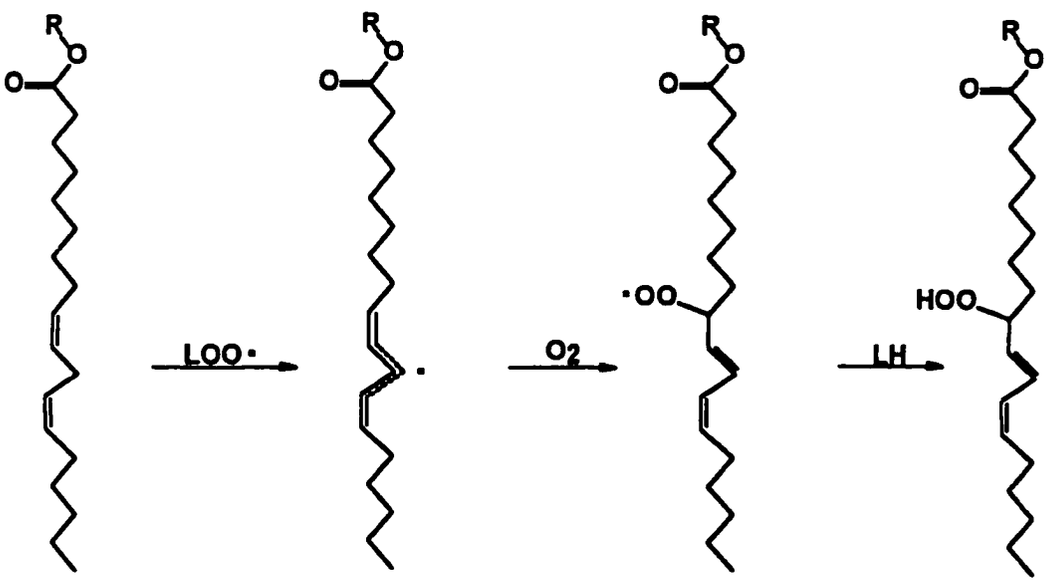

Figure 1.1. Oxidation of the phospholipid fatty acyl side chain.

oxidative attack. Note that it is the unsaturated fatty acyl side chains of the phospholipids in the bilayer membrane that are attacked by free radicals. In particular, it is the bis-allylic hydrogen atoms that are abstracted by lipid peroxyl radicals to produce LOOH and lipid alkyl radical (L$^{\cdot}$), thus propagating further oxidative damage. [16]

Free radicals have been shown to be involved in inflammation. [17,18] Human phagocytes are cells which engulf and destroy cells foreign to the body, such as bacteria. Part of the process of destroying these foreign materials is through the use of superoxide, generated by the one-electron reduction of singlet oxygen by NADPH to yield $NADP^{+}$.[19]

During inflammation phagocytes tend to produce far more superoxide than necessary. [5,20] Some of this superoxide can react with protons to form H_2O_2. and O_2 (eq 1.1). [11] Though H_2O_2 alone is not highly reactive, the presence of iron

$$O_2^{\cdot -} + 2H^{+} \rightarrow H_2O_2 + O_2 \qquad (1.1)$$

can initiate lipid peroxidation which damages tissues surrounding the inflammed area. [21]

Iron-dependent lipid peroxidation can be initiated by several mechanisms. [22] First of all, Fe^{II} can undergo autoxidation to Fe^{III} to form superoxide (eq 1.2). The reverse reaction does occur, but it must compete with the dismutation of superoxide by superoxide dismutase to form H_2O_2. Fe^{II} also reacts with H_2O_2,

$$Fe^{II} + O_2 \longrightarrow Fe^{III} + O_2^{\cdot -} \quad (1.2)$$

however, by one of the following mechanisms (eqs 1.3,1.4). In this case, $^{\cdot}OH$ and $Fe^{III}OH$ serve as powerful oxidants for initiating oxidation. Thus, with only

$$Fe^{II} + H_2O_2 \longrightarrow Fe^{III} + {}^{\cdot}OH + OH^- \quad (1.3)$$

$$Fe^{II} + H_2O_2 \longrightarrow Fe^{III}OH + OH^- \quad (1.4)$$

trace amounts of iron in biological systems, the iron-catalyzed Haber-Weiss reaction (equations 1.5,1.6) may occur.

$$Fe^{III} + O_2^{\cdot -} \longrightarrow Fe^{II} + O_2 \quad (1.5)$$

$$Fe^{II} + H_2O_2 \longrightarrow Fe^{III} + {}^{\cdot}OH + OH^- \quad (1.6)$$

Iron can additionally react with lipid hydroperoxide (LOOH) formed during lipid peroxidation (Figure 1.1) to produce either the lipid alkoxyl radical ($LO^{\cdot}$) or lipid peroxyl radical ($LOO^{\cdot}$), shown in equations 1.7 and 1.8. The resulting lipid peroxyl radical and lipid alkoxyl radical can then react with more lipid to

$$LOOH + Fe^{II} \longrightarrow LO^{\cdot} + OH^- + Fe^{III} \quad (1.7)$$

$$LOOH + Fe^{III} \longrightarrow LOO^{\cdot} + Fe^{II} \quad (1.8)$$

produce LOOH or LOH and lipid alkyl radical, propagating the chain of free radical damage to cell membranes (eqs 1.9,1.10).

$$LO^{\cdot} + LH \longrightarrow LOH + L^{\cdot} \qquad (1.9)$$

$$LOO^{\cdot} + LH \longrightarrow LOOH + L^{\cdot} \qquad (1.10)$$

Following traumatic injury, various biological reactions occur that ultimately result in the proliferation of a large number of free radicals. Traumatic injury such as that to the central nervous system eventually results in a condition known as ischemia. [22] Ischemia is the partial or complete depletion of oxygen to a tissue. Following the onset of ischemia a number of cellular metabolic activities begin to occur which are conducive to the formation of oxygen free radicals. Due to its lack of oxygen, the cell first switches to anaerobic respiration. [23] As this respiratory pathway is energetically less efficient, the levels of ATP decrease dramatically. All available high energy phosphates are consumed. [23] Due to the onset of anaerobic respiration, the levels of lactic acid (a by-product of this process) in the tissues increase. [24] Tissue pH thus falls from approximately 7.4 to between 5.9 and 6.4. [25]

As ATP is consumed in the ischemic tissue, AMP begins to accumulate and is eventually degraded to hypoxanthine. [24] Hypoxanthine in normal tissues is converted to uric acid by xanthine dehydrogenase. [26] During ischemia, however, xanthine dehydrogenase is converted proteolytically to xanthine oxidase. [27] The

xanthine oxidase thus formed catalyzes the production of superoxide *via* the oxidation of hypoxanthine to produce xanthine (Figure 1.2). [28] The resulting

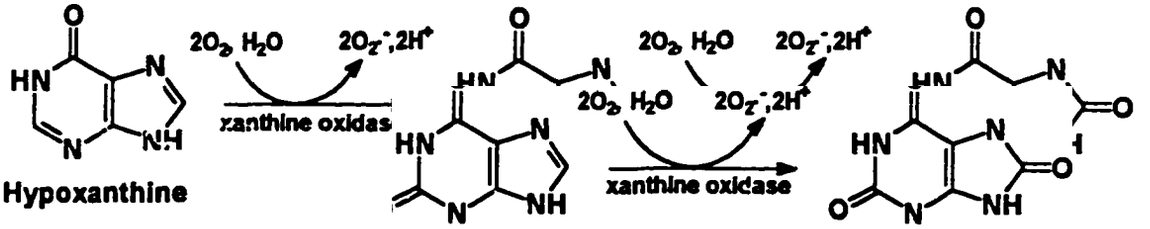

Figure 1.2. Mechanism of superoxide production by xanthine oxidase.

xanthine can again be oxidized by xanthine oxidase to produce uric acid and more superoxide, or eventually, H_2O_2. [28]

After the development of these cellular activities return of oxygen to the tissue results in a proliferation of superoxide and H_2O_2 production. [22,27] The inevitable consequence is thus lipid peroxidation and tissue damage.

Recently, free radical research has focused on another free radical called nitric oxide, $NO^{\cdot}$, shown to be important to the body. It was discovered that nitric oxide is the vasodilator that relaxes smooth muscle in the vessel wall to consequently reduce blood pressure. [29,30] It is also important to various other biological functions such as neurotransmission, blood clotting, learning and memory. [29,30] Though nitric oxide is a relatively unreactive free radical, it can react with superoxide to produce the highly reactive peroxynitrite radical, shown in eq 11. [31-33] This highly reactive free radical has been implicated in oxidative damage to membrane lipids, [34] sulfhydryl amino acids, [35] and methionine

$$NO\cdot + O_2\cdot^- \longrightarrow ONOO^- \qquad (1.11)$$

residues. [36] It has also been shown to hydroxylate and nitrate aromatic amino acids. [37,38]

1.2. Antioxidation *in vivo*.

Antioxidants are compounds the body uses to eliminate free radicals. Antioxidants are divided into two basic classes based on their mechanism of inhibition. Antioxidants which prevent the initiation of oxidation are called primary or preventive antioxidants. [39] Secondary or chain-breaking antioxidants are those which terminate chain-propagating free radicals, such as the peroxyl radical. [39]

A number of enzymes exist *in vivo* to prevent lipid oxidation. One of these is superoxide dismutase (SOD). SOD converts superoxide into the less reactive H_2O_2, as shown in eq. 1.12 below. [40] The hydrogen peroxide is then eliminated

$$O_2\cdot^- + 2H^+ \xrightarrow{SOD} H_2O_2 + O_2 \qquad (1.12)$$

by one of two enzymes - catalase and glutathione peroxidase. Catalase reacts with H_2O_2 to produce H_20 and O_2 (eq 1.13). [7,9] Glutathione peroxidase reacts with H_2O_2 in the presence of glutathione (GSH) to produce H_2O and oxidized

$$2H_2O_2 \xrightarrow{\text{catalase}} 2H_2O + O_2 \qquad (1.13)$$

glutathione (GSSG), as shown in Figure 1.3. [7,41] Glutathione peroxidase has also been shown to reduce lipid hydroperoxides, formed during lipid peroxidation, to

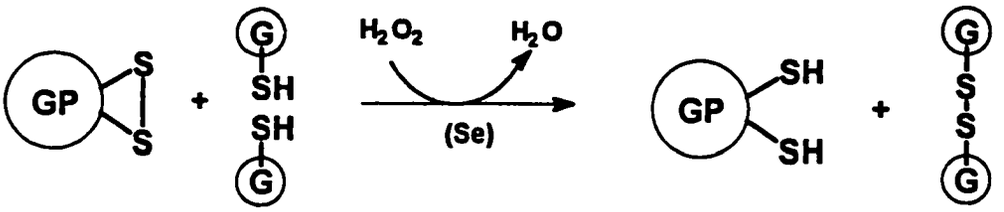

Figure 1.3. Mechanism of reduction of H_2O_2 *via* the oxidation of glutathione by glutathione peroxidase.

the less reactive alcohol. Selenium is often considered an antioxidant, because it is important to the function of glutathione peroxidase. [42] The oxidized glutathione species (GSSG) is then converted back to glutathione by glutathione reductase *via* the oxidation of NADPH to $NADP^+$ (Figure 1.4). [7,41]

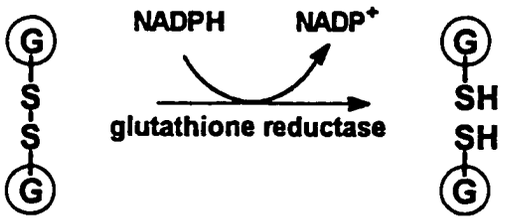

Figure 1.4. Reduction of oxidized glutathione by glutathione reductase.

The body possesses chelating glycoproteins which usually keep iron and copper in forms which are not conducive to the initiation of lipid oxidation. Iron, for example, is transported through plasma bound to the protein transferrin. [43] Copper, capable of initiating oxidation by a similar mechanism as Fe, is carried through plasma by the protein ceruloplasmin. [44] In these bound forms, the metal ions are not available for initiating free radical reactions.

The body also requires other non-enzymatic natural antioxidants normally present in healthy diets. [13,45-47] One such antioxidant is α-tocopherol (one of a group of tocopherols collectively known as Vitamin E). Antioxidants such as α-tocopherol (α-T) are compounds capable of inhibiting the oxidative chain of reactions and are thus biologically important. During typical inhibition of lipid peroxidation by a phenolic antioxidant such as α-T, LOO$^{\bullet}$ abstracts a H-atom from the antioxidant to produce a stable and persistent free radical called a phenoxyl radical (Figure 1.5). [48] The phenoxyl radical can then react with another lipid peroxyl radical to produce several possible non-radical products,

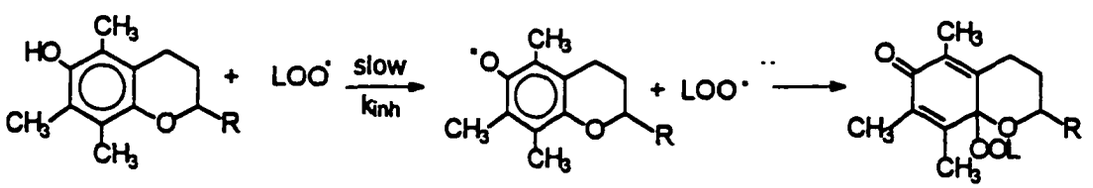

Figure 1.5. Mechanism for antioxidation by α-tocopherol.

one of which is illustrated above.[48] BHT (butylated hydroxytoluene), also a phenolic antioxidant, is a food additive used to prevent the oxidation of food

which causes rancidification. [49] Its antioxidant activity is believed to proceed by the same mechanism as α-T.

Ascorbic acid (Vitamin C) is a water-soluble antioxidant. It has been shown to react with H_2O_2 to produce dehydroascorbate. [50] It was shown that α-T and ascorbic acid are synergistic antioxidants, in that the ascorbic acid regenerates the oxidized α-T into a usable form. [51,52]

Various lipid-soluble carotenoids of plant origin, including β-carotene (the biological precursor to Vitamin A) have been shown to inhibit lipid oxidation in LDL (low density lipoprotein). [53] Characterization of the oxidation products of related carotenoids suggests that the inhibition by β-carotene is probably due to its coupling to lipid peroxyl radicals to form non-radical products. [54]

1.3. Kinetic Modeling of lipid peroxidation and its antioxidation.

Important to the study of lipid peroxidation is the use of membrane models. Simple and uncomplicated, biologically realistic membrane models allow for a quick and easy elucidation of many aspects of both lipid peroxidation and its antioxidation. These include the interpretation of the kinetics of lipid peroxidation and evaluation of the effectiveness of antioxidants. Figure 1.2 shows the structure of two membrane models, liposomes and micelles. Surfactants such as sodium dodecyl sulfate are conical in structure and preferentially assume a spherical micellar structure when placed in aqueous solution. [55] Phospholipids are tubular in shape and tend to form a bilayer

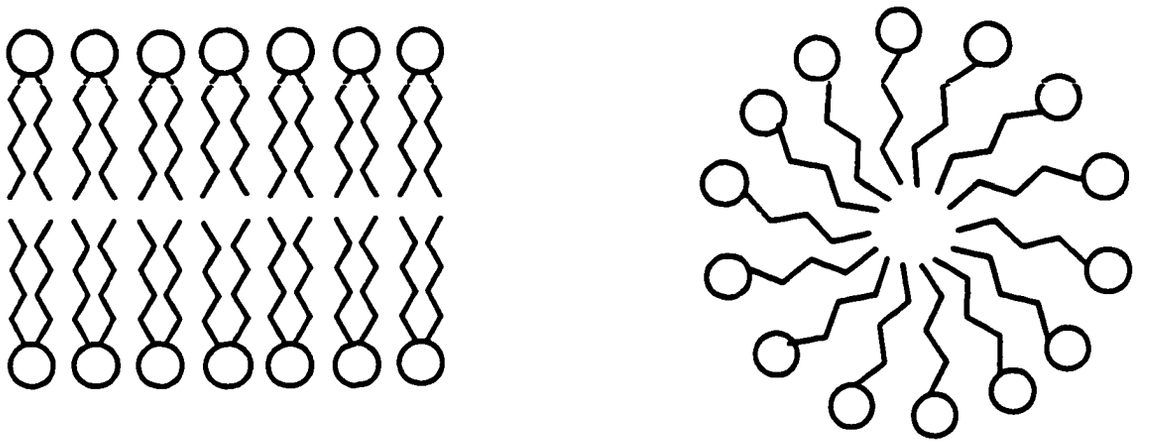

Figure 1.6. Structures of micelles and liposomes.

structure when placed in aqueous solution. [55] They align themselves as to minimize contact between the hydrophobic hydrocarbon side chains and the aqueous layer. [55] This bilayer structure is similar to the lipid bilayer of cell membranes. The hydrocarbon tails of the bilayer sheet thus formed further minimize their contact with water by folding back on themselves to form a hollow vesicle known as a liposome. [55]

Liposomes can be classified as either unilamellar vesicles (ULVs) or multilamellar vesicles (MLVs), both of varying sizes. The two liposome models studied here are the medium-sized ULVs and large MLVs. As shown in Figure 3.3, unilamellar vesicles contain only one lipid bilayer, while MLVs contain several stacked or concentric lipid bilayers. Between micelles, ULVs, and MLVs, ULVs are structurally the most biologically similar to the cell membrane.

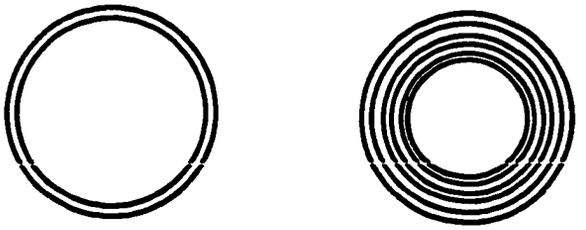

Unilamellar Vesicles (ULVs) **Multilamellar Vesicles (MLVs)**

Figure 1.7. Liposomal membrane models.

Systematic kinetic work done in homogeneous solution has elicited the reactions shown in equations 1.14-1.19. [56,57] These are the reactions proven to occur during lipid peroxidation initiated by an azo compound (R-N=N-R) in organic solution. [58,59] Azo compounds are a convenient source of initiating free radicals, in this case alkyl radicals (R$^{\bullet}$). Oxidizable substrate (e.g., linoleic acid) is represented here by LH. The first three equations are those for initiation. In these reactions the azo compound decomposes into two alkyl radicals that can react with a polyunsaturated fatty acid (linoleic acid) to produce lipid alkyl radicals. These lipid alkyl radicals further react with oxygen in aerobic conditions to produce lipid peroxyl radicals.

This dissertation suggests that some of the membrane models, such as micelles and homogeneous solutions of lipid, used previously by other investigators [51,58,60-62] are not suitable model systems. Firstly, the two are not structurally similar to the cell membrane's lipid bilayer. Most importantly, the kinetics of these two systems are not the same as those of the more biologically realistic membrane models studied here - liposomes [58,63-65]

Initiation

$$R\text{-}N{=}N\text{-}R \rightarrow 2R^{\bullet} + N_2 \quad (1.14)$$

$$R^{\bullet} + LH \rightarrow RH + L^{\bullet} \quad (1.15)$$

$$R^{\bullet} + O_2 \rightarrow ROO^{\bullet} \quad (1.16)$$

Propagation

$$LOO^{\bullet} + LH \rightarrow LOOH + L^{\bullet} \quad (1.17)$$

$$L^{\bullet} + O_2 \rightarrow LOO^{\bullet} \quad (1.18)$$

Termination

$$2LOO^{\bullet} \rightarrow \text{Non-radical products} \quad (1.19)$$

Figure 1.5, shown previously in section 1.2, gives an example of H-atom abstraction from α-tocopherol, a phenolic antioxidant, to produce a stable phenoxyl radical. The phenoxyl radical then reacts with a second $LOO^{\bullet}$ to produce one of a variety of non-radical products, one of which is illustrated in Figure 1.5. [48] The initial H-atom abstraction is the slow, rate-determining step. [59] The rate constant for this step, k_{inh}, determines the effectiveness of antioxidants.[59] Previous investigators have used this constant, k_{inh}, to compare the efficiencies of various antioxidants in a variety of membrane models. [58,62,66-68]

1.4. Release of free fatty acids in lipid peroxidation.

As mentioned earlier in section 1.1, a large amount of superoxide and other free radicals are produced during inflammation. It is commonly believed that free radicals and prostaglandins are involved in the inflammatory process. [17,18] Free radical insult has been shown to stimulate phospholipases to degrade phospholipids, liberating free fatty acids (FFA). [69] Marion and Wolfe used radiolabeled arachidonic acid to determine the source of unesterified FFA in rat forebrain post-mortem. [70] They determined that it came from a variety of lipid sources, including phosphatidylcholine and phosphatidylinositol. Phosphatidylcholine and phosphatidylethanolamine are degraded by phospholipase A_2 to generate arachidonic acid, the predominate FFA observed in rat brain tissues following insult. [71] After the release of FFA from the phospholipid bilayer, cyclooxygenase converts the arachidonic acid to prostaglandins and lipid peroxides. [18,72] Alternatively, lipoxygenase converts the arachidonic acid to hydroxy fatty acids and leukotrienes.[18,72] Once introduced into cell cultures and tissues, arachidonic acid has been shown to disrupt membrane integrity. [69,72-74]

1.5. The antioxidant efficiency of the synthetic CNS antioxidant U74006.

It is estimated that each year 1 million Americans suffer from stroke or trauma to the head or spinal cord .[22] Because no successful therapy exists as yet for these central nervous system (CNS)-related injuries, much research into this area is currently underway.

In traumatic CNS injury, the initial insult results in a tearing of the neurons and axons, resulting in death of the affected cells. [22] At some point after this occurs, there is a loss of blood flow to the brain or spinal cord tissue, a condition known as ischemia. [75,76] The reintroduction of blood flow and oxygen to this tissue, however, results in a sudden burst of oxygen free radicals and thus, lipid peroxidation. [77] The CNS is particularly prone to oxidative damage due to the large percentage of unsaturated lipids that make up the neuronal cell membranes. [22] There is reportedly also a lack of cellular antioxidants, including catalase and glutathione peroxidase, in CNS tissue. [7,78] Because of its inability to regenerate itself, any damage to CNS tissue results in permanent loss of cell and tissue function. Much effort has thus been exerted into developing new antioxidants to defend against free radical oxidative damage.

Initially, it was observed that large doses of steroids such as methylprednisolone (Figure 1.8) inhibited lipid peroxidation in CNS tissues. It was shown that administration of this drug improves recovery from damage to the CNS in mice [79] and in cats. [80] The problem associated with the use of these drugs is that they are known to elicit glucocorticoid activity, including hormonally-related elevation of blood glucose levels; immunosuppression, and weight loss. [81]

More recently, a new, but similar class of antioxidants called 21-aminosteroids has been developed that lack this glucocorticoid activity. [82] Two representative compounds from this class include U74500A (pregna-1,4,9(11)-triene-3,20-dione, 21-[4-[5,6-bis(diethylamino)-2-pyridinyl]-1-piperazinyl-16-

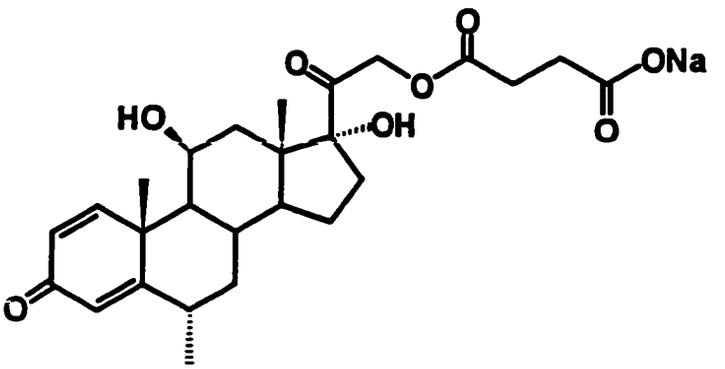

Figure 1.8. Structure of methylprednisolone.

methyl-,hydrochloride) and U74006F (21-[4-(2,6-di-1-pyrrolidinyl-4-pyrimidinyl)-1-piperazinyl]-16-methyl-(16.alpha.)-pregna-1,4,9(11)-triene-3,20-dione monomethanesulfonate mesylate) shown in Figure 1.9. Both contain a nonglucocorticoid steroid bound to an amine which serves as its antioxidant functionality. While very similar in structure, the two inhibit lipid peroxidation by different mechanisms. The U74500A is an iron chelator and thus inhibits iron-dependent lipid peroxidation. [83,84] U74006F, though not an iron chelator, is capable of inhibiting both iron- and noniron-dependent lipid peroxidation. [83,84]

Certain pyridine compounds were shown to have affinity for Fe^{II}. [85] These compounds contain a N-C-C-N fragment that enable them form bidentate ligands to the metal. [86] Similarly, U74500A contains a N-C-C-N fragment that renders it an excellent chelator of Fe^{II}. As such, it is capable of inhibiting Fe^{II}-dependent lipid peroxidation. [87] Interestingly, this amine was less effective at inhibiting

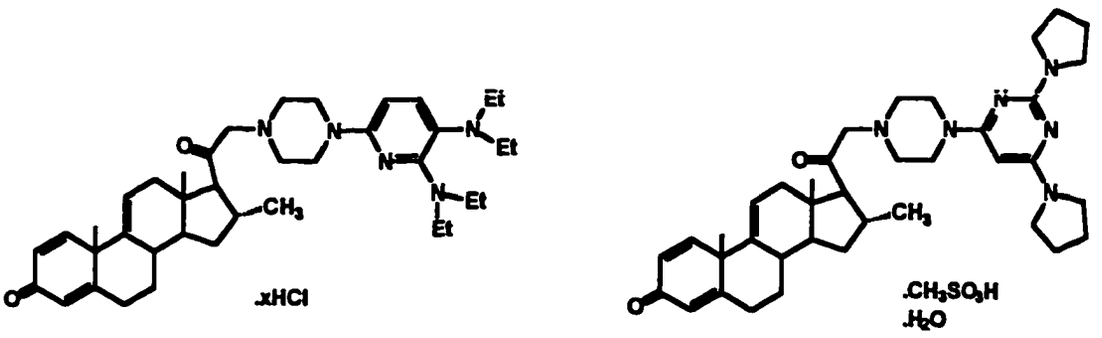

U74500A **U74006F**

Figure 1.9. Structures of 21-aminosteroids in clinical trials.

oxidation when not bound to the steroid. [86] Although most of the iron added to lipid systems is located within the more aqueous region of the membrane, it has been found that iron can actually bind to the membrane itself. [88] Steroids, including the 21-aminosteroids, are already known to partition themselves within the lipophilic region of the membrane. [89,90] The fact that addition of a steroid to an iron chelator was capable of increasing its ability to inhibit iron-dependent oxidation could suggest that the membrane-bound iron is the actual initiating species.

U74006F prevents lipid peroxidation but is not an iron chelator. It was shown to exhibit inhibition comparable to α-tocopherol in membranes. [91] Both U74006F and U74500A were proven reactive toward lipid peroxyl radicals (LOO$^{\bullet}$) and phenoxyl radicals (PhO$^{\bullet}$), [91] and were able to spare α-tocopherol in membrane

models as well as *in vivo*. [91,92] An interesting finding was that U74006Fshowed a smaller antioxidant effectiveness in systems of arachidonic acid in ethanol than in membranes. [91] Perhaps the antioxidant role of U74006F includes membrane stabilization by the steroid group. This 21-aminosteroid was in fact shown to elicit similar effects as cholesterol on lipid packing order in membrane models. [90] In this study, U74006F was proven to have a wide distribution between the two layers and contributed to a higher order in lipid packing within the hydrophobic lipid domain. Higher order and increased membrane packing may result in the entry of fewer free radicals into the lipid bilayer to initiate oxidation.

U74006F was chosen for development in clinical trials for antioxidant protection against brain and spinal cord injury, stroke, and brain hemorrhage. [93] Although U74500A in some instances was proven to be a more potent inhibitor of iron-dependent lipid peroxidation, it lacks pharmaceutic stability and is rapidly eliminated *in vivo*. [93] It was for these reasons that we chose U74006F for our investigation.

1.6. Goals for this research.

The first goal of this study was to compare the kinetics of homogeneous solution [62] and micelles [58,66] with that of liposomes, whose lipid bilayer makes for a better model of the cell membrane. The data and results for work done in this area are described in detail in chapter 2. The kinetics of the two liposome models presented here, multilamellar vesicles (MLVs) and unilamellar vesicles (ULVs), are further compared. Results from these data show that the

traditionally accepted rate equation determined for homogeneous solution and for micelles is not valid in either of the liposome models studied here.

Secondly, the antioxidant effectiveness of α-tocopherol was determined for micelles and for MLVs and ULVs. The results are compared to that observed by others in the same or different systems. The data show that the effectiveness of α-tocopherol decreases from homogeneous solution and micelles to liposomes. This indicates that as the membrane model becomes more biologically realistic, the antioxidant effectiveness of α-tocopherol decreases. This could suggest that α-tocopherol may not actually be very effective *in vivo.* It was also observed that the antioxidant was less effective at high concentrations. This, in conjunction with findings by other researchers, may suggest that at high concentrations there is a competition between antioxidation and prooxidation by α-tocopherol.

The third goal of this research was to determine the role of free fatty acids in lipid oxidation and antioxidation. In chapter 3 we present data that clearly show there is an increase in the antioxidant efficiency of α-tocopherol in the presence of FFA. This effect becomes important in oxidatively damaged tissue where FFA have been shown to be released. [70,94,95]

Evidence from differential scanning calorimetry (also in chapter 3) is presented here that suggests there is a change in membrane fluidity when both α-T and FFA are present. It is possible that an increase in membrane fluidity in the presence of FFA is responsible for the increase in α-T's efficiency in liposomes containing FFA. A more fluid membrane may allow for greater mobility of α-tocopherol to encounter and trap free radicals.

Finally, the antioxidant effectiveness of U74006F was compared with that of α-tocopherol in systems of noniron-dependent lipid peroxidation in ULV liposomes. These data are presented in chapter 4. Results show that there is a decrease in the antioxidant effectiveness of U74006 between pH 7.0 and pH 6.5. This could indicate that U74006 may not be effective in damaged tissue, where the pH was shown to decrease to about 5.4-6.9. [25]

CHAPTER 2: EFFECT OF MEMBRANE STRUCTURE ON THE KINETICS OF LIPID PEROXIDATION

2.1. INTRODUCTION

Systematic kinetic work done in homogeneous solution has elicited the following reactions (eqs 2.1-2.6), given previously in chapter 1 but repeated here for convenience [59] These are the reactions generally believed to occur during lipid peroxidation initiated by an azo compound (R-N=N-R) in organic solution.[58,59] Oxidizable substrate (e.g., linoleic acid) is represented here by LH.

Initiation

$$R\text{-}N{=}N\text{-}R \rightarrow 2R^{\bullet} + N_2 \quad (2.1)$$

$$R^{\bullet} + LH \rightarrow RH + L^{\bullet} \quad (2.2)$$

$$R^{\bullet} + O_2 \rightarrow ROO^{\bullet} \quad (2.3)$$

Propagation

$$LOO^{\bullet} + LH \rightarrow LOOH + L^{\bullet} \quad (2.4)$$

$$L^{\bullet} + O_2 \rightarrow LOO^{\bullet} \quad (2.5)$$

Termination

$$2LOO^{\bullet} \rightarrow \text{Non-radical products} \quad (2.6)$$

The first three equations are those for initiation. In these reactions the azo compound decomposes into two alkyl radicals that can react with a polyunsaturated fatty acid (linoleic acid) to produce lipid alkyl radicals. These lipid alkyl radicals further react with oxygen in aerobic conditions to produce lipid peroxyl radicals.

Most common biological initiators of membrane lipid peroxidation, for example, the hydroxyl radical from the metal-mediated reduction of hydrogen peroxide or superoxide, are hydrophilic. [7,11] These initiating free radicals form in the extracellular medium or at the membrane interface between the lipophilic and hydrophilic regions. [7,11] Thus, the radicals must partition into the lipophilic region of the membrane at least slightly in order to abstract a reactive bis-allylic lipid hydrogen atom and initiate the lipid peroxidation chain process. [16]

In this study, we have used the cationic, water-soluble azo compound ABAP (2,2'-azobis-2-amidinopropane dihydrochloride), shown in Figure 2.1, to mimic the hydrophilic nature of most biological initiators. Azo compounds are known to decompose unimolecularly at a known and constant rate. [96] The decomposition of the azo initiator is thus quantitative, making interpretion of the kinetic results feasible. [58] Many researchers have used ABAP as an initiator in *in vitro* models for membrane lipid peroxidation because of its ease of study. [58,66,97] One assumption that is commonly made is that the mechanism of the ABAP decomposition is similar to that observed with other azo compounds

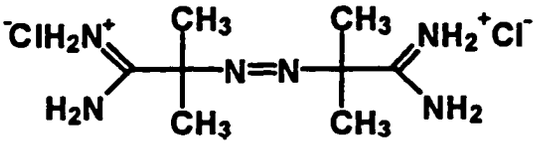

Figure 2.1. Structure of ABAP, a water-soluble azo initiator.

(see eqs 2.7-2.9). [58] The first step results in the formation of a caged radical complex *via* either concerted or stepwise bond dissociation (eq 2.7). [58,96] The caged radicals can then either combine in the cage (eq 2.8) or escape as free radicals available for initiating chain processes (eq 2.9).

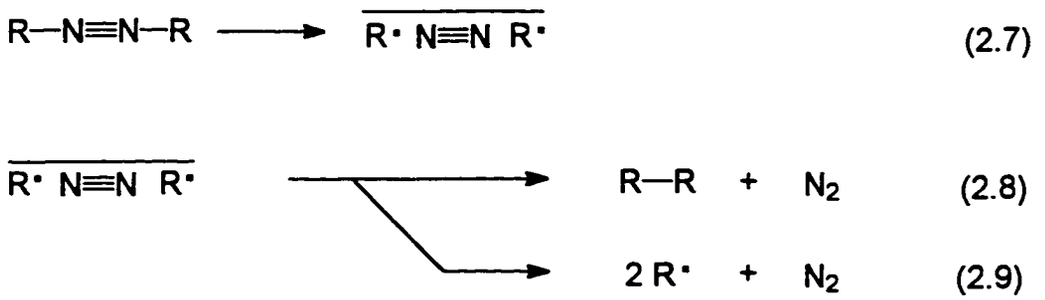

Previous studies probing the kinetics of lipid oxidation in homogeneous solution and in SDS micelles elucidated the rate equation shown in eq 2.10. [57] The rate constants denoted in this equation are those for the free radical

$$-\frac{d[O_2]}{dt} = \frac{k_p}{(2k_t)^{1/2}}[LH]R_i^{1/2} \qquad (2.10)$$

oxidation reactions described in eqs 2.1-2.6. Here, k_p is the rate constant for initiation (eq 2.4), k_t is the rate constant for termination (eq 2.6), R_i is the rate of initiation (eq 2.1), and LH is the oxidizable substrate (polyunsaturated fatty acid).

More recently, liposomes are being used as membrane models, because their lipid bilayers make for a better model of the cell membrane. [98] In aqueous solution, two types of liposomes are possible, multilamellar vesicles (MLVs) and unilamellar vesicles (ULVs). Unilamellar vesicles are phospholipid spheres containing only one lipid bilayer, while MLVs contain several concentric or stacked lipid bilayers. ULVs are a more biologically realistic model of the cell membrane's lipid bilayer.

The goal of this study was to determine whether homogeneous kinetics applied to more biologically realistic membrane models such as liposomes. The results obtained for SDS micelles were compared to results reported in the literature for the same system to confirm that the method used here for measuring lipid oxidation was valid. Furthermore, comparison of the kinetic data obtained for the ULV and MLV membrane models studied here with data reported in the literature show that indeed the kinetics of these two systems are different from that of other previously studied model systems. Neither MLVs nor ULVs seems to abide by the traditionally accepted rate equation.

2.2. RESULTS

2.2.1. Medium effects on the effective rate of decomposition of ABAP, a water-soluble azo initiator.

Rates of oxygen consumption were determined at 37°C as a function of the concentration of ABAP (2,2' azobis-2-amidinopropane) in each of the different media used in this study (buffer, SDS micelles, MLVs, and ULVs). No unsaturated lipids were present in the SDS, MLV, or ULV systems. Tabulated raw data for these experiments can be found in the Appendixes, Table A.1.

The rate of decomposition of initiator is represented below as R_i. This rate depends on the rate constant for the decomposition of the initiator, k_d, and

$$R_i = nek_d[ABAP] \qquad (2.11)$$

the efficiency, e, which is the fraction of alkyl radicals that react with oxygen to produce peroxyl radicals. The stoichiometric factor, n, is assumed to have a value of 2, because the decomposition of azo compound results in the production of two molecules of free radicals. In homogeneous systems, ne is approximately equal to 1.0, and k_d for ABAP is equal to $3.72X10^{-7}s^{-1}$.[58] The slope of the lines generated by least squares treatment of rates of initiation (R_i) versus [ABAP] gives the quantity nek_d (Figure 2.2). From the slope of R_i versus [ABAP] and with n equal to 2, we can calculate the quantity ek_d, which is the

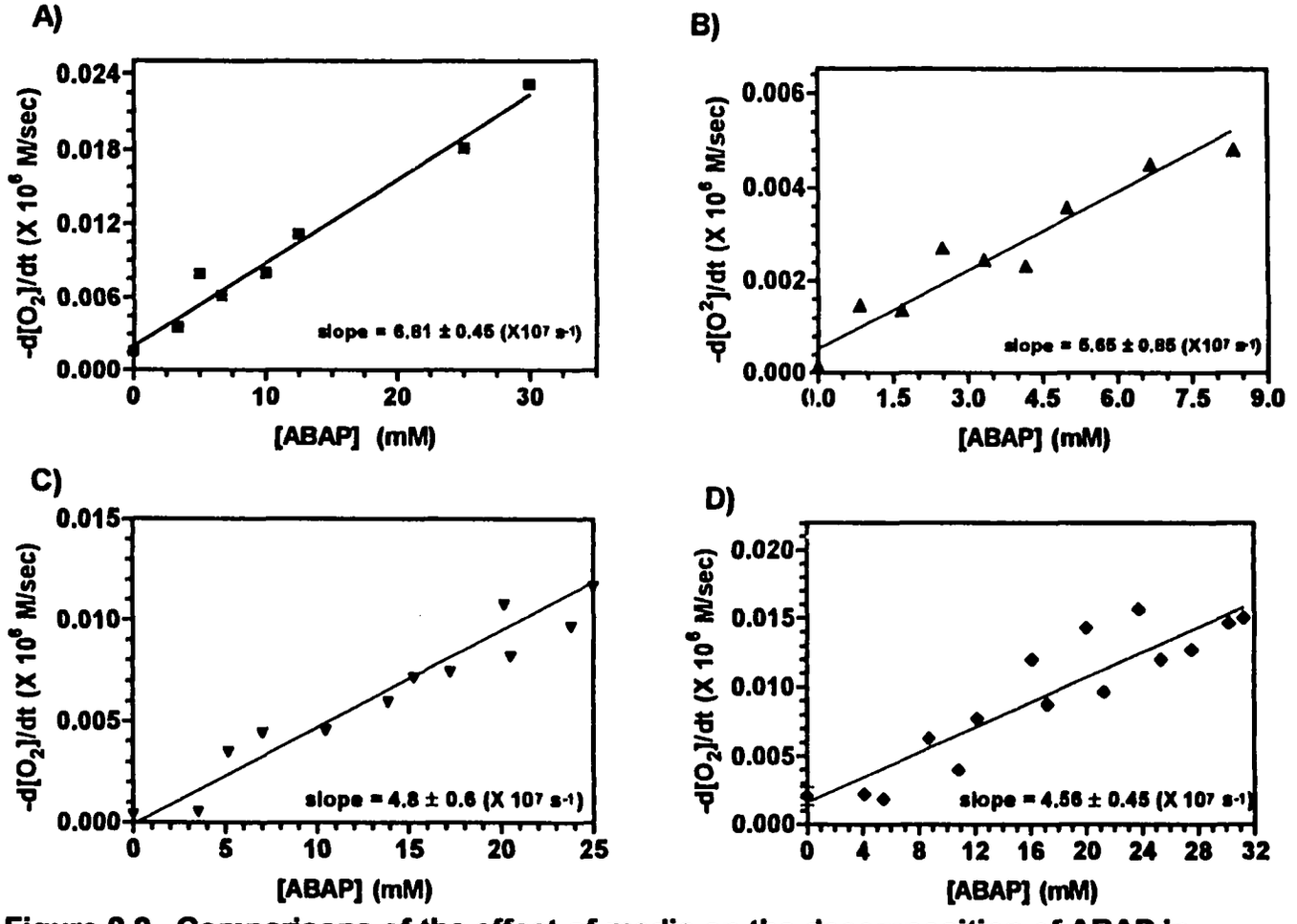

Figure 2.2. Comparisons of the effect of media on the decomposition of ABAP in A) phosphate buffer, B) SDS micelles, C) MLVs, and D) ULVs. Samples contained the following: 50mM phosphate buffer, pH 7.4, 88.3 μM DTPA, B) 0.5 M SDS in phosphate buffer, 88.3 μM DTPA, C) 20 mg/mL MLV hydrogenated egg PC in phosphate buffer, 88.3 μM DTPA, D) 20 mg/mL MLV hydrogenated egg PC in phosphate buffer, 88.3 μM DTPA. Data were obtained using the oxygen electrode method.

effective rate of formation of radicals available for initiating lipid peroxidation chain processes. Thus, we calculate values of ek_d at 37°C (Table 2.1) of 3.1 ± 0.4 X $10^{-7}s^{-1}$ and 2.8 ± 0.4 X $10^{-7}s^{-1}$ in the presence of buffer alone and SDS, respectively. In MLVs and ULVs the values were similar, at 2.4 ± 0.3 X $10^{-7}s^{-1}$ and 2.3 ± 0.2 X $10^{-7}s^{-1}$, respectively. Calculations for comparison of the means at 95% confidence were performed on these data. [99] These calculations show that ek_d for MLVs and ULVs is different from that of buffer. In addition, values for ek_d in micelles and buffer were statistically the same. Figure 2.3 illustrates these results graphically.

Table 2.1. Results for measuring the dependence of media on the rate of decomposition of ABAP in buffer, micelles, MLVs and ULVs.*

Model System	$ek_d \pm \sigma$ (X10^7 s^{-1})
phosphate buffer	3.12 ± 0.43
SDS micelles	2.83 ± 0.43
MLV hydrogenated PC	2.40 ± 0.30
ULV hydrogenated PC	2.28 ± 0.23

* Data obtained from the slopes of the lines generated from data in Figure 2.1.

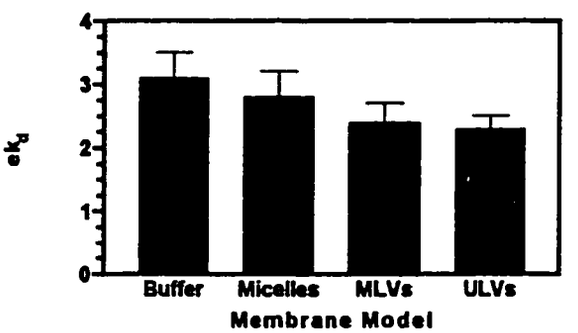

Figure 2.3. Error associated with calculated values of ek_d in various membrane models.

2.2.2. Effect of [ABAP] on rates of oxidation in micelles, MLVs and ULVs.

Rates of oxygen consumption, R_{ox}, were determined for different concentrations of ABAP in various membrane models, this time containing oxidizable substrate. Experiments were done in SDS micelles containing linoleic acid, and in ULVs and MLVs prepared from soy PC. Tabulated raw data for these experiments can be found in Table A. 2 of the Appendixes. Log-log plots of log(Rox) *versus* log([ABAP]) were constructed for each model system and are shown in Figure 2.4. The slope of these plots gives the order for ABAP in each of the systems. These results are tabulated in Table 2.2.

Table 2.2. Results obtained for measuring the order in ABAP for SDS, MLVs, and ULVs.*

Membrane Model	Order $\pm \sigma$
SDS micelles	0.43 ± 0.02
MLVs	1.37 ± 0.10
ULVs	1.35 ± 0.18

* Data were obtained for slopes of lines generated in the graphs in Figure 2.2.

2.2.3. Effect of the concentration of unsaturated lipid, [LH], on the rate of oxidation in micelles, MLVs, and ULVs.

Log-log plots were constructed for data collected in systems containing varying concentrations of MLV and ULV soy PC diluted with 20 mg/mL hydrogenated egg PC (unoxidizable lipid) (Figure 2.5, with tabulated raw data in

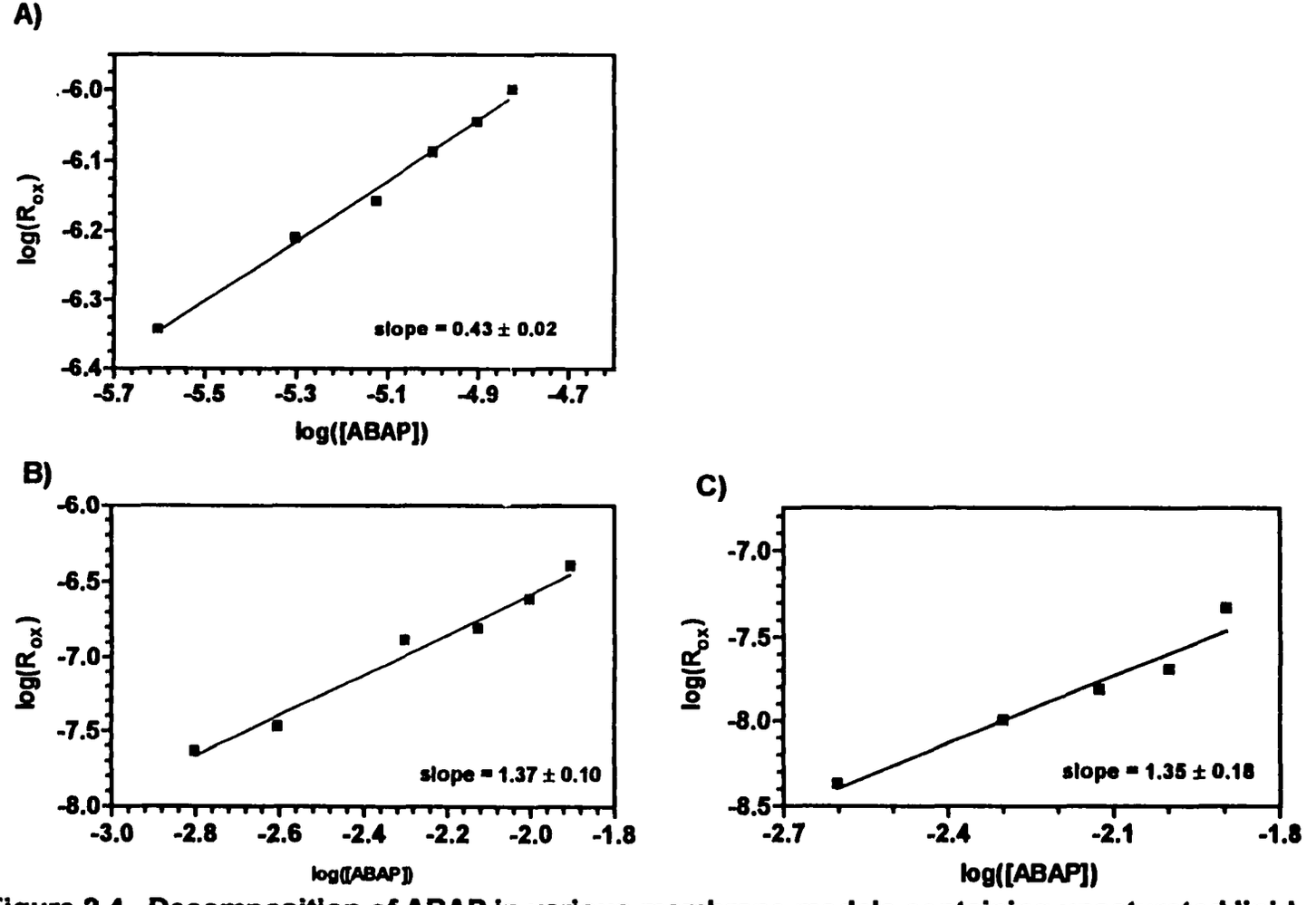

Figure 2.4. Decomposition of ABAP in various membrane models containing unsaturated lipid. Varying concentrations of ABAP (0-15 mM) were added to samples containing A) 0.5 M SDS micelles in phosphate buffer, 88.3 μM DTPA, 46.7 mM linoleic acid, B) 20 mg/mL MLV soy PC in buffer, 88.3 μM DTPA, C) 20 mg/mL ULV soy PC in 88.4 buffer, 88.3 μM DTPA. Data were obtained using the oxygen electrode method.

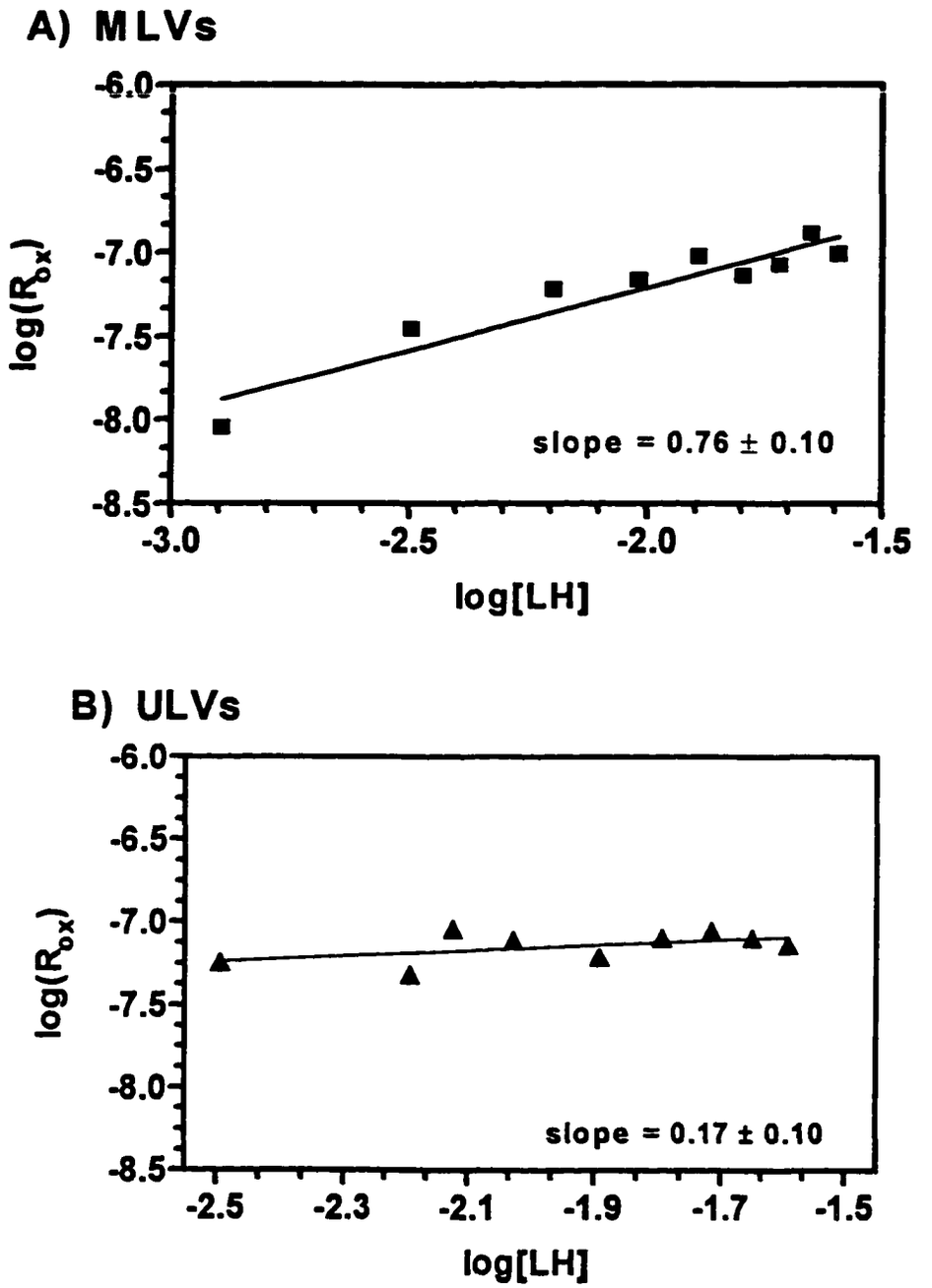

Figure 2.5. Effect of varying oxidizable substrate concentration on the rate of decomposition of ABAP in A) MLVs, and in B) ULVs. Both systems contained varying amounts of soy PC diluted with 20 mg/mL hydrogenated egg PC in 50 mM phosphate buffer, pH 7.4, 88.3 μM DTPA, and 21.2 mM ABAP. Rates of oxidation were measured using the oxygen electrode method.

Table A. 3 of the Appendixes). The slope of this line gives the order in LH. Results show that the order in both systems is less than 1 (Table 2.3). The two systems appear to be kinetically different, in that the calculated order in MLVs (0.76 ± 0.10) is significantly different from the order in ULVs (0.17 ± 0.10). Calculations for comparison of the means at 95% confidence [98] show that the two values for the order in LH are stastically different.

Table 2.3. Results for measuring the order in LH in MLVs and ULVs.*

Membrane Models	Order $\pm \sigma$
MLVs	0.76 ± 0.10
ULVs	0.17 ± 0.10

* Data were obtained from the slopes of the lines generated from the data in Figure 2.3.

2.2.4. Effect of $[O_2]$ on rates of oxidation in MLVs and ULVs.

The effect of oxygen concentration on rates of oxidation in MLVs and ULVs is shown in Figure 2.6. Rates of oxygen consumption were determined in both MLVs and ULVs containing oxygen concentrations of 62.5, 250 and 1250 μM. Tabulated raw data from this study can be found in the Appendices in Table A. 5. Log-log plots were constructed using rates of oxidation and $[O_2]$ (Figure 2.6). The slope of the line generated by least squares for the MLV system 0.09 ± 0.05 was greater than that for the ULV system, 0.05 ± 0.01 (Table 2.4). Calculations for comparison of the means at 95% confidence [99] show that these two numbers are not different. Using this same calculation, however, the two orders in O_2 for the same two systems is statistically different from zero.

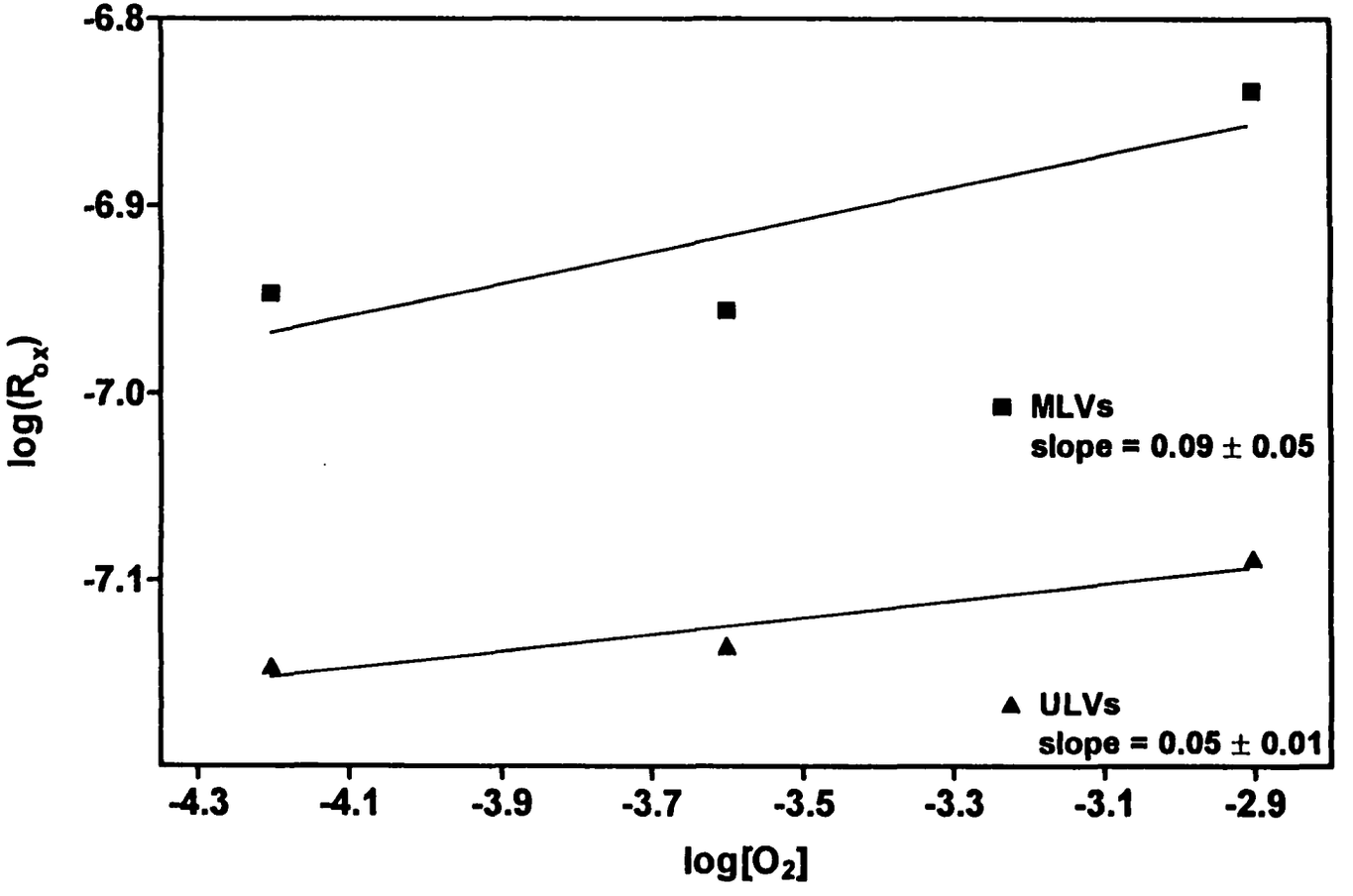

Figure 2.6. Effect of varying oxygen concentration on initiation by ABAP in ULVs.
System contained 20 mg/mL ULV soy PC in 50 mM phosphate buffer, pH 7.4, 88.3 μM DTPA, and 21.2 mM ABAP. Samples were bubbled with gas of varying O_2 concentrations. Rate of oxidation were measured by oxygen electrode method.

Table 2.4. Results for measuring the order in $[O_2]$ in MLVs and ULVs.

Membrane Model	Order $\pm \sigma$
MLVs	0.09 ± 0.05
ULVs	0.05 ± 0.01

* Data were obtained from slopes of the lines generated from the data in Figure 2.6.

2.3. DISCUSSION

2.3.1. Rate of intiation resulting from ABAP decomposition in micelles, MLVs and ULVs.

It has often been assumed that the decomposition chemistry and kinetics of ABAP are essentially independent of its environment. [100,101] The results presented here tend to suggest that such assumptions are not always justified. Apparently, SDS micelles (containing no oxidizable substrate) do not have an appreciable effect on ABAP decomposition; the product of the rate constant for decomposition and the efficiency is the statistically the same in this system as in buffer alone (Figure 2.2). Statistical analysis of data do show, however, that the decomposition of ABAP in MLVs and ULVs (also containing no oxidizable substrate) is different from its decomposition in buffer alone.

Strickland, Pryor, et al [58] reports a value of k_d equal to 3.7×10^{-7} s^{-1} for ABAP in micelles. Using the value of e they reported, 0.49, k_d is thus calculated to be 5.7×10^{-7} s^{-1}. From the slopes of the lines shown in Figure 2.1 and assuming the stoichimetric factor n equal to 2, ek_d was calculated. The results are presented in Table 2.1. These results show that the rates of decomposition of ABAP in MLVs and ULVs are different from the rates of decomposition in buffer

and micelles. The decomposition of ABAP thus does not appear to be independent of the environment or media.

The order in LH was determined by measuring the rates of oxidation for varying concentrations of unsaturated lipid (Table 2.3). The orders in LH for MLVs and ULVs are statistically different and are different from 1, the order in LH for homogeneous solution.

Barclay, et al, have reported attempts at elucidating the kinetics of azo-initiated liposome systems. [102] They argue that the rate law confirmed for homogeneous systems (determined for eqs 2.1-2.6 and given in eq 2.10) holds for liposomes, since they were able to calculate an order of 1.07 in LH and 0.54 in ABAP. There are two problems with these data. First of all, the order in ABAP was calculated in MLVs prepared by vortex-stirring followed by freeze-thaw. The order in LH, on the other hand, was determined in ULVs prepared by passing the liposomes through a French pressure cell. The first problem with Barclay's experiments is that he assumes the kinetics of ULVs and MLVs are the same. The results presented here show a large difference in the kinetics of ULV and MLV systems. The second problem with Barclay's study is that the ULVs prepared using the French pressure cell are very small, on the order of 15-30 nm [103]. The liposomes prepared using the extrusion method, as was utilized here, are much larger, with a diameter of about 70 nm [104]. The kinetics of these two systems should therefore be different, since the fluidity of the liposome system decreases as the size of the ULV increases. [105-108] As will be discussed in chapter 3, fluidity of the membrane model has a large effect on the kinetics of

the system. The small ULVs prepared by Barclay and his coworkers would thus be more fluid and more kinetically similar to homogeneous solution.

In summary, it is likely that the kinetics for oxidation in MLVs and ULVs are quite different. This work also suggests that the traditional rate equation reported for homogeneous solution and for micelles does not necessarily apply to liposomes.

2.4. EXPERIMENTAL

2.4.1. Materials.

Linoleic acid (cis,cis-9, 12, octadecadienoic acid) and diethylenetriaminepenta-acetic acid (DTPA) were obtained from Sigma Chemical Co. Hydrogenated L-α-phosphatidylcholine from frozen egg yolk was purchased from Avanti Polar Lipids (Alabaster, AL). A convenient and inexpensive source for the soy phosphatidylcholine used in this study was found to be commercial L-α-Lecithin capsules, purified as described below. Granular 2,2' azobis-2-amidinopropane dihydrochloride (ABAP), type V-50, was obtained from Wako Pure Chemical Industries, Ltd. These, and all other incidental chemicals and solvents, were of high purity and were used as received.

2.4.1.1. Purification of L,α lecithin.

The flash chromatography column apparatus was obtained from Ace Glass, Inc. (cat. no. 5872). It consisted of a column with a 10 mm I.D. and a 45.7 cm effective length, a 250 mL reservoir, and a flow control adapter. A chloroform

slurry containing 40 g silica gel was poured into the column such that the column bed was 35-37 cm in length.

One lecithin capsule was dissolved in 10 mL chloroform and loaded onto the column. The column was then pressurized using nitrogen (> 10 psi) such that the flow rate was approximately 10 mL/min. The column was first eluted with 400 mL ethyl acetate/methanol (50:50). This fraction presumably contained less polar compounds such as α - tocopherol, β - carotene, and diglycerides. The PC was then eluted off the column using 200 mL methanol. The methanolic solution was evaporated to dryness under vacuum leaving the purified lipid as a thin film on the walls of the flask. The yield was approximately 200 $\pm$ 75 mg, depending on the source of lecithin. The purified material was dissolved in chloroform and was stored under nitrogen at -20°C.

2.4.1.2. Analysis of the purified phosphatidylcholine.

The purity of the sample was confirmed using reverse-phase HPLC and comparison to a 99% soy PC sample. A Perkin-Elmer Series 410 pump with a 235C diode array detector were used. The column used was a Spherisorb 25 cm X 4.6 mm I.D. C_8 reverse-phase column with 5 μm particle size (Regis, 8210 Austin St., Morton Grove, IL, 60053). A solvent mixture consisting of 90% acetonitrile and 10% water was formed using the HPLC pump. Conditions for the separation included a 1.0 mL/min flow rate run isocratically at 25°C and UV detection at 215 nm. Data were collected and analyzed using LabCalc software (Galactic Industries).

The HPLC chromatograms obtained for the soy PC purified as described above and for a commerical sample of soy PC (99% purity) are shown in Figure 2.7. Both chromatograms show a similar group of peaks that elute from 14-23 min. These peaks reflect the mixture of phosphatidylcholines having various fatty acid composition (probably of varying degrees of unsaturation). One additional large peak was observed at 26.5 min in the commercial soy PC sample that was not observed in the purified soy PC. In addition, several small impurity peaks were observed between 5 and 15 min in the commercial sample that were not observed for the chromatographically purified PC. The peak eluting at 3 min in both samples was shown to be due to solvent passage. Based on the HPLC analysis, it appears that the PC purified by this method is of higher purity than PC obtained commercially. However, note that the size of the peaks observed with UV detection is not directly indicative of the quantity of material present. [109,110]

Fast-atom bombardment-mass spectra (FAB-MS) were aquired using a Finnigan MAT TSQ - 70 triple quadrapole mass spectrometer with an Antek PS-4 cesium ion gun. Samples were applied to both glycerol and 3-nitrobenzyl alcohol matrices and each were run separately. Sample mixing was accomplished by placing the matrix material on a stainless steel probe tip and applying the sample to the matrix. The heater current for the Cs pellet was run at 150 μA, the extractor at 2.5 kV, the focussing lens at 5.5 kV, and the acceleration voltage at 6.4 kV.

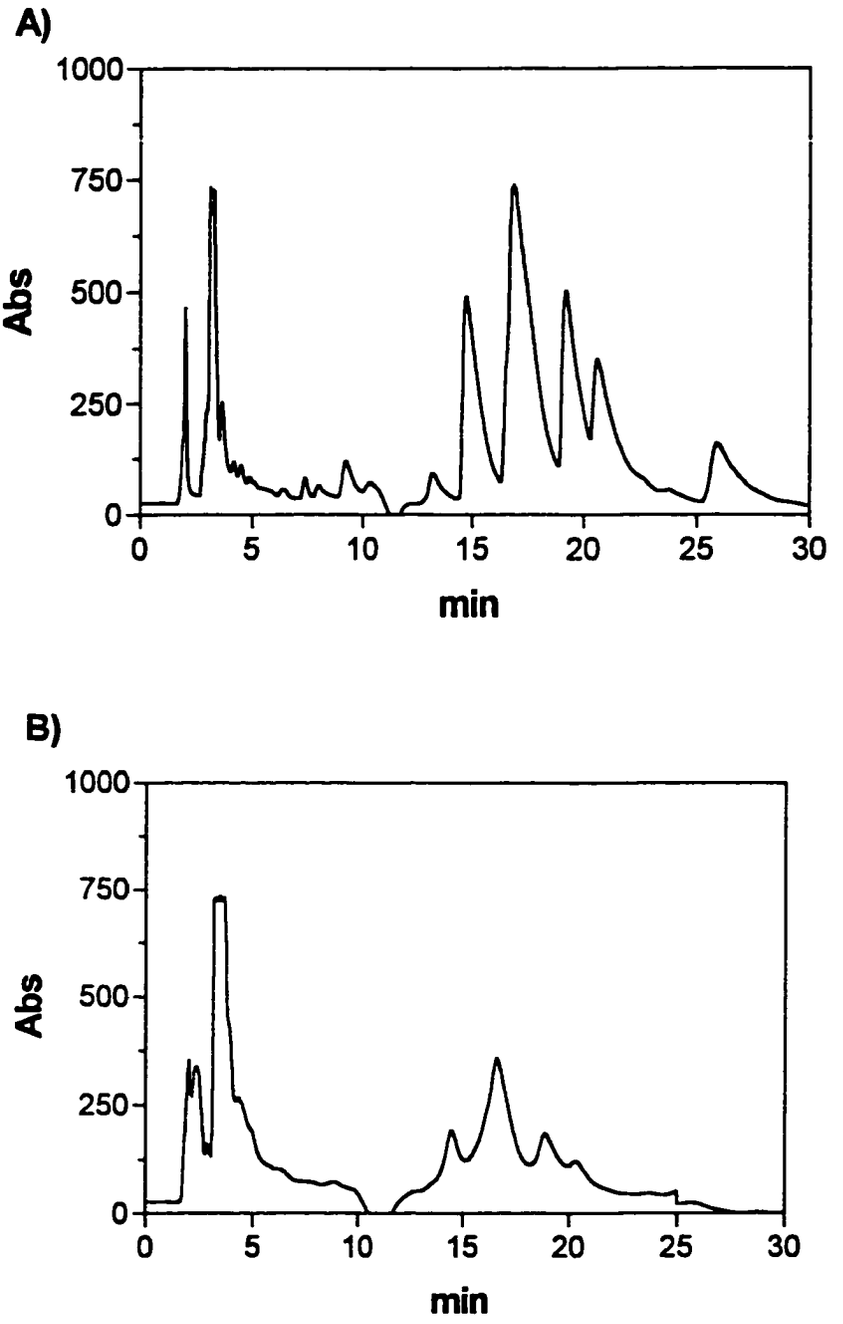

Figure 2.7. HPLC chromatogram for L-α-phosphatidylcholine. Samples contained A) 100 mg/mL chloroform solution of 99% L-α-phosphatidylcholine, and B) 20 mg/mL chloroform solution of L-α-phosphatidylcholine purified from lecithin.

The chromatographically-purified soy PC, Figure 2.8, gave FAB-MS that show mass clusters centered at 695.9, 717.9, 739.0, 759.1, 783.2, and 805.2 m/e while the commercial soy PC sample showed mass clusters centered at 759.1 and 783.1 m/e.

Table 2.5 shows the fatty acid composition of some common phospholipids, including PC extracted from soybean. Possible combinations for fatty acyl side chains that would have combined masses corresponding to the mass clusters observed by FAB-MS were calculated (Table 2.6). The presence of the cluster

Table 2.5. Fatty acid composition of commonly used phospholipids [55]

Fatty acid abbreviation	Common name	Percent abundance (%) in natural source of PC		
		Soy PC	Egg PC	Rat PC
14:0	myristic			
16:0	palmitic	17.2	35.3	28.8
18:0	stearic	3.8	13.5	18.0
18:1	oleic	22.6	26.8	8.4
18:2	linoleic	47.8	5.7	19.4
18:3	linolenic	8.6	0.2	
20:3				1.0
20:4	arachidonic		1.0	17.0
20:5			3.6	2.4
22:5			1.3	1.5
22:6			12.6	3.5

at 805.2 m/e in the FAB-MS of the purified soy PC indicates that this sample contained more arachidonic acid (20:4) than did the commercial sample. Since no arachidonic acid should be present in soy PC (Table 2.5), PC from some other source may have been added to the commercial lecithin capsules. The peak with mass 717.9 m/e for the purified lecithin is likely another phospholipid

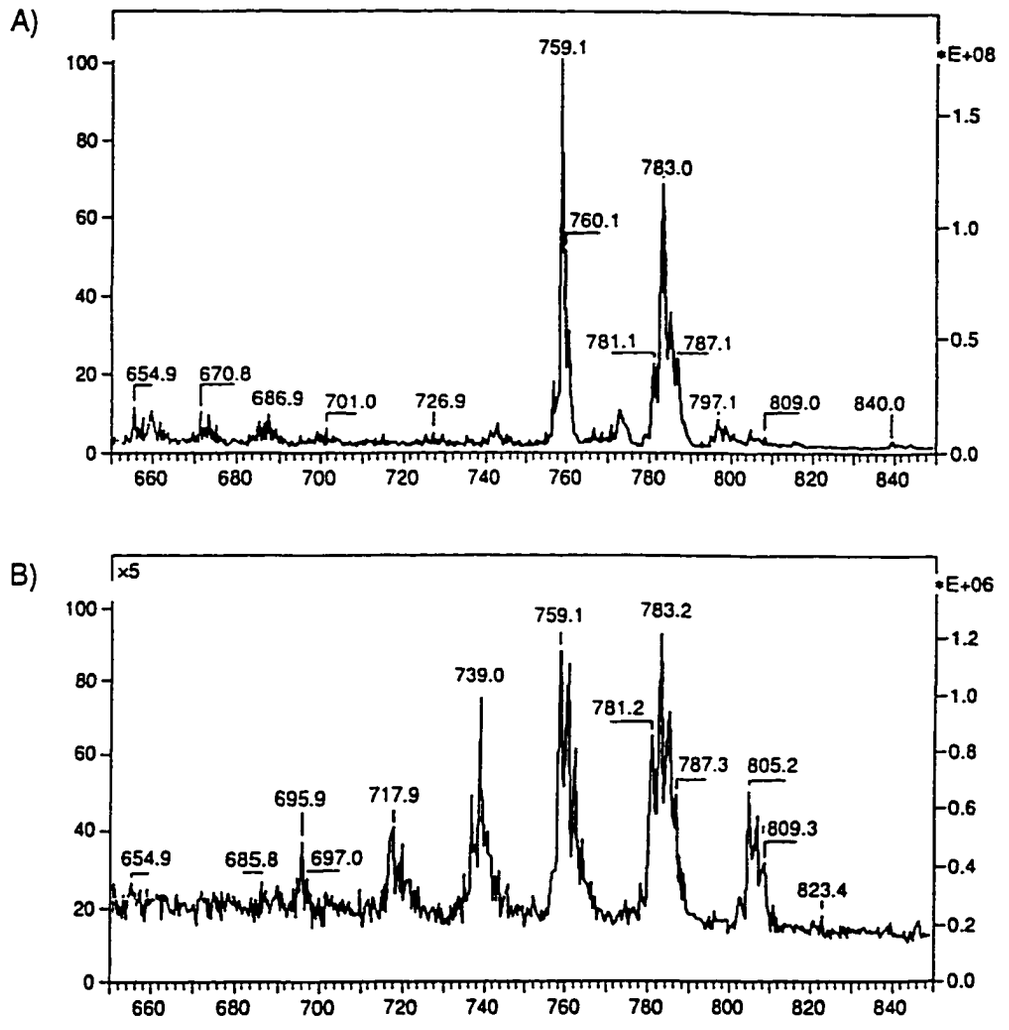

Figure 2.8. FAB-MS obtained for A) 99% L-α-phosphatidylcholine, and B) L--α-phosphatidylcholine purified from a lecithin capsule.

Table 2.6. Possible combinations of R_1, R_2 for the observed FAB-MS mass clusters.

Mass cluster	Possible R_1, R_2 combinations	Mass
759.1	16:0/18:0	761
	16:0/18:1	759
	16:0/18:2	757
	16:0/18:3	755
783.1	18:0/18:1	789
	18:0/18:2	787
	18:0/18:3	785
	18:1/18:2	783
	18:1/18:3	785
	18:2/18:3	783
	18:0/18:0	781
	18:1/18:1	781
	18:2/18:2	779
	18:3/18:3	777
805.2	20:4/18:0	809
	20:4/18:1	807
	20:4/18:2	805
	20:4/18:3	803

of the same family but is not identified here. Note that the masses reported by FAB-MS are one mass unit greater than the actual mass because the analyzed species are protonated. Also, as is true of UV detection, size of the peak produced by FAB-MS is not necessarily proportional to the quantity present. [111]

It is likely that the purification procedure reported here results in a purer lecithin sample than was available in the particular commercial sample used as a standard. Evidence of this was the appearance of the extra impurity peaks observed in the HPLC chromatogram for the commercial sample. From the MS

data, however, its fatty acid composition appears slightly different. Although the FAB-MS showed that the two samples contained different types of fatty acyl side chains, their properties should be the same.

2.4.2. Methods.

2.4.2.1. Preparation of multilamellar and unilamellar vesicles.

To produce multilamellar vesicles (MLVs) the suspension of soy PC in buffer was sonicated in a low energy bath-type sonifier for 5 min, making sure that all PC on the sides of the flask were in solution.[112] Liposomes produced in this manner are very large and heterogeneous in size, on the order of 0.1-5.0 μM in diameter. [98] For unilamellar vesicles (ULVs), the sample was then extruded 10 times or until clear through 2 X 100 nm polycarbonate filters using an Avestin liposome extrusion device (Ottawa, Canada). [104] ULVs prepared using this method have been shown to be on average about 70 μM in diameter. [104]

2.4.2.2. Measurement of the effect of SDS micelles and phosphatidylcholine liposomes on the rate of decomposition of ABAP.

The rate of decomposition of ABAP was first determined in 50 mM potassium phosphate buffer, pH 7.4. This was accomplished by placing 3 mL of the phosphate buffer (containing 88.3 μM DTPA) in a Clark-type oxygen electrode cell. DTPA (diethylenetriaminepenta-acetic acid) was added to chelate any iron present that may initiate iron-dependent lipid oxidation. The Biological Oxygen Monitor, Model YSI 5300 (Yellow Springs Instrument Co., Yellow Springs, Ohio)

was interfaced to computer software *via* a 12 bit A/D converter. Oxygen concentration was thus followed over time. Increasing amounts of 0.5 M ABAP in water were added (a few μL at a time), and after each addition, oxygen concentration was followed. Rates of oxidation (R_{ox}) were determined from the slopes of lines generated from plots of oxygen concentration *versus* time. A plot of R_{ox} versus [ABAP] was then constructed and its slope was measured.

To determine the effect of SDS micelles or PC liposomes on the rate of decomposition of ABAP, a 3 mL solution of either 0.5 M SDS or 20 mg/mL hydrogenated soy PC in 50 mM potassium phosphate buffer, pH 7.4, was prepared. MLVs or ULVs were then prepared from soy PC using the methods described previously, section 2.4.2.1. DTPA was added so that its final concentation was 88.3 μM. Increasing volumes of 0.5 M ABAP in water were added (a few μL at a time), and after each addition, the rate of decrease in oxygen concentration was followed.

2.4.2.3. Measurement of the effect of [ABAP] on rates of oxidation in SDS micelles, MLV, and ULVs.

To determine the effect of [ABAP] on rates of oxidation in SDS micelles or soy PC liposomes, a 3 mL solution of either 0.5 M SDS or 20 mg/mL soy PC in 50 mM potassium phosphate buffer, pH 7.4, was prepared. MLVs or ULVs were then prepared from soy PC using the methods described in section 2.4.2.1. DTPA was added so that its final concentation was 88.3 μM. To the samples containing SDS, linoleic acid was added so that its final concentration was 46.7

mM. Increasing amounts of ABAP in water were added (a few μL at a time), and after each addition, the rates of oxidation were measured as described in section 2.4.2.2.

2.4.2.4. Measurement of the effect of [LH] on rates of oxidation in MLVs and ULVs.

To determine the effect of oxidizable substrate concentration, 3 mL solutions of varying concentrations of soy PC diluted with 20 mg/mL hydrogenated egg PC were prepared in 50 mM potassium phosphate buffer, pH 7.4. The solutions were then either sonicated in a sonic bath (for MLVs) or extruded (for ULVs), as previously described. A 2.7 mL aliquot of the solution was then placed in an oxygen electrode cell. Stock solutions DTPA and ABAP in buffer were added, so that their final concentrations were 88.3 μM and 21.2 mM, respectively. The concentration of oxygen was followed over time. The rates of oxidation, R_{ox}, were determined as described in section 2.4.2.2. Plots of the rate of oxidation versus [LH] were constructed.

2.4.2.5. Measurement of the dependence of oxygen concentration on rates of oxidation in MLVs and ULVs.

Solutions of 20 mg/mL ULV or MLV soy PC in phosphate buffer were prepared as described previously. These solutions were maintained at 62.5, 250 and 1250 μM O_2 by bubbling each with gas of varying O_2 concentrations (5, 20, and 100%, respectively). The 5% O_2 gas contained an O_2/N_2 mixture, the

20% O_2 gas was a typical air mixture, and the 100% gas contained pure O_2. The concentration of oxygen in the sample was estimated using the assumption that air-saturated solution contains 250 μM O_2, [113] and that air itself is 20% O_2. The concentration of O_2 in samples bubbled with 5% O_2 is 62.5 μM; with 20% O_2, 250 μM; and with 100% O_2, 1250 μM. Stock solutions of DTPA and ABAP in phosphate buffer were added so that their final concentrations were 88.3 μM and 21.2 mM, respectively. The rate of oxygen consumption was then measured by oxygen electrode method.

2.4.2.6. Error analysis for the oxygen electrode method.

The oxygen electrode method described previously included error that was associated with that of the A/D converter, solution preparation, drift of the electrode itself, and error from imperfections in the electrode membrane. Each of these instrumental errors analysis is listed in Table 2.7. As long as the measurement was performed over a short period of time, all of these errors should be very small in comparison to that derived from the imperfections in the

Table 2.7. Instrumental error associated with the oxygen electrode method.

Source of error	Percent error
A/D converter	± 0.02%
solution preparation	± 0.32%
drift of electrode	± 0.13% per 15 min
Physical imperfections in membranes	± 10%

membrane, which is reportedly 10%. Thus, the total error associated with the use of the oxygen electrode over a 15 minute period can thus be assumed to be ±10.47%.

CHAPTER 3: EFFECT OF FREE FATTY ACIDS AND MEMBRANE STRUCTURE ON ANTIOXIDANT EFFICIENCY OF α-TOCOPHEROL

3.1. INTRODUCTION

As discussed in Chapter 1, the inhibition of lipid peroxidation by a phenolic antioxidant occurs due to competition between chain propagation (eq 3.1) and H-atom abstraction from an antioxidant (eq 3.2) to produce a stable and

$$LH + LOO^{\bullet} \rightarrow L^{\bullet} + LOOH \qquad (3.1)$$

$$ArOH + LOO^{\bullet} \rightarrow ArO^{\bullet} + LOOH \qquad (3.2)$$

persistent phenoxyl radical ($ArO^{\bullet}$). The phenoxyl radical can further react with a second $LOO^{\bullet}$ to produce a non-radical product (illustrated in Chapter 1, Figure 1.1). The initial H-atom abstraction is the slow, rate-determining step. Previous investigators measured the rate constant for this step, k_{inh}, in order to compare the effectiveness of antioxidants. This constant was calculated using the rate equation (eq 3.3) determined for inhibited oxidation in homogeneous

$$R_{ox,inh} = \frac{k_p R_i [LH]}{2k_{inh}[ArOH]} \qquad (3.3)$$

solution. In order to calculate k_{inh}, k_p, the rate constant for the propagation reaction (eq 2.4), and R_i, the rate of initiation (eq 2.1), would first have to be experimentally determined. This problem can be alleviated by instead calculating an antioxidant efficiency, AE. Antioxidant efficiency is

mathematically defined as k_{inh}/k_p and has been calculated as such in previously reported work. [66] The method used here to calculate AE assumes as little

$$LOO\cdot + LH \xrightarrow{k_p} L\cdot + LOOH \qquad (3.4)$$

$$LOO\cdot + ArOH \xrightarrow{k_{inh}} ArO\cdot + LOOH \qquad (3.5)$$

knowledge about mechanism as possible. In these calculations the "50% inhibition concentration" is first determined experimentally. This is the concentration of antioxidant required to produce a 50% decrease in the rate of oxidation. An assumption about the kinetics of the system is then made in order to calculate AE without first calculating k_{inh} or k_p. When the rate of lipid peroxidation is inhibited by an antioxidant by 50%, the rate of the reactions in eqs 3.4 and 3.5 are assumed to be equal and, therefore, k_p and k_{inh} are equal. If this assumption is accurate, then eqs 3.6 and 3.7 must also be valid. In these

$$k_p[LH]_{50}[LOO^{\cdot}] = k_{inh}[LOO^{\cdot}][ArOH]_{50} \qquad (3.6)$$

$$\frac{k_{inh}}{k_p} = \frac{[LH]_{50}}{[ArOH]_{50}} \qquad (3.7)$$

equations, $[LH]_{50}$ and $[ArOH]_{50}$ represent the concentrations of oxidizable lipid and phenolic antioxidant at 50% inhibition, respectively.

This work demonstrates that the antioxidant efficiency (AE) calculated in this manner for α-tocopherol decreases dramatically from homogeneous to heterogeneous systems of lipid, such as micelles, liposomes, and microsomes. In addition, it is concluded that free fatty acids actually enhance AE for α-tocopherol. This becomes important in damaged tissue, where free fatty acids have been shown to be released. [70,94] To determine what effect FFAs have on the membrane that enhances α-tocopherol's antioxidant efficiency, physical characteristics of the liposome before and after addition of FFA were investigated.

An electron spin resonance (ESR) assay was used to measure the entrapped or internal volume of the liposome vesicle. In this assay the liposomes were prepared containing the stable nitroxyl radical TEMPOL (Figure 3.1). Due to its membrane permeability, TEMPOL partitions both within the

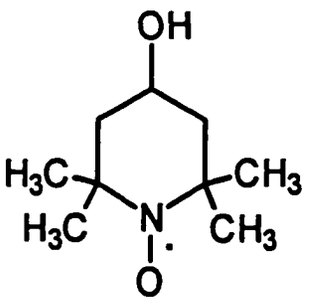

Figure 3.1. Structure of TEMPOL, a membrane permeable nitroxyl radical.

aqueous interior of the vesicle, as well as outside the vesicle in solution. [114] A relatively membrane impermeable spin-label broadening agent, tris(oxalato)chromate(III), is then added. This paramagnetic ion reportedly

remains only on the outside of the liposome [115,116] Spin-label broadening agents work by both spin exchange and through dipole-dipole interactions. [117,118] Spin exchange occurs as a result of a contact interaction, and dipole-dipole, a pseudocontact interaction. [117,118] In both cases, shorter relaxation times are the overall result and line broadening occurs. ESR signal represented by the extravesicular nitroxyl radical is thus broadened by the chromium oxalate (Figure 3.2). Chromium oxalate is added in increasing concentrations until no further broadening occurs. The signal thus reaches a limiting minimum peak height in

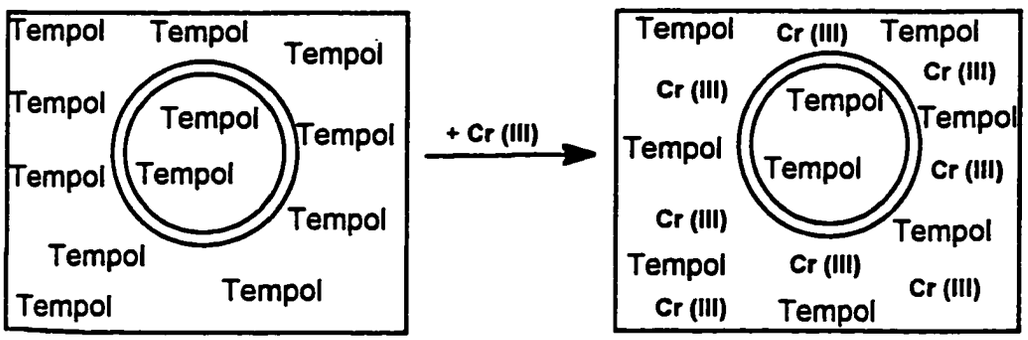

Figure 3.2. Method of measuring entrapped volume in liposome vesicles using the nitroxyl radical TEMPOL and the paramagnetic ion Cr (III).

the presence of Cr (III). The signal that remains is that of the TEMPOL within the vesicle, and the intensity of the remaining signal is manipulated to determine entrapped or internal volume within the liposome vesicle. If the membrane becomes leaky, signal from intravesicular TEMPOL may then become broadened by Cr (III) that has permeated the membrane, and the effective entrapped volume or observed signal should thus be smaller. In these studies,

entrapped volume was determined for ULVs with and without FFAs to detect differences in entrapped volume and/or "leakiness" of the membrane.

Differential scanning calorimetry (DSC) is often used to measure membrane fluidity. [119-121] There are two phases that can exist in the liposome - the more ordered gel state and the less ordered or more fluid liquid crystalline state. DSC is used to measure the temperature of the transition from one phase to another and the enthalpy of this transition. Shifts in the liposome's gel to liquid crystal transition temperature or enthalpy correlate to a change in membrane fluidity. Results show that when FFAs are present the liposome is more fluid.

3.2. RESULTS

3.2.1. Comparison of inhibition by α-tocopherol in micelles and in liposomes.

Plots of percent inhibition *versus* concentration of α-tocopherol in systems of ABAP-initiated oxidation in SDS micelles, and MLV and ULV soy PC liposomes showed that inhibition in these systems were not similar (Figure 3.3, with tabulated raw data listed in Table A.5 of the Appendixes). Inhibition in the SDS micelles increased to 90 ± 4 % at 10 μM α-T and then decreased gradually. Inhibition in the MLV system increased to 108 ± 2 % around 25 μM and then decreased more dramatically. In the ULV system inhibition increased to 115 ± 15 % at 75 μM before its sharp decrease in inhibition.

Note that in calculating the rates of oxidation, the rate of decomposition of ABAP (determined in the same system, except with no oxidizable substrate

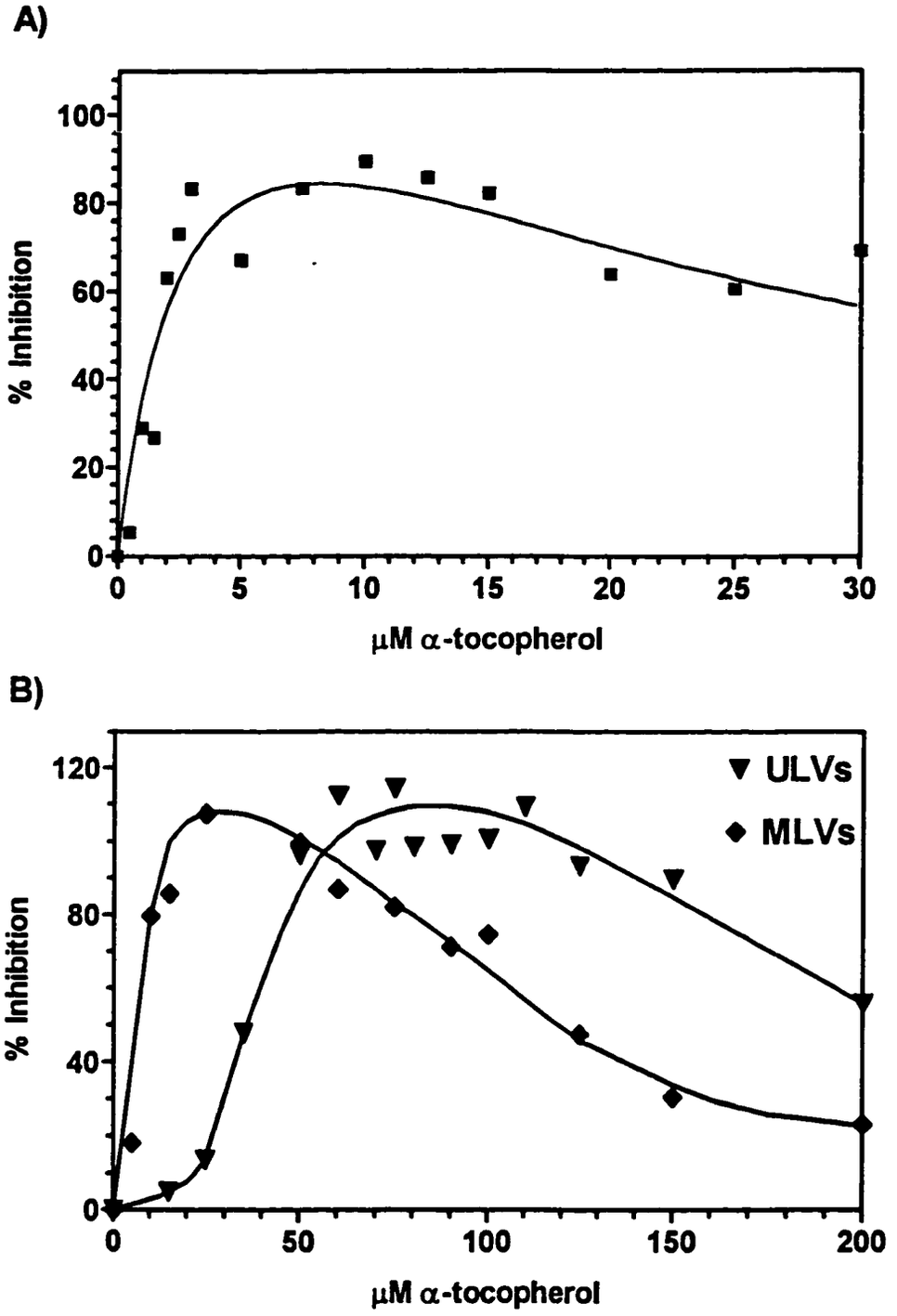

Figure 3.3. Inhibition by α-tocopherol in A) SDS micelles , and in two liposomes models, B) unilamellar vesicles (ULVs) and multilamellar vesicles (MLVs). Sample A) contained 0.5 M SDS, 46.7 mM linoleic acid, 88.3 μM DTPA, and 20 mM ABAP. Samples B) and C) contained 20 mg/mL ULV or MLV soy PC, 21.2 mM ABAP, and 88.3 μM DTPA. Rates of oxidation were measured using the oxygen electrode.

present) was subtracted from the rate of oxidation measured by the electrode. These rates of decomposition are described in chapter 2, Figure 2.2. The purpose of this calculation was to describe the rate of oxidation as only that derived from the oxidation of the membrane. The ratio of k_{inh} to k_p was calculated by dividing the initial concentration of the total oxidizable lipid substrate by the 50% inhibition concentration. These 50% inhibition concentrations are shown in Table 3.1.

Based on the percent inhibition *versus* concentration plots, α-tocopherol was much less efficient in ULVs than in MLVs or micelles. In fact, the 50% inhibition concentration calculated for α-tocopherol in ULVs is an order of magnitude greater than that in micelles (Table 3.1). It is also about five times greater than that for MLVs.

Table 3.1 Inhibition data for α-tocopherol in various membrane models.

Membrane Model	50% Inhibition Concentration (μM)	Estimated AE ($[LH]_{50}/[ArOH]_{50}$)
SDS micelles	2.0 ± 0.6	24,000
MLV Soy PC[a]	7.2 ± 6.2	3500
ULV Soy PC[a]	36.4 ± 5.2	700
ULV Soy PC[b]	60.5 ± 14.7	100

a. 20 mg/mL soy PC in phosphate buffer. b. 5 mg/mL soy PC in phosphate buffer.

The 50% inhibition concentration determined for α-tocopherol in SDS micelles is 2.0 ± 0.6 μM. This is comparable to the value obtained by Strickland,

Pryor, et al. [58] Using the same concentrations of SDS, ABAP, and LH, they obtained a value of approximately 3 μM.

Antioxidant efficiencies ($[LH]_{50}/[ArOH]_{50}$ ratios) observed in SDS micelles and several different liposomal systems, including those from the literature, are given in Table 3.2. The AE ($[LH]_{50}/[ArOH]_{50}$ ratio) calculated from data reported in the literature for inhibition in SDS micelles is an order of magnitude less than the AE calculated from data presented here for the same system. Interestingly, the AE calculated for inhibition data presented here for micelles is very similar to the AE calculated from data reported for homogeneous solution. Another interesting trend was observed for AE results within the liposomal group. There is apparently a trend to lower AE as the system changes from MLVs to ULVs prepared at high phospholipid concentration (20 mg/mL) to ULVs prepared at low phospholipid concentrations (5 mg/mL).

One discrepancy between the method for calculating AE presented here, where AE = $[LH]_{50}/[ArOH]_{50}$, and the traditional calculation using the rate equation for homogeneous kinetics is apparent for the SDS system (Tables 3.1, 3.2). The antioxidant efficiency calculated using the $[LH]_{50}/[ArOH]_{50}$ ratio for SDS micelles was 24,000, but using the traditional calculation (AE = k_{inh}/k_p), AE for micelles was instead 4300.

3.2.2. Effect of free fatty acids on inhibition by α-tocopherol in liposomes.

Concentrations of α-tocopherol required to produce a 50% decrease in the rate of lipid peroxidation were compared for liposomal systems with and without

Table 3.2. Antioxidant Efficiencies for α-Tocopherol in Various Heterogeneous and Homogeneous Systems.

System	Estimated AE ($[LH]_{50}/[ArOH]_{50}$)	Reference
Homogeneous		
18:2 / t-BuOH / AIBN [a]	12,400	Niki, et al[62]
Micelles		
18:2 / SDS / ABAP [b]	24,000	
18:2 / SDS / ABAP[c]	1830	Pryor, Wu, et al[66]
18:2 / SDS / ABAP[d]	1000	Pryor, Strickland, et al[58]
18:2 / SDS / TBHN[e]	600	Pryor, Strickland, et al[58]
Membrane Models		
MLVs / ABAP[f]	3500	
ULVs / ABAP / 18:0[g]	2600	
ULVs / ABAP[h]	700	
ULVs / ABAP[i]	100	
microsomes / ABAP[j]	109	Krinsky, et al [67]

a. Results tabulated from data obtained for 3.99 M AIBN, 0.604 M LH in t-butyl alcohol, and 0.272 - 1.71 μM Vitamin E. Rate of oxidation was measured using a pressure transducer. b. This work. c. Data reported for 0.1 M SDS in 0.3 M phosphate buffer, pH 7.4, 2.6 mM LH, and 0.5 M ABAP. Oxidation was measured by following conjugate diene formation. d. Calculated from data reported from using 0.5 M SDS in 0.5 M phosphate buffer, pH 7.6, 46.7 mM 18:2, 4.85-5.24 mM ABAP, and 0.97-1.95 μM Vitamin E. e. Results obtained using 0.015 M SDS in 50 mM sodium phosphate buffer, pH 7.0, 3 mM 18:2, and 0.3 mM di-tert-butyl hyponitrite. Data were aquired using a Clark-type oxygen electrode. f. Used 20 mg/mL MLV soy PC. g. Used 5 mg/mL ULV soy PC in phosphate buffer with 100 μM 18:0. h. Same as f., except ULV liposomes were used. i. Same as g., except no 18:0 was added. j. Results reported using 25 mM ABAP, 0.5 mg/mL microsomes in 0.1 M phosphate buffer, pH 7.5, and 2.5 - 9.0 nmol/mg Vitamin E. Data were obtained by following malonaldehyde (TBARS) formation. All original work presented in this paper done using a Clark-type oxygen electrode.

added free fatty acid (Tables 3.2 and 3.3). Tabulated raw data for this experiment can be found in the Appendixes, Table A.6. The systems containing free fatty acid required less α- tocopherol for inhibition than those without FFA. The model containing 5 mg/mL soy PC and 100 μM oleic acid (Figure 3.4) showed that at lower concentrations the added free fatty acid increased inhibition substantially. At α-tocopherol concentrations greater than 150 μM percent inhibitions calculated with and without FFA were about the same.

Table 3.3. Effect of Free Fatty Acids on the 50% Inhibition Concentrations for Vitamin E in Various Liposome Systems.

System	FFA	50% Inhibition Concentration (μM)	Estimated AE ($[LH]_{50}/[ArOH]_{50}$)
SDS micelles	18:2	1.98 ± 0.56	24,000
MLV Soy PC[b]	-	7.15 ± 6.15	3500
ULV Soy PC[a]	18:0	2.50 ± 0.18	2600
ULV Soy PC[b]	-	36.4 ± 5.20	700
ULV Soy PC[a]	-	60.5 ± 14.7	100

a. 5 mg/mL soy PC in phosphate buffer. b. 20 mg/mL soy or egg PC in phosphate buffer.

3.2.3. Effect of FFA on entrapped volume in ULVs.

The results for the comparison of entrapped volumes for ULVs with and without stearic acid or α-T are shown in Figure 3.5 (with raw data tabulated and reported in Table A.7 of the Appendixes). All concentration ratios of α-T or FFA to LH were consistent with those present in the oxidation experiments using 5 mg/mL soy PC and 100 μM oleic acid. This figure shows the intensity of an ESR signal from a membrane permeable nitroxyl radical (TEMPOL) in the presence of a relatively membrane-impermeable, paramagnetic, spin-broadening Cr (III)

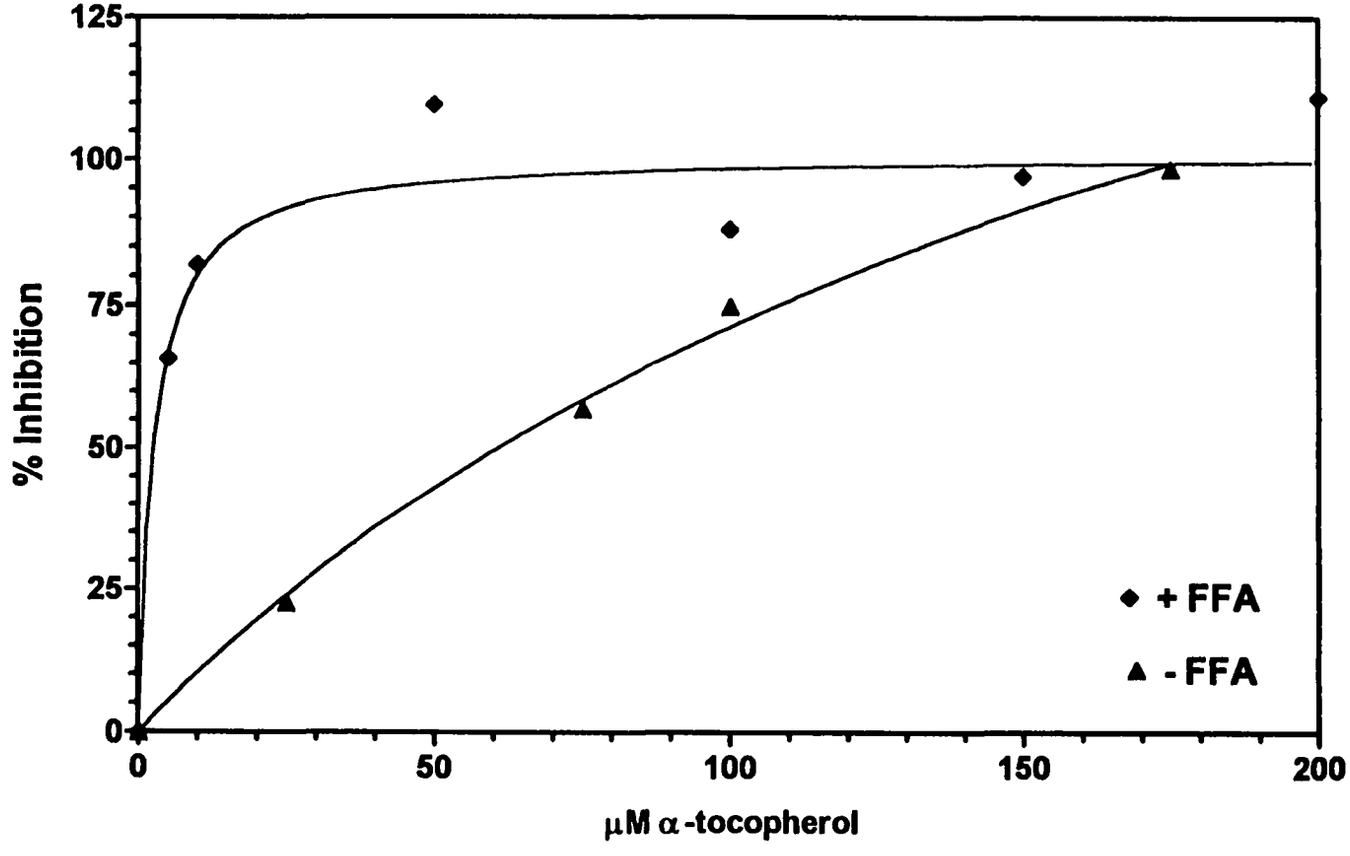

Figure 3.4. Effect of free fatty acids on inhibition by α-tocopherol in ULVs. Model system contained 5 mg/mL soy PC ULVs in phosphate buffer, 100 μM DTPA, 5 mM ABAP, and 100 μM oleic acid in some samples. Rates of oxidation were measured using the oxygen electrode method.

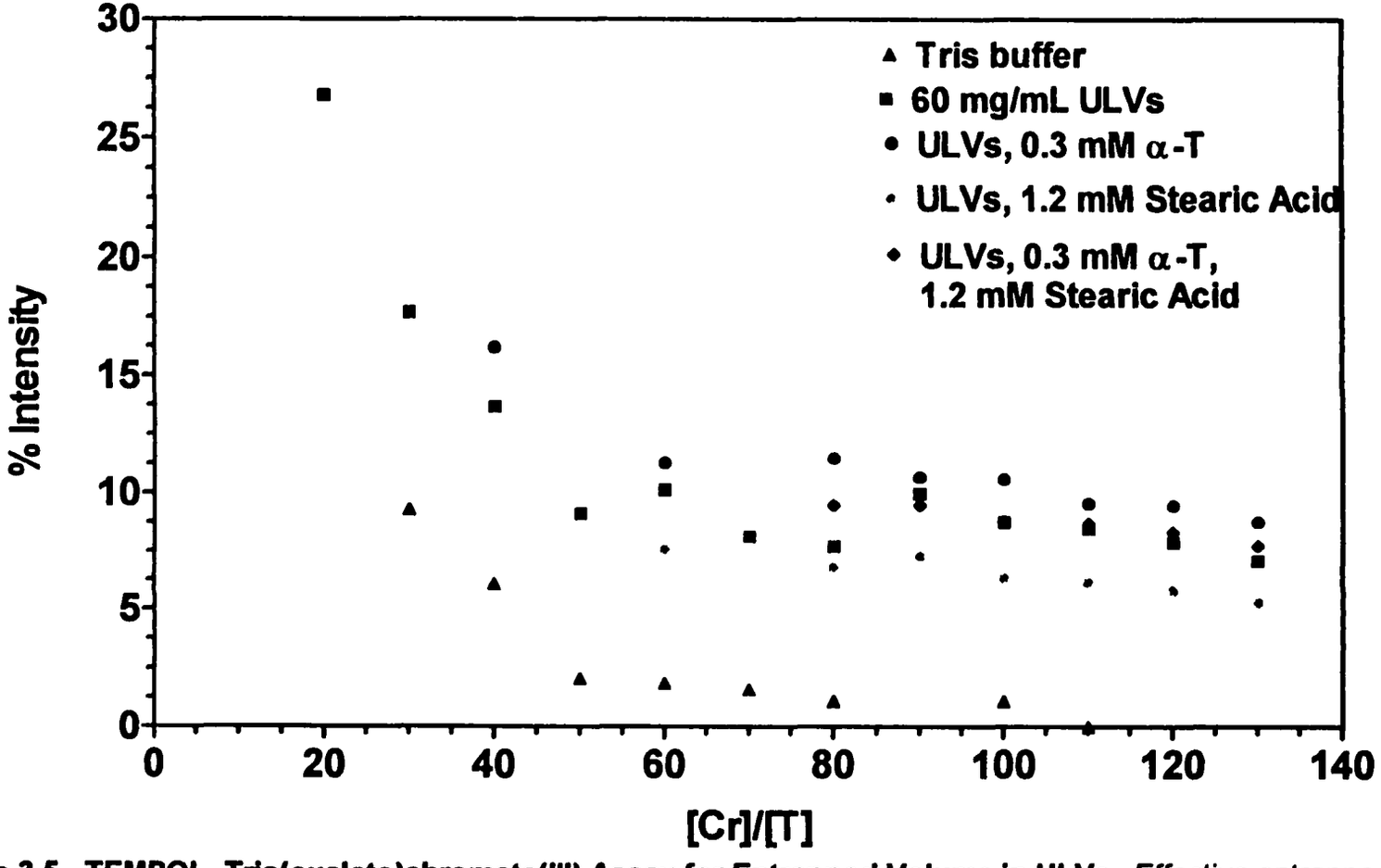

Figure 3.5. TEMPOL, Tris(oxalato)chromate(III) Assay for Entrapped Volume in ULVs. Effective entrapped volume was measured for 50 mM Tris buffer, and for 60 mg/mL ULVs in Tris buffer containing either 300 μM α-T, 1.2 mM stearic acid, or both.

reported in Table A.7 of the Appendixes). All concentration ratios of α-T or FFA to LH were consistent with those present in the oxidation experiments using 5 mg/mL soy PC and 100 μM oleic acid. This figure shows the intensity of an ESR signal from a membrane permeable nitroxyl radical (TEMPOL) in the presence of a relatively membrane-impermeable, paramagnetic, spin-broadening Cr (III) ion. Any remaining ESR signal intensity after addition of Cr(III) represents signal from intravesicular TEMPOL radical. Percent intensity depicted in the graph is explained in more detail in the section 3.4.2.4 of this chapter. The amount of remaining signal can further be manipulated to determine the internal or entrapped volume of the liposome vesicles. As illustrated in the graph (and in Table 3.4 below), in Tris buffer alone the signal decreases to zero near a Cr (III) to TEMPOL molar ratio ([Cr]/[T]) of approximately 110. For ULVs, the signal

Table 3.4. Results for measuring the entrapped volume of liposomes containing α-tocopherol, stearic acid, both or neither.

Membrane Model	% Intensity
buffer	0.0
ULVs	8.0 ± 0.8
ULVs, α-T	9.8 ± 0.8
ULVs, stearic acid	6.2 ± 0.9
ULVs, α-T, stearic acid	8.6 ± 0.6

* Data obtained from minimal signal intensities observed for those data graphed in Figure 3.3.

intensity decreased to about 8.0 ±0.8% at a molar ratio of about 130. In the presence of FFA, however, the signal intensity decreased to approximately 6.2 ± 0.9%. With α-T present percent intensity was 9.8 ± 0.8% at a molar ratio of 130 and with both FFA and α-T, 8.6 ± 0.6%. Calculations for comparison of the

3.2.4. Differential Scanning Calorimetry for ULVs with and without FFA and for MLVs.

DSC was conducted for liposomes containing either α-T or stearic acid or both. Concentration ratios of α-T or FFA to LH were comparable to those used in the previous oxidation experiment using 5 mg/mL ULVs and 100 μM oleic acid. DSC data showing the effect of α-T in liposomes are given in Table 3.5 and Figure 3.6. Note that the addition of α-T to the liposome produces a broadening of the melting transition and a lower ΔH. A broadening effect is normally observed for the introduction of an impurity into the liposome. [122] Here, T_m is the temperature of transition between the less fluid gel state and the more fluid liquid crystalline state (Figure 3.7), and ΔH is the standard enthalpy change of that transition. [122] Calculations for comparison of the means [99] using 95% confidence limits shows that the ΔH for ULVs and that for ULVs containing 200 μM α-T were statistically different.

DSC data, shown in Table 3.6, Figure 3.8, were then compared for liposomes with and without stearic acid. Addition of stearic acid to the ULVs also produced a broadening of the transition. In this case, there was a shift to lower T_m, and a considerable increase in ΔH, indicating an increase in the fluidity of the liposome. [119] Comparison of the means [99] at 95% confidence showed that the observed values for ΔH in ULVs and in ULVs containing stearic acid were statistically different. Samples containing both α-T and stearic acid showed a

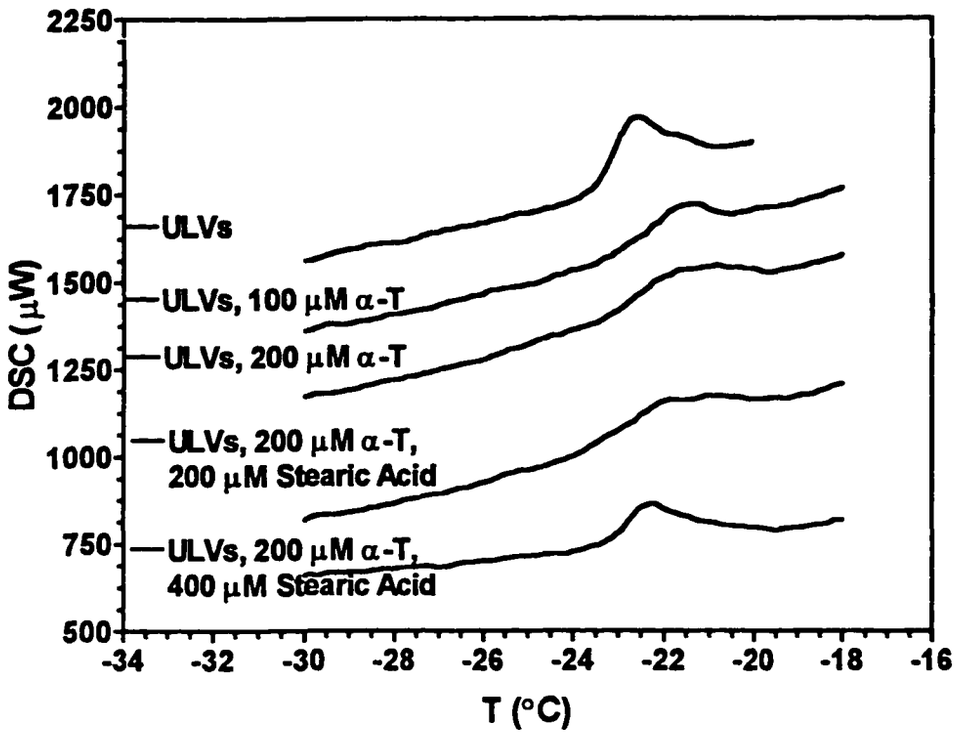

Figure 3.6. Differential Scanning Calorimetry for ULVs Containing α-Tocopherol. Samples contained 20 mg/mL ULV dioleoyl PC and varying amounts of α-T and stearic acid.

Table 3.5. Differential Scanning Calorimetry for ULVs Containing Various Amounts of α-Tocopherol and Stearic Acid.

[α-T] (μM)	[Stearate] (μM)	Tm (°C)	ΔH (mJ/mg)
-	-	-25.2 ± 2.01	20.6 ± 1.44
100	-	-24.8 ± 1.08	18.7 ± 3.37
200	-	-24.3 ± 0.85	17.5 ± 3.28
200	200	-24.0 ± 0.44	20.7 ± 1.37
200	400	-23.6 ± 0.11	19.1 ± 0.77

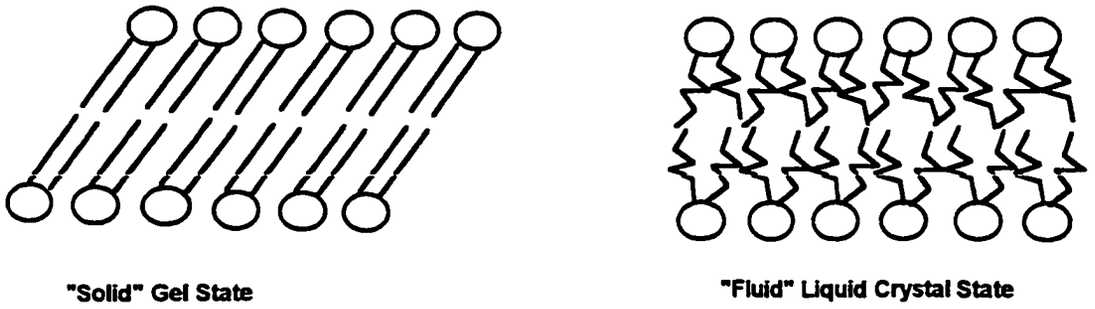

Figure 3.7. Structures of the two phases for liposomes - gel state and liquid crystal.

decrease in ΔH and the T_m shifted back to the transition temperature measured for ULVs alone.

Finally, DSC data were compared for MLVs and ULVs (Table 3.7, Figure 3.9). Results show that there is a noticeable increase in ΔH in MLVs over ULVs. Interestingly, the transition recorded for MLVs was much more broad than that of ULVs. In addition, T_m for MLVs was lower than that of ULVs. Comparison of the means [99] at 95% confidence, however, showed that the results obtained for MLVs and ULVs were not stastically different.

3.3. DISCUSSION

3.3.1. Comparison of AE for homogeneous and heterogeneous systems of lipid.

The kinetic analysis used here requires that the majority of peroxyl radicals come from substrate. Given that the rate of oxidation in the presence of substrate is at least an order of magnitude greater than the rate of oxidation in

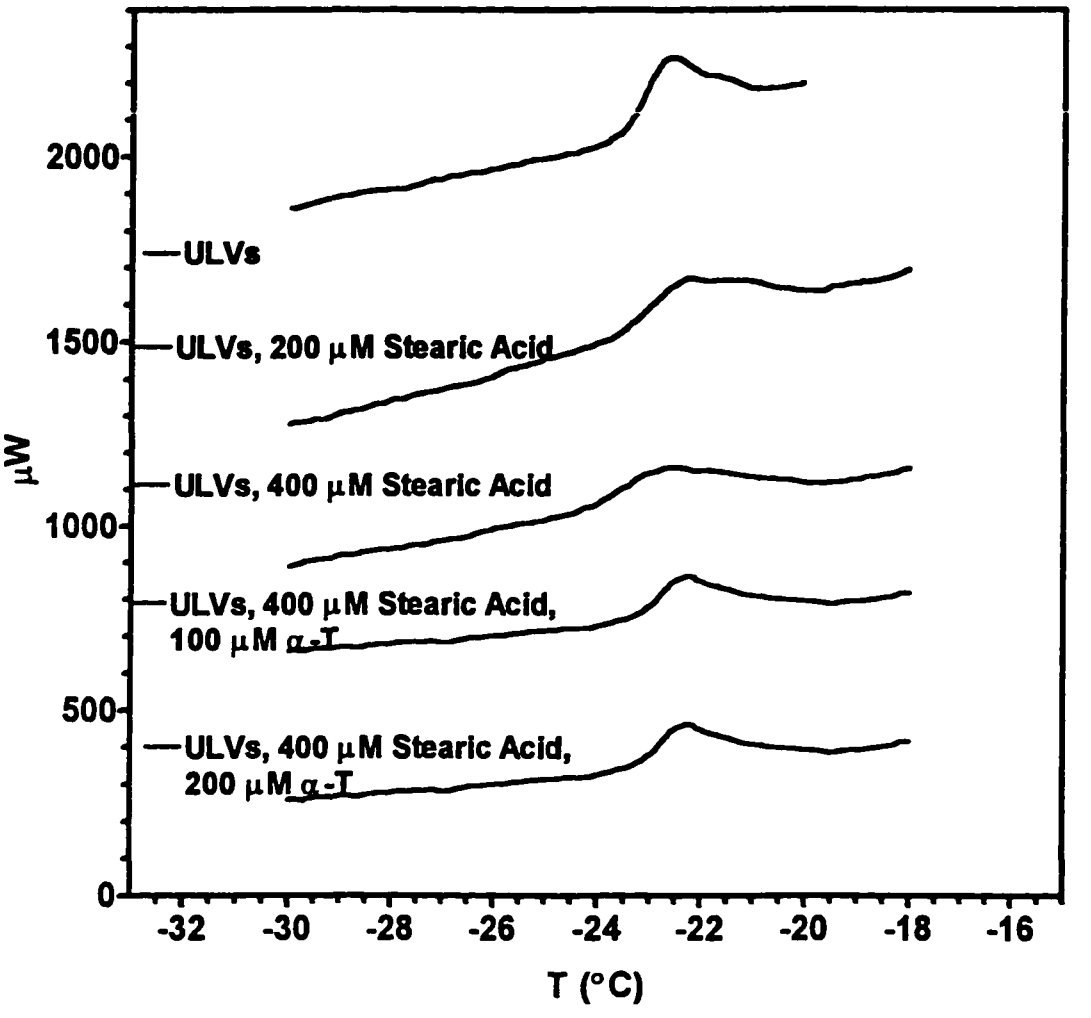

Figure 3.8. Differential scanning calorimetry for ULVs containing stearic acid. Samples contained 20 mg/mL ULV dioleoyl PC and varying amounts of α-T and stearic acid.

Table 3.6. DSC data for ULVs containing varying amounts of stearic acid and α-T.

[α-T] (μM)	[Stearate] (μM)	Tm (°C)	ΔH (mJ/mg)
-	-	-25.2 ± 2.01	20.6 ± 1.44
-	200	-24.9 ± 0.99	21.4 ± 3.47
-	400	-25.5 ± 1.30	27.6 ± 3.56
100	400	-24.6 ± 1.35	20.6 ± 2.59
200	400	-23.6 ± 0.11	19.1 ± 0.77

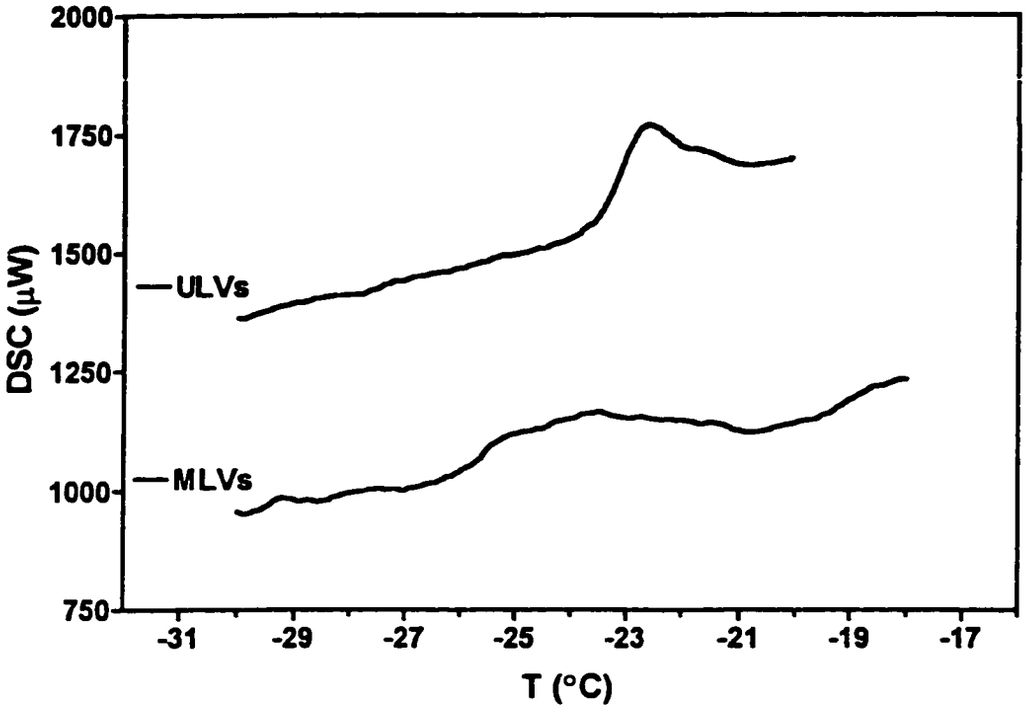

Figure 3.9. Differential scanning calorimetry for ULVs and MLVs. Samples contained 20 mg/mL ULV or MLV dioleoyl PC in phosphate buffer.

Table 3.7. Differential scanning calorimetry data for some membrane models.

Type of Liposome	n (# observations)	T_m (°C)	ΔH (mJ/mg)
ULVs	5	-25.2 ± 2.01	19.8 ± 1.44
MLVs	3	-26.3 ± 0.1	24.6 ± 4.7

its absence (Figures 2.2 and 2.5), the rate of initiation due to peroxyl radicals derived from the azo initiator is not important. Moreover, the reactivities of peroxyl radicals derived from the azo initiator and of peroxyl radicals derived from lipid should be the same.

Antioxidant efficiency was calculated for data reported by Niki, et al[62] in their homogeneous system of lipid (Table 3.2). The calculated value, 12,000, was an order of magnitude greater than that for data reported for micelles by Strickland, et al (1000)[58] and Pryor, et al (1800).[66] By comparison, the AE calculated from data obtained for microsomes, reported by Krinsky, et al[67] was only 110, two orders of magnitude less than in homogeous solution. It appears that as the model system becomes more membrane-like, α-tocopherol becomes less efficient in trapping peroxyl radicals. In addition, the AE calculated for ULVs, 700, was less than the AE calculated for MLVs, 3500. This decrease in efficiency could be due to less fluidity in the liposome. Fluidity in the liposome determines various physical characteristics of the liposome, including diffusion. A less fluid liposome might restrict the diffusion of α-T through the membrane.

Interestingly, as discussed in section 3.3.1., the AE calculated here for inhibition in micelles using the $[LH]_{50}/[ArOH]_{50}$ ratio (24,000) was an order of magnitude greater than if AE were calculated using the classical rate equation (4300). The $[LH]_{50}/[ArOH]_{50}$ ratio calculated for data reported by Niki and his coworkers for inhibited oxidation in homogeneous solution (12,400) was also an order of magnitude greater than the value for AE that could be calculated using

the traditional rate equation (5000). [62] This suggests that the classically accepted mechanism and kinetics for inhibited autoxidation may not be completely valid.

DSC data obtained for MLVs and ULVs show that MLVs may be more fluid than ULVs (Figure 3.9, Table 3.7). Once again, a decrease in fluidity and decrease in diffusion of α-T may account for the smaller AE in ULVs.

Table 3.8 shows lipid-to-α-tocopherol mole ratios in several tissues, which ranges from 400-5000. This ratio was calculated for work presented here, using concentrations of α-tocopherol where inhibition was most efficient. In micelles the ratio is 5800, while in ULVs and MLVs the ratio is 280 and 1000, respectively. Inhibition data for α-tocopherol in MLVs thus show that α-tocopherol can only be effective in tissues such as the heart, blood serum and the brain, but not in the lung or liver. Inhibition data for α-tocopherol in ULVs, which is the more biologically realistic membrane model, show that α-tocopherol may not be effective in any of these tissues.

Table 3. 8. Approximate lipid-to-α-tocopherol ratio in selected tissues.

Tissue	mol lipid / mol α-T	Reference
Heart	750	Mitchell, et al [123]
Lung	4500	Pacht, et al [124]
Liver	2000	Mitchell, et al [123,125]
Brain and Spinal Cord	700	Muller, et al [126]
Blood Serum	450	Sokol, et al [47,127]

3.3.2. Dependence of the concentration of α-tocopherol on its inhibition.

Inhibition data for α-T show that in micelles, ULVs, and MLVs inhibition by α-T decreases, rather dramatically in the case of ULVs and MLVs, at higher concentrations of α-T (Figure 3.3). This could be due to competition of the $ArO^{\cdot}$ for LOOH or LH to propagate the chain of free radical reactions. Cillard, et al [128,129] saw similar results for α-tocopherol in their oxidation studies of linoleic acid emulsions in phosphate buffer. Results such as these were also observed by Bowry, Ingold, et al. To explain their results, they measured both the rates of formation of LOOH and the consumption of α-T in low-density lipoprotein (LDL) at varying concentrations of α-T. At concentrations of 1.8 μM LDL (approximately 2.5 mM PUFA) and greater than 66 μM α-T (lipid-to-α-T mole ratio of 37.9), the rate of oxidation was greater than R_{ox} with no antioxidant present. The lipid-α-T mole ratio for the observation of decreased antioxidant efficiency of α-T in the MLV and ULV systems presented here were approximately 120-200 and 120-960, respectively. This decrease in inhibition at higher concentrations of α-T could possibly be due to prooxidation by α-tocopherol.

3.3.3. Effect of free fatty acids on membrane fluidity and lipid oxidation.

It has been shown that free fatty acids (FFAs) are released in damaged tissue. One example is the release of unesterified free fatty acid in the brain

after trauma. [70,94] It is therefore important to study their effect on the kinetics of lipid peroxidation and its inhibition. This work clearly shows that the efficiency of inhibition by α-tocopherol is increased by addition of an essentially non-oxidizable fatty acid such as oleic acid to the liposome system. Oleic acid is not likely to participate directly in lipid peroxidation (eq 3.1), because as stated in chapter 1, it is the bis-allylic H atom that is abstracted from the fatty acid. Since oleic acid has no bis-allylic position, it can be considered to have low oxidizability. One possible explanation for the increased effectiveness of the antioxidant in the presence of oleic acid is that FFAs serve to increase fluidity and diffusion across the membrane.

In order to explain this theory, an understanding of the physical characteristics of membranes is first necessary. First of all, membrane *fluidity* is a thermodynamic description of the membrane's phase behavior. Remember that membranes can exist in either an ordered gel phase or a more *fluid* liquid crystalline phase. In the gel phase, the fatty acyl chains are more tightly packed than in the liquid crystal. [55] For this reason, a decrease in *fluidity* in the membrane generally indicates an increase in *order*, a physical description of the lipid chain packing. [55] It has been shown that small ions or molecules permeate the membrane more readily in the membrane's liquid crystalline phase. [55] Increases in membrane permeability thus suggest increases in fluidity. Because increases in fluidity and decreases in order imply less lipid packing, greater diffusion of membrane proteins usually also coincide with increases in fluidity.

Studies have shown that FFA does appreciably increase membrane permeability, calcium transport, and protein diffusion. [69,72-74]

3.3.4. Effect of FFA on entrapped volume.

Measurements for the entrapped volume of the liposome vesicle show that there is no significant change in entrapped volume or size of the liposome in the presence of either α-T, stearic acid, or both. This means that the increase in inhibition of oxidation by α-T was not due to a disruption of the integrity of the liposomes. The presence of α-T did cause a slight increase in the entrapped volume of ULVs, thus suggesting a small increase in chain packing in the liposome. It has been shown that an increase in lipid chain order actually causes the bilayer to become thinner. [55] This could then result in an increase in the entrapped volume of the vesicle. [55] The increase in chain packing could result from both the hydrogen-bonding of α-T to the polar head groups on the lipid and the hyrodrophobic interactions between α-T's hydrocarbon tail and the phospholipid side chain (Figure 3.10).

3.3.5. Effect of FFAs and α-T on T_m.

Differential scanning calorimetry data were obtained for ULVs with and without α-tocopherol and stearic acid. It has been shown that T_m is dependent on the intermolecular attractive forces between the phospholipid headgroups. [122,130] An increase in these attractions produces more stability in the

liposome, thus less fluidity, and the observed T_m increases. On the other hand, ΔH depends on the distance between the hydrocarbon chains. [122,130] An increase in the van der Waals attractions between these hydrocarbons produces more stability in the liposome, thus less fluidity, and there is a decrease in the observed ΔH. Though there was no obvious change in T_m, there was a slight

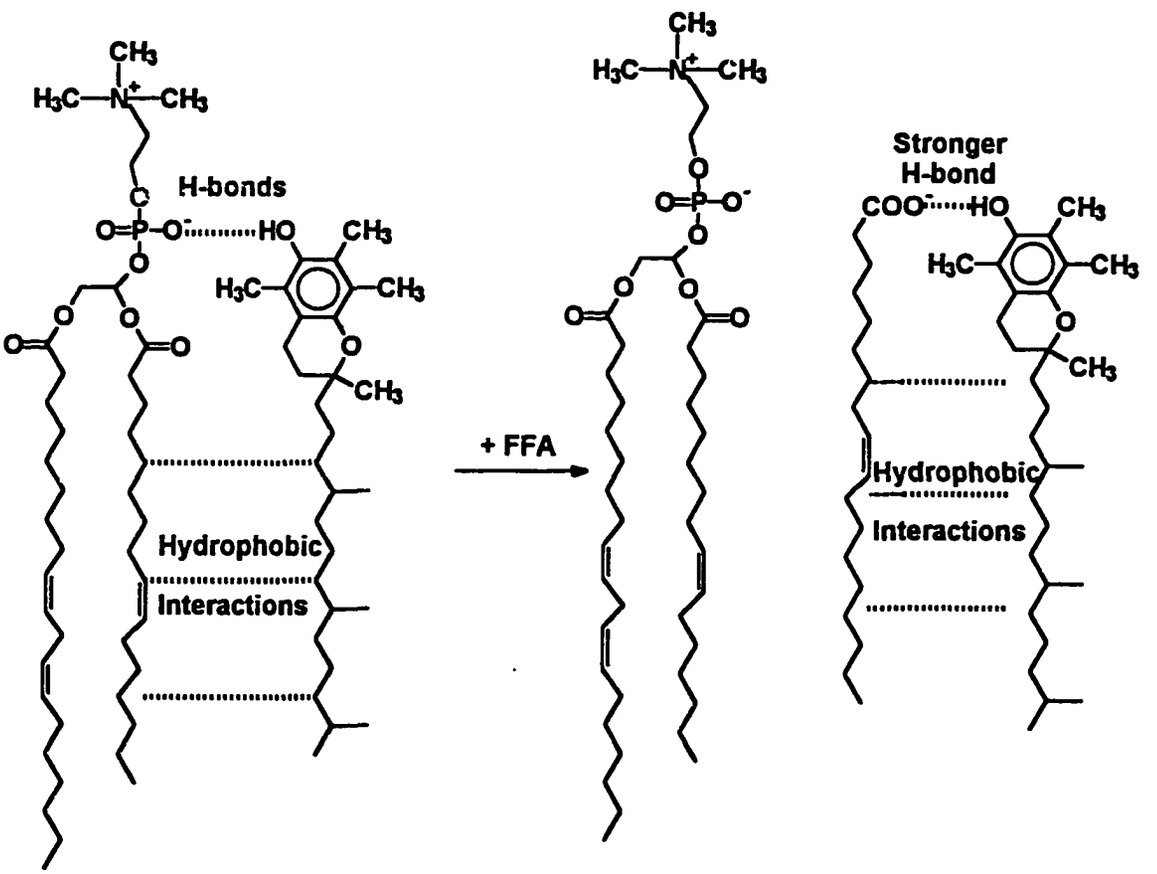

Figure 3.10. Disruption of both hydrophobic interactions and hydrogen bonding between α-T and lipid by free fatty acid.

decrease in ΔH in the presence of α-T, suggesting α-T might cause the liposome to be more stable or less fluid. This had been previously observed by Suzuki and coworkers when they measured molecular motion of a spin label in liposomes. [131]. They showed that the addition of α-T elicited less molecular motion of a spin label, thus showing the liposome containing α-T was more ordered.

Stearic acid, however, produced an increase in ΔH for the liposome's gel to liquid crystal transition, suggesting it produces more fluidity in the membrane. Mabrey and Sturtevant, on the other hand, showed by DSC that addition of saturated fatty acids to the membrane model increased order. [120] They argued that the introduction of the FFA into the bilayer decreases crowding in the polar head groups by increasing the distance between them. This, in turn, increases stability or order in the membrane. The difference between their data and the data presented in this paper is that they used a 2:1 lipid to FFA mole ratio and the mole ratio here was at least a 65:1 molar ratio. At the concentrations they used, the stearic acid - fatty acyl van der Waals attractions become more important than the fatty acyl - fatty acyl attractions. In the case of the data presented here, the stearic acid served merely as an impurity that produced less order in the membrane. Results similar to those shown here were also reported by Schaeffer and Zadunaisky when they measured diffusion of immunofluorescently-labeled proteins in plasma membranes treated with low

concentration of fatty acids. [73] They observed greater greater diffusion of the labeled protein in the presence of FFA, and thus, less order.

The results presented in this research indicate that there is an increase in the fluidity of the membrane model when FFA are present. The increase in AE for α-T in the presence of FFA may therefore be due to an increase in fluidity in the liposome. It is possible that in ULVs containing α-T, there are strong intermolecular forces, as mentioned earlier, that produce tighter packing in the liposome, and thus, less fluidity and more order (Figure 3.10). When the FFA are introduced, there are stronger interactions between the FFA and α-T than between α-T and the phospholipid. This disrupts the packing of the phospholipid and results in less order or more fluidity in the membrane. It is therefore possible that there is an increase in the diffusion of α-T through the more fluid membrane when FFA are present. A more mobile α-T may be thus more effective at trapping free radicals in damaged tissue than in normal tissue *in vivo*.

This paper shows that the choice of membrane model used to evaluate the effectiveness of an antioxidant is highly important. While biomembranes contain many components such as proteins that make interpretation of various aspects of lipid peroxidation difficult, membrane models provide a simple and uncomplicated picture of the chemistry within lipid membranes. The data clearly show that the effectiveness of α-tocopherol decreases dramatically as the membrane models become more rigid and, hence, more biologically relevant. The effectiveness of α-tocopherol *in vivo* may also be questionable, especially at

higher concentrations, where prooxidation may take place. The data do suggest that α-T may be more effective in damaged tissue, where FFAs are present.

3.4. EXPERIMENTAL

3.4.1. Materials.

Linoleic acid (cis,cis-9, 12, octadecadienoic acid), Oleic acid (*cis*-9-octadecenoic acid), diethylenetriaminepenta-acetic acid (DTPA), L-α-phosphatidylcholine from frozen egg yolk (egg PC), type V-E and I-α-phosphatidylcholine from soybean (soy PC), type IiI-S were obtained from Sigma Chemical Co. A crude source of soy phosphatidylcholine was obtained commercially in the form of L-α-lecithin capsules and was purified by flash column chromatography using silica gel (Chapter 2, section 2.4.1.1.). Granular 2,2' azobis-2-amidinopropane (ABAP), type V-50, was obtained from Wako Pure Chemical Industries, Ltd. D,L-α-tocopherol was obtained from Hoffman-La Roche, Inc. TEMPOL (4-hydroxy-2,2,6,6-tetramethyl-piperidinyl-1-oxy) was a gift from Exxon Chemicals (8320 Stedman, Houston, TX). Potassium tris(oxalato)chromate(III) trihydrate was prepared as described by Bergmann, et al. [115] Dioleoyl phosphatidylcholine (1,2-dioleoyl-*sn*-glycero-3-phosphocholine) was purchased from Avanti Polar Lipids (Alabaster, AL). These and all other incidental chemicals and solvents were of high purity and were used as received.

3.4.2. Methods.

3.4.2.1. Determination of 50% inhibition concentration of α-tocopherol for SDS micelles using ABAP initiation.

A 15 mM solution of sodium dodecyl sulfate (SDS) was prepared in 50 mM sodium phosphate buffer (pH 7.4). To 3 mL of this solution, linoleic acid, DTPA, and ABAP were added, so that their final concentrations were 46.7 mM, 88.3 μM, and 20 mM, respectively. The decrease in oxygen concentration was followed using a Clark-type oxygen electrode. Plots of oxygen concentration as a function of time were constructed using computer software interfaced to the oxygen electrode *via* a 12 bit A/D converter. Increasing amounts of α-tocopherol in ethanol were added a few μL at a time. After each addition, the decrease in oxygen concentration was measured over time.

3.4.2.2. Measurement of the inhibition of oxidation in MLVs and ULVs.

Multilamellar and unilamellar vesicles were prepared by first evaporating under vacuum a 20 mg/mL purified soy phosphatidylcholine (PC) solution in chloroform and containing varying amounts of α-tocopherol. The PC was resuspended in 50 mM phosphate buffer, pH 7.4, so that its final concentration was again 20 mg/mL. MLVs and ULVs were then formed using the methods described for each in chapter 2, section 2.4.2.1. To 2.7 mL of either MLVs or ULVs in buffer, 10 μL of a 25 mM solution of DTPA in water and 120 μL of a 0.5 M solution of ABAP in water were added, so that the final concentrations were

88.3 μM DTPA and 21.2 mM ABAP. After equilibration, oxygen concentration was monitored as described previously.

3.4.2.3. Measurement of the effect of free fatty acid on inhibition by α-tocopherol.

A stock solution of soy PC in chloroform containing varying amounts of α-tocopherol was evaporated to a film under vacuum. To demonstrate the effect of free fatty acids on antioxidant efficiency, this mixture for rotor evaporation also included oleic acid for some experiments. The mixture was resuspended in 3 mL of 50 mM high ionic strength phosphate buffer (containing 100 μM DTPA), pH 7.4, so that the final concentrations were 5 mg/mL PC, 0-200 μM α-tocopherol, and 100 μM oleic acid in some samples. Ionic strength buffer is often used to prevent liposome aggregation in solution. [55] Though high ionic strength phosphate buffer was used in this experiment, rates of oxidation in normal phosphate buffer were shown to be very similar. ULVs were then prepared using the method described in chapter 2, section 2.4.2.1. A 2.7 mL aliquot of the resulting ULV solution was placed in the oxygen electrode cell, and 75 μL of a 0.5 M ABAP solution in water was added, so that its final concentration was 13.5 mM in the phosphate buffer. The rate of decrease in oxygen concentration was measured by oxygen electrode method. Plots of percent inhibition of the rate of oxidation versus concentration of α-tocopherol were constructed for data obtained with and without added oleic acid.

3.4.2.4. Measurement of the entrapped volume in ULVs.

Entrapped volumes of the liposomes were determined according to the method described by Vistnes and Puskin.[116] Liposomes containing the membrane-permeable spin label TEMPOL[132] and with and without added FFA were extruded as described previously. Tris(oxalato)chromate(III), a relatively impermeable paramagnetic ion,[132] was then added in increasing concentrations as a spin label broadening agent. Because the solvent in these samples was water, special steps were taken in the aquisition of ESR spectra. Water is known to absorb microwave energy very strongly. [133] As a result, the added energy causes a large decrease in relaxation time and the signal is quenched. [133] To reduce signal quenching due to water, each sample was placed in a capillary tube under vacuum, and the capillary tube, inside an ESR tube. The ESR spectrum for the spin label was obtained using an X-band Micro-Now Instrument Co. 8300A ESR spectrometer with a center field of 341 mT. Spectral parameters included a 5G modulation amplitude, a 100 G field width, a 100 s scan time, and a 0.1 s time constant. ESR spectra were then obtained for each of the samples. Signal intensity was determined by measuring peak heights using computer software. Percent intensity was calculated for each sample by dividing the signal intensity for each sample containing chromium oxalate by the intensity of the control sample containing no added chromium oxalate (eq 3.8). The percent intensity of the signals were plotted versus the mole ratio of Cr(III) to moles of

$$\%\text{Intensity} = \frac{\text{Int}_{(\text{Tempol+CrIII})}}{\text{Int}_{(\text{Tempol})}} \times 100 \qquad (3.8)$$

TEMPOL. Note that the liposomes were prepared in 50 mM Tris buffer, pH 7.4. Though deionized water may be used, phosphate buffer may not, since it appears to coordinates to the chromium oxalate and prevents its action as a spin broadening agent. Also, NaCl was added to each sample in a manner to maintain ionic strength throughout. Maintaining ionic strength is important in preventing liposome aggregation. [55]

3.4.2.5. Measurement of T_m using Differential Scanning Calorimetry.

Chloroform solutions of soy PC (purified as described in chapter 2, section 2.4.1.1) containing varying amounts of stearic acid and α-T were evaporated to a film using rotory evaporation. The samples were redissolved in 0.5 mL 50 mM Tris buffer, pH 7.4, such that the final concentration of PC was 20 mg/mL. Samples were then either sonicated to produce MLVs or extruded to produce ULVs (both prepared as described in chapter 2, section 2.4.2.1). Samples for DSC were placed in aluminum hermetic pans and DSC data were obtained using a Seiko DSC 220C calorimeter, operating at a scan rate of 1°C/min.

CHAPTER 4: EVALUATION AND pH DEPENDENCE OF INHIBITION BY THE 21-AMINOSTEROID U74006

4.1. INTRODUCTION

The goal of this research was to compare the antioxidant efficiency of U74006 with that of α-tocopherol in systems of noniron-dependent lipid peroxidation in ULV phosphatidylcholine liposomes. Furthermore, we compared the antioxidant efficiency of U74006 and a similar 21-aminosteroid, U74389 (Figure 4.1), with that of the amine functionality alone, designated here as MAC-acetamide.

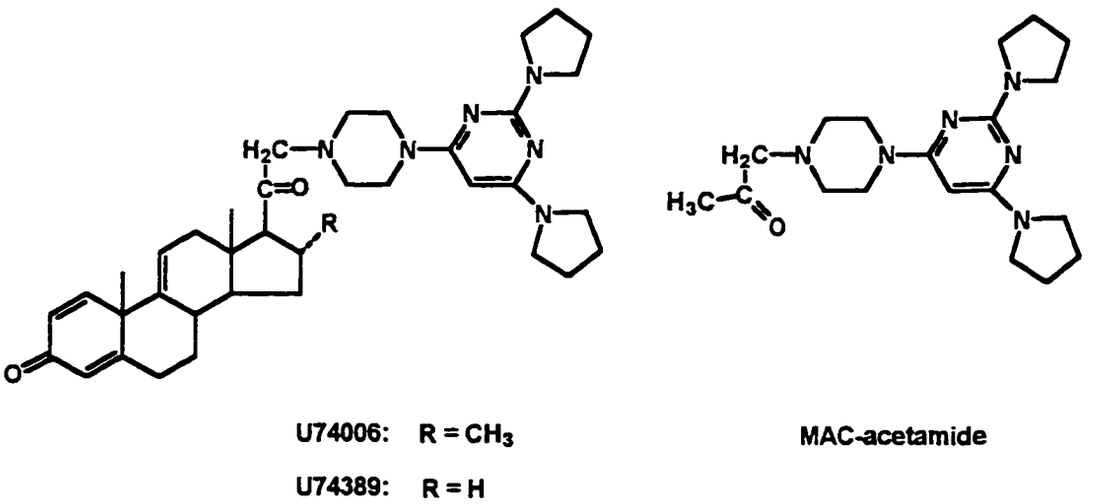

Figure 4.1. Structures for 21-aminosteroids used in this study.

Finally, we studied the pH dependence of the antioxidant efficiency of U74006. This aspect becomes increasingly important in damaged tissue, where the pH is known to be fairly acidic. [25] We find that the antioxidant is greatly affected by pH and is much less efficient below pH 7.

4.2. RESULTS

4.2.1. Comparison of the inhibitions of the 21-aminosteroids with α-tocopherol in ULVs.

Inhibition of oxidation in ULVs by MAC-acetamide, U74006, and U74389 are compared in Figure 4.2 (with the raw data and their error analysis in the appendixes, Table A.8). Percent inhibition here represents the decrease in the rate of oxidation (in the presence of antioxidant) divided by the uninhibited rate of oxidation (with no antioxidant present). All three antioxidants, U74006, U74389, and MAC-acetamide, inhibited oxidation. None of the 21-aminosteroids tested, however, demonstrated anything close to 100% inhibition. Maximum inhibition was approximately 75% for U74389, 60% for U74006. and 55% for the MAC - acetamide.

In order to compare inhibition by α - tocopherol with that by the 21-aminosteroids, 50% inhibition concentrations were calculated. The 50% inhibition concentration represents the concentration of antioxidant required to produce a 50% decrease in the rate of uninhibited oxidation. Thus, a smaller 50% inhibition concentration corresponds to a more effective antioxidant. For a more detailed discussion of 50% inhibition concentrations and their implications, see chapter 3, section 3.1. As shown in Table 4.1, the 50% inhibition concentration for α-tocopherol, 39 μM, was less than any of the other antioxidants studied. The 50% inhibition concentration measured for U74389 and U74006 were 104 and 205 μM, respectively. These values were greater than that of α-tocopherol by a factor of 2 - 3. Finally, the 50% inhibition

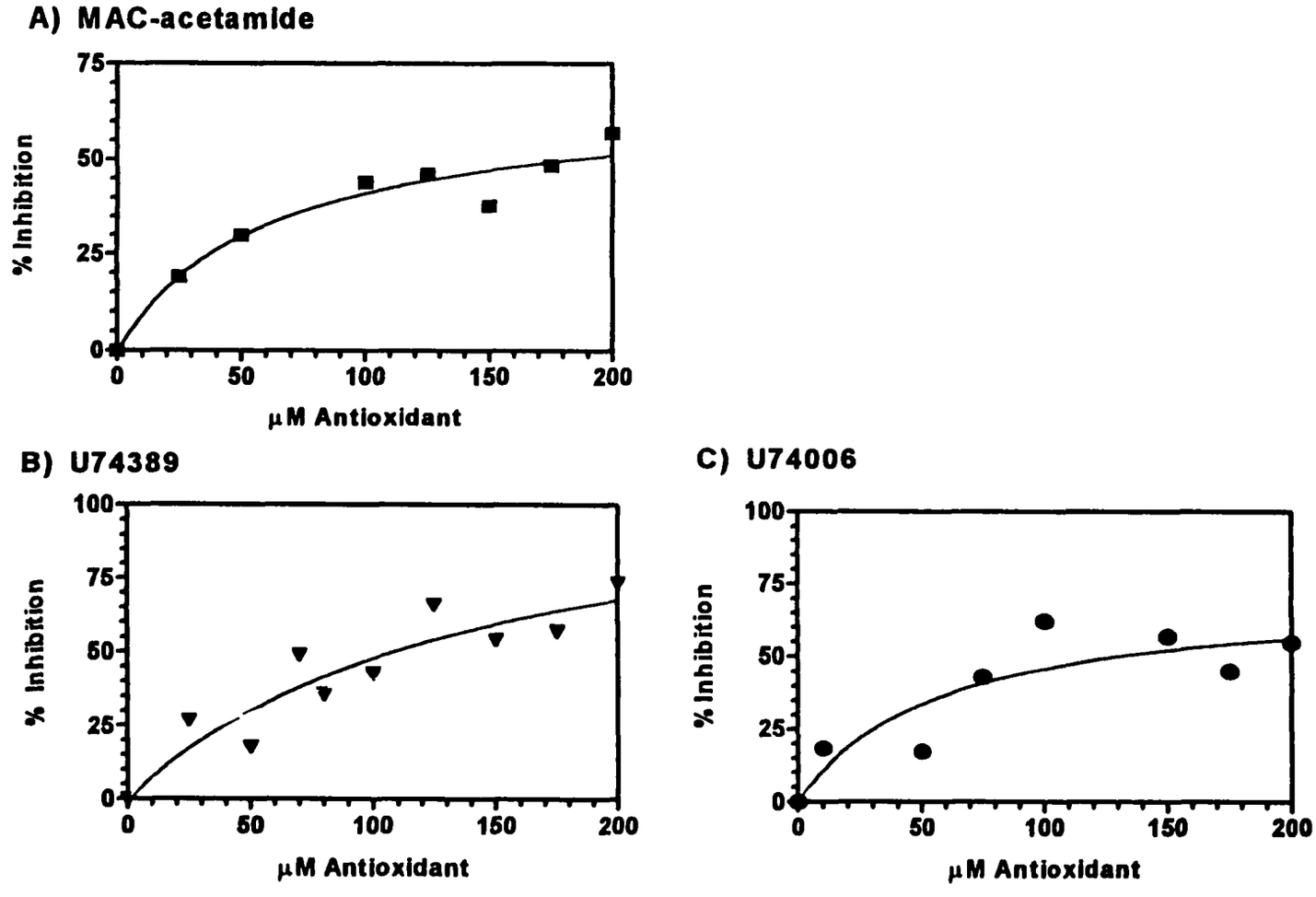

Figure 4.2. Comparison of percent inhibition measurements for A) MAC-acetamide B) U74389, and C) U74006. Systems contained 21.2 mM ABAP and 88.3 μM DTPA in 20 mg/mL ULV soy PC. Rates of oxidation were measured by oxygen consumption method using an oxygen electrode.

concentration calculated for MAC-acetamide was 206 μM, greater than that of α-tocopherol by a factor of 5. In this liposome system, α-tocopherol was thus a much more effective antioxidant than either of the 21-aminosteroids or MAC-acetamide.

Table 4. 1. Comparison of Inhibition by 21-Aminosteroids and α-Tocopherol in ULV Liposomes.

Antioxidant	50% Inhibition Concentration (μM)
MAC-acetamide	206 ± 38
U74389	104 ± 7
U74006	205 ± 81
α-Tocopherol	36 ± 5

Inhibition was measured in 20 mg/mL ULV soy PC in 50 mM phosphate buffer, pH 7.4, and containing 21.2 mM ABAP and 88.3μM DTPA.

4.2.2. Effect of pH on inhibition by U74006.

As shown in Figure 4.3, the antioxidant effectiveness of U74006 decreased dramatically when the pH changed from 7.0 to 6.5. In particular, the 50% inhibition concentration increased from 100μM at pH 7.0 to 200μM at pH 6.5.

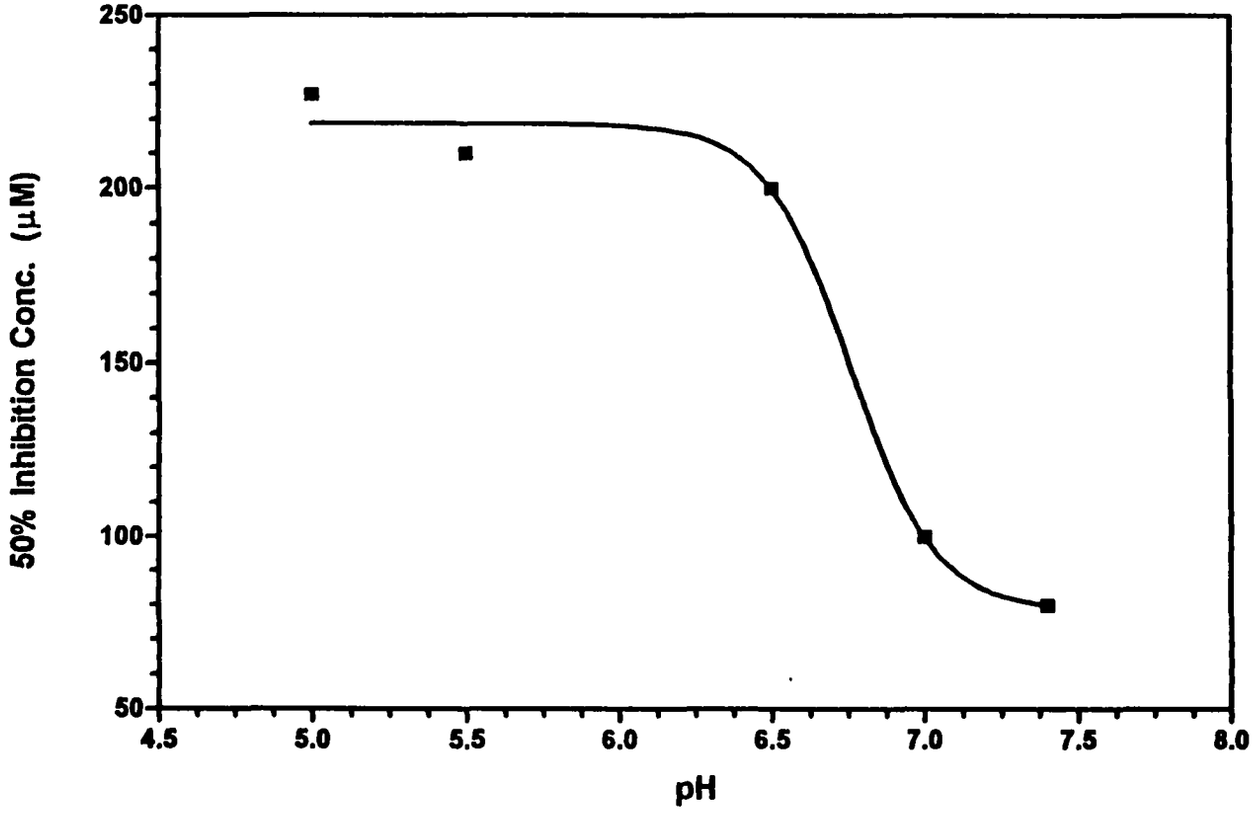

Figure 4.3. Effect of pH on inhibition by U74006 in 20 mg/mL ULV soy PC liposomes. The system also contained 21.2 mM ABAP and 88.3 μM DTPA in 50 mM phosphate buffer of varying pH. The rate of oxygen consumption was followed by oxygen electrode method.

This means that the antioxidant was only half as effective at pH 6.5 as compared to pH 7.0.

4.3. DISCUSSION

Results presented here show that U74389 and U74006 exhibit about the same antioxidant effectiveness in ABAP-initiated ULV liposomes. This is shown in Figure 4.2 and Table 4.1. Furthermore, U74389 demonstrated the same or perhaps a greater antioxidant effectiveness than MAC-acetamide. If indeed the 21-aminosteroids are better antioxidants than MAC-acetamide, this could be due to the added benefit of the steroid functionality on the U74389. Steroids such as cholesterol have been shown to be membrane stabilizers, in that they bring about more order in the membrane. [134,135] Creating a more rigid bilayer may decrease the number of free radicals capable of diffusing through to the hydrophobic region of the membrane to initiate lipid oxidation. A second explanation could be that addition of the steroid affords the antioxidant more favorable partitioning into the hydrophobic lipid bilayer where lipid peroxyl radicals reside.

In comparison to α-tocopherol, U74006 and U74389 are not as effective in inhibiting oxidation. In ULV liposomes, α-tocopherol proved to be more effective than MAC-acetamide and the 21-aminosteroids by factors of 3-5. Neither the 21-aminosteroids nor MAC-acetamide, however, was ever completely effective in

the liposomes, in that percent inhibition never reached 100% in either case. This means that the antioxidants do not shut down autoxidation in this liposomal membrane model.

Finally, the efficiency of U74006 appears to have associated with it a very large pH dependence. In fact, the antioxidant efficiency of U74006 decreases by half between pH 6.5 and pH 7.0. This means that in oxidatively damaged tissues where the pH is shown to be somewhat acidic, [25] U74006 may be even less effective at terminating lipid peroxyl radicals.

This research thus indicates that while U74006 and U74389 do exhibit antioxidant activity, they are not as effective as α-tocopherol in the liposome model. Furthermore, in oxidatively damaged tissue *in vivo* where the pH is reduced, the 21-aminosteroids might actually be very inefficient antioxidants. It is possible that the observed decrease in antioxidant effectiveness at lower pH is due to a change in the geometry of the molecule when the antioxidant becomes protonated. The protonated molecule may assume a geometry that decreases its ability to insert into the membrane to both trap free radicals and to increase membrane stability.

Though the 21-aminosteroids were shown here to be somewhat ineffective, they have been shown to be effective clinically. It is therefore possible that they inhibit lipid peroxidation by some other non-chemical mechanism.

4.4. EXPERIMENTAL

4.4.1. Materials:

Soy phosphatidylcholine was purified from lecithin tablets using flash-column chromatography (described in Chapter 2, section 2.4.1.1). MAC-acetamide, or U98982 (4-(2,6-di-1-pyrrolidinyl-4-pyrimidinyl)-1-piperazinyl acetate), and the 21-aminosteroids U74389 (21-[4-(2,6-di-1-pyrrolidinyl-4-pyrimidinyl)-1-piperazinyl]-pregna-1,4,9(11)triene-3,20-dione) and U74006 (21-[4-(2,6-di-1-pyrrolidinyl-2-pyrimidinyl)-1-piperazinyl]-16.alpha.)-pregna-1,4,9(11)-triene-3,20-dione) were gifts from Pharmacia Upjohn, Inc. Note that U74389 and U74006 were the organic soluble versions of U74389G and U74006F and were used here for experimental convenience. Diethylenetriamine penta-acetic acid (DTPA) was purchased from Sigma Chemical Co. Granular 2,2' azobis-2-amidinopropane (ABAP), type V-50, was obtained from Wako Pure Chemical Industries, Ltd. These and all other incidental chemicals used were of high purity and were used as obtained.

4.4.2. Methods:

4.4.2.1. Measurement of the inhibition by U74389, U74006, and MAC - acetamide in ULV soy PC liposomes.

ULVs containing varying concentrations of U74006, U74389, or MAC-acetamide were prepared by first rotory evaporating together a solution of soy PC in chloroform and various amounts of a chloroform stock solution of the antioxidant to be studied. A 20 mg/mL soy PC solution was then formed by

redissolving the lipid in the appropriate amount of 50 mM phosphate buffer, pH 7.4. ULVs were then prepared using the method described in chapter 2, section 2.4.2.1. Diethylenetriamine penta-acetic acid (DTPA), an iron chelator, and 2,2'-azobis-2-amidinopropane (ABAP), an azo initiator, were then added so that the final solution contained 88.3 μM DTPA and 22 mM ABAP. The rate of oxidation was followed by measuring the decrease in oxygen concentration *versus* time using a Clark-type oxygen electrode interfaced *via* a 12 bit A/D converter to computer software.

4.4.2.2. Evaluation of the effect of pH on inhibition by U74006.

The effect of pH was determined in samples of 20 mg/mL ULV soy PC liposomes containing U74006, prepared as described in chapter 2, section 2.4.2.1. To evaluate the AE of the 21-aminosteroids as a function of pH, the samples were extruded in 50 mM phosphate buffer of varying pH. Oxidation was initiated using ABAP and its rate was followed by oxygen electrode method.

CHAPTER 5: CONCLUSIONS

Important to the study of lipid peroxidation is the use of membrane models. Simple and uncomplicated, biologically realistic membrane models allow for a quick and easy elucidation of many aspects of both lipid peroxidation and its inhibition. [98] The primary goal of this research was to explore lipid peroxidation and its inhibition in membrane models. To accomplish this objective, three sets of experiments were performed. First of all, the kinetics of lipid peroxidation in two liposome models, unilamellar vesicles (ULVs) and multilamellar vesicles (MLVs), were studied. The results of these experiments were presented in chapter 2. Secondly, the inhibition of lipid peroxidation by α-tocopherol in MLVs and ULVs was investigated. Furthermore, the effects of membrane structure and free fatty acids on this inhibition were explored. The discussion of these experiments was covered in chapter 3. Finally, the inhibition of lipid peroxidation in liposomes by a group of synthetic antioxidants called 21-aminosteroids as compared to inhibition by α-tocopherol was presented in chapter 4.

5.1. Kinetics of lipid peroxidation in membrane models.

Data resulting from this research as well as that found in the literature show that the kinetics of homogeneous solution and of micelles may not be the same as those of the more biologically realistic membrane models studied here - liposomes (Table 5.1).[58,63-65] . It was observed that the kinetics of autoxidation were different in the large ULVs and in the MLVs studied here.

Table 5.1. Comparison of orders obtained for measuring the kinetics of lipid peroxidation in membrane models.

Membrane Model	[ABAP]	[LH]	$[O_2]$
Homogeneous	0.50[a]	1.00	0[b]
SDS micelles	0.50[a]	1.00	0[b]
MLVs	1.37 ± 0.10	0.76 ± 0.10	0.09 ± 0.05
ULVs	1.35 ± 0.18	0.17 ± 0.10	0.05 ± 0.01

a. Data reported by Pryor, et al. [58] b. As reported by Burton, Ingold, and others.[136]

One explanation for the kinetic differences between all of the model systems compared here may be the differences in O_2 concentrations in the membrane models. While autoxidation was shown to be virtually independent of $[O_2]$ in solution and in micelles, Barclay and Ingold noticed that the rate law for autoxidation in liposomes is slightly affected by the oxygen partial pressure. [100] They argue that as the oxygen partial pressure decreases, chain transfer may begin to occur by a cross termination mechanism (eq 5.2), as opposed to termination by coupling of two lipid peroxyl radicals (eq 5.1).

$$2LOO\cdot \longrightarrow \text{non-radical products} \qquad (5.1)$$

$$LOO\cdot + L\cdot \longrightarrow \text{non-radical products} \qquad (5.2)$$

Cross terminations such as that in eq 5.2 in addition to the reaction in eq 5.3 might become increasingly important in oxygen-deprived membranes, where the ratio of $L^{\cdot}$ to $LOO^{\cdot}$ increases. [100] There may likewise be a dependence of

autoxidation on [O_2] in the membrane models studied here (Table 5.1). Statistically, the orders in O_2 in both MLVs and ULVs are different from zero.

$$2L\cdot \longrightarrow \text{non-radical products} \qquad (5.3)$$

While Barclay's group observed classical kinetics in their membrane models of small ULVs and MLVs, they did note that ULVs were more susceptible to oxidation than MLVs. [102] They rationalized this based on lipid chain packing in the two models. They argue that the higher oxidative susceptibility of ULVs is due to higher local concentrations of oxidizable methylene groups. This would then result in higher rates of propagation.

The large order with respect to R_i observed in both MLVs and ULVs (Table 5.1) could be due to induced decomposition. [137] With the occurrence of induced decomposition the order in R_i has been shown to be greater than $^3/_2$. [137]

Induced decomposition is a bimolecular process in which free radicals attack a non-radical compound and cause it to decompose. [137] One plausible mechanism for induced decomposition in the MLVs and ULVs studied here is given in eq 5.4. In this mechanism, $LOO^{\cdot}$ attacks the peroxidic (O-O) bond of the non-radical LOOH. It is possible that as lipid chains become more restricted, the probability of a lipid peroxyl radical encountering another of its kind for termination is much smaller.

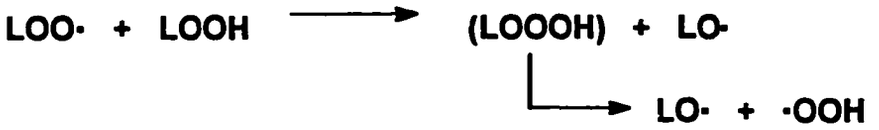

Overall:

(5.1)

Overall, ULVs appear to be more kinetically different from the classical rate law than MLVs. This may be because MLVs are more fluid and ULVs, more rigid. It is thus reasonable to assume that ULVs are both the most biologically and kinetically realistic membrane models of the model systems compared here.

5.2. Inhibition of lipid peroxidation by α-tocopherol.

Fortunately, the body possesses several natural antioxidants to prevent against oxidative damage. [7] These include α-tocopherol (Vitamin E), β-carotene, ascorbic acid, and enzymes such as superoxide dismutase and catalase, to name a few. [7] Recently, a pharmaceutical movement toward developing synthetic antioxidant drugs has emerged. [7,22,86,91] The use of realistic membrane models is important to the study of antioxidants, as they provide a route to simple and fast comparisons of the effectiveness of antioxidants. The results presented in this dissertation suggest that the choice of membrane model is critical, as the kinetics of inhibition in each may be quite different. In this set of experiments, the antioxidant efficiency of α-T was therefore determined for

oxidation in SDS micelles, MLVs and ULVs. These efficiencies were compared with others reported in the literature for the same or different systems.

The antioxidant efficiency of α-T was measured here by comparing 50% inhibition concentrations. This value was used for comparison because it can be calculated without first determining the rate equation for inhibited oxidation. There was a dramatic decrease in the antioxidant efficiency of α-T from micelles to liposomes. [58,62,66,67] Comparing these results with others in literature, antioxidant efficiency decreases from homogeneous solution to micelles, and from micelles to microsomes and liposomes. [58,62,66,68] Perhaps as the model becomes more rigid, it becomes increasingly difficult for α-T to encounter and trap peroxyl radicals.

Oxidation data show that α-T is more efficient in MLVs than in ULVs. DSC data suggest that MLVs may be more fluid than ULVs. MLVs should thus allow α-T to diffuse more readily. An interesting result observed from DSC data was the decrease in the fluidity of ULVs in the presence of α-T. This may be evidence that in liposome models α-T is more restricted and less efficient at encountering and trapping free radicals than it is in homogeneous solution.

The inhibition data for α-tocopherol do suggest that α-T may not be very efficient in real tissues. In liposomes, especially in ULVs, α-T was only completely efficient at concentrations greater than that that exists is real tissues. It is difficult to predict what the efficiency of α-T may be in real tissues, though, since real membranes contains a large amount of protein, and these proteins have been shown to participate in autoxidation. [138]

Interestingly, at high concentrations of α-T, antioxidant efficiency decreased substantially. This was also observed by several other groups for both α-T and Trolox. [128,129,139-141] Bowry and Ingold have reasoned that this is probably due to chain propagation *via* the tocopheroxyl (phenoxyl) radical. [139,140,142] They further argue, perhaps incorrectly, that at high concentrations, the persistent tocopheroxyl (phenoxyl) radical located in lipophilic region rarely encounters free radicals ($LOO^{\bullet}$) residing in aqueous solution. This assumption is probably based on the "Floating" Peroxyl Radical Hypothesis. [101,143] It has been theorized that once formed, the peroxyl radical, shown to have a very high dielectric constant, "floats" toward the aqueous layer to hydrogen bond with water. [101,143] The phenoxyl radical generated from α-T then instead terminates by abstracting a hydrogen atom from a molecule of lipid in close proximity to produce a chain-propagating lipid alkyl radical. [139] The problem with the "Floating" Peroxyl Radical Hypothesis is that it suggests a decrease in order or increase in fluidity during autoxidation. Moderate levels of lipid peroxidation, however, were shown to increase order and decrease membrane permeability and fluidity in microsomes. [144]

Perhaps a better explanation comes from analysis of oxidation products for α-T, reported by Leibler, et al. [48] Leibler observed an α-T oxidation product that could be the result of a prooxidation reaction (Figure 5.3). In this mechanism the phenoxyl radical produced by H-atom abstraction by $LOO^{\bullet}$, now of high concentration, reacts with $LOO^{\bullet}$ to form an epoxy alkyl radical and $LO^{\bullet}$ by β-

scission (Figure 5.3). The epoxy alkyl radical then reacts with O_2 to produce a peroxyl radical. This α-tocopherol-derived peroxyl radical can then abstract a H-atom from another molecule of lipid to terminate itself and produce a chain propagating lipid alkyl radical. This is an important consequence, because in this case α-T has terminated only one $LOO^{\cdot}$ and has generated one $LO^{\cdot}$ and one $L^{\cdot}$.

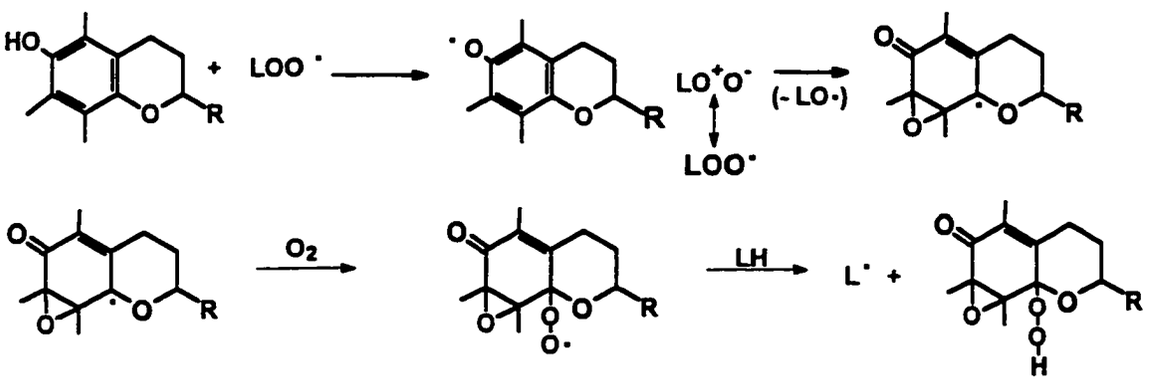

Figure 5.3. Oxidation products of α-T that may suggest mechanism for prooxidation.

It was observed that α-T was highly effective at low concentrations in the presence of free fatty acids. This could infer that α-T may be more effective in damaged tissue, where FFA have been shown to be released. [70,94] This increase in antioxidant efficiency may be due to an increase in fluidity in the membrane when FFA are present. A similar increase in fluidity in the membrane in the presence of FFA was observed by.Schaeffer and Zadunaisky, measuring diffusion of immunofluorescently-labeled proteins in plasma membranes. [73] This

suggests that lipid packing is smaller in the presence of FFA. DSC data presented here likewise show that FFAs produce more fluidity in the liposome. A more fluid lipid bilayer may allow for greater diffusion of α-T through the membrane to terminate lipid peroxyl radicals.

5.3. Inhibition of oxidation by 21-aminosteroids.

The recent trend toward developing synthetic antioxidant drugs seems promising. [7] Pharmacia & Upjohn, Inc., have developed an antioxidant, the 21-aminosteroid U74006, it hopes will prove effective against CNS trauma and prevent tissue damage following stroke. [145]

Antioxidant efficiencies of α-T, U74006, U74389, and MAC-acetamide,the acetylated pyrimidine with no attached steroid, were compared in ULVs. It was observed that none of the 21-aminosteroids studied were as effective as α-T. In addition, none of the 21-aminosteroids studied were completely efficient, in that percent inhibition never reached 100%. Of the 21-aminosteroids, U74389 was more effective than either U74006 or MAC-acetamide by a factor of 2.

The antioxidant efficiency of U74006 was shown here to decrease by half from pH 7.0 to pH 6.5. This could be due to a change in geometry in the molecule after protonation. The protonated molecule may assume a "bent" orientation that penetrates the liposome only minimally. It is thus possible that U74006 may be ineffective in already damaged tissues, which are typically of lower pH. [25] This finding, in conjunction with its low efficiency in comparison to α-

T, leave doubt as to the effectiveness of this drug as an antioxidant, effective by only a chemical mechanism. Since it has been shown effective *in vivo* in preventing reperfusion injury, [92,146] it is possible that it inhibits lipid peroxidation by some other mechanism. Perhaps it inhibits one of the biological processes involved in ischemia.

5.4. Summary.

This dissertation thus demonstrates that the choice of membrane model for evaluating lipid peroxidation is critical, as the kinetics of each are quite different. Comparing liposomes and other membrane models, it is shown here that α-T appears effective in homogeneous solution, micelles, and liposomes modeling damaged membranes. Its antioxidant efficiency, however, is much lower in liposome models for undamaged membranes. Finally, while the effort toward developing synthetic antioxidant CNS drugs is promising, more work may need to be done to find an antioxidant that is at least as effective as α-T and whose activity has little or no pH dependence.

BIBLIOGRAPHY

1. Lewis, G. N. *Chem. Rev.* **1924**, *1*, 243.

2. Weiss, J. *Trans. Faraday Soc.* **1935**, *31*, 966.

3. Sato, R.; Omura, T. *Cytochrome P450*; Academic Press: New York, 1978.

4. Klebanoff, S. J. *Ann. Intern. Med.* **1980**, *93*, 480.

5. Porter, N. N. Prostaglandin endoperoxides. In *Free Radicals in Biology;* Pryor, W. A. Ed.; Academic Press: New York, 1980; Vol. 4; p. 261.

6. Beauchamp, C.; Fridovich, I. *J. Biol. Chem.* **1970**, *255*, 1970.

7. Halliwell, B.; Gutteridge, J. M. C. *Free Radicals in Biology and Medicine*; Claredon Press: Oxford, 1985.

8. Farhataziz; Ross, A. B. *NSRDS-NBS* **1977**, *59*, 1.

9. Singh, A.; Singh, H. *Prog. Biophys. Mol. Biol.* **1982**, *39*, 69.

10. Halliwell, B. *Free Rad Res Commun* **1990**, *9*, 1.

11. Miquel, J.; Quintanilha, A. T.; Weber, H. *Handbook of Free Radicals and Antioxidants in Biomedicine*; Miquel, J.; Quintanilha, A. T.; Weber, H., Ed.; CRC Press: Boca Raton, Florida, 1989; Vol. I.

12. Sies, H. *Oxidative Stress, Oxidants and Antioxidants*; Sies, H., Ed.; Academic Press: New York and London, 1991.

13. Byers, T.; Perry, G. *Annu. Rev. Nutr.* **1992**, *12*, 139.

14. Hall, E. D.; Braughler, J. M. *Free Rad Biol Med* **1989**, *6*, 303.

15. Halliwell, B.; Gutteridge, J. M. C.; Cross, C. E. *J. Lab. Clin. Med.* **1992**, 598.

16. Wagner, B. A.; Buettner, G. R.; Burns, C. P. *Biochemistry* **1994**, *33*, 4449.

17. Higgs, G. A.; Moncada, S.; Vane, J. R. *Advanc. Inflam. Res.* **1979**, *1*, 413.

18. Samuelsson, B.; Hammarstrom, S.; Borgeat, P. *Advanc. Inflamm. Res.* **1979**, *1*, 405.

19. Morehouse, I. A.; Thomas, C. E.; Aust, S. D. *Arch. Biochem. Biophys.* **1984**, *232*, 366.

20. Babior, M. B. *N. Engl. J. Med.* **1978**, *298*, 659.

21. Pryor, W. A.; Stawley, J. P. *J. Org. Chem.* **1975**, *40*, 3615.

22. Braughler, J. M.; Hall, E. D. *Free Rad. Biol. Med.* **1989**, *6*, 289.

23. Marcy, V. R.; Welsh, F. A. *J. Cereb. Blood Flow Metab.* **1984**, *4*, 362.

24. Welsh, F. A. Acidosis and energy metabolism. In *Cerebral Ischemia;* Bes, A., Braquet, P., Paoletti, R. and Seisjo, B. K. Eds.; Elsevier: Amsterdam, 1984; p. 177.

25. Abiko, Y.; Sakai, K. *Eur. J. Pharmacol.* **1980**, *64*, 239.

26. Battelli, M. G.; Corte, E. D.; Stripe, F. *Biochem. J.* **1972**, *126*, 747.

27. McCord, J. M. *N. Engl. J. Med.* **1985**, *312*, 159.

28. McCord, J. M.; Fridovich, I. *J. Biol. Chem.* **1968**, *243*, 5753.

29. Snyder, S. *Cell* **1992**, 705.

30. Galla, H. *Angew. Chem. Int. Ed. Engl.* **1993**, *32*, 378.

31. Padmaja, S.; Huie, R. E. *Free Radical Res. Commun.* **1993**, *18*, 195.

32. Ischiropoulos, H.; Zhu, L.; Beckman, J. S. *Arch. Biochem. Biophys.* **1992**, *298*, 446.

33. Beckman, J. S.; Beckman, T. W.; Chen, J.; Marshall, P. A.; Freeman, B. A. *Proc. Natl. Acad. Sci. USA* **1990**, *87*, 1620.

34. Radi, R.; Beckman, J. S.; Bush, K. M.; Freeman, B. A. *Arch. Biochem. Biophys.* **1991**, *288*, 481.

35. Radi, R.; Beckman, J. S.; Bush, K. M.; Freeman, B. A. *J. Biol. Chem.* **1991**, *266*, 4244.

36. Moreno, J. J.; Pryor, W. A. *Chem. Res. Toxicol.* **1992**, *5*, 425.

37. Halfpenny, E.; Robinson, P. L. *J. Chem. Soc.* **1952**, 939.

38. Trifonow, I. *Z. Anorg. Chem.* **1922**, *124*, 136.

39. Burton, G. W.; Cheeseman, K. H.; Doba, T.; Ingold, K. U.; Slater, T. F. Vitamin E as an antioxidant *in vitro* and *in vivo*. In *Biology of Vitamin E*; Pittman Books: London, 1983; p. 4.

40. Fee, J. A. On the question of superoxide toxicity and the biological function of superoxide dismutases. In *Oxidases and related redox systems;* King, T. E., Mason, H. S. and Morrison, M. Eds.; Pergamon Press: New York, 1982; p. 101.

41. Singh, A. *Can. J. Physiol. Pharmacol.* **1982**, *30*, 1330.

42. Fleming, C. R.; Lie, J. T. *Gastroenterology* **1982**, *83*, 689.

43. Aisen, P.; Listowsky, I. Iron transport and storage proteins. In *Annual Review of Biochemistry;* Snell, E. E., Boyer, P. D., Meister, A. and Richardson, C. C. Eds.; Annual Reviews: Palo Alto, Calif, 1980; Vol. 49; p. 357.

44. Osaki, S.; Johnson, D. A.; Frieden, E. *J. Biol. Chem.* **1966**, *241*, 2746.

45. Diplock, A. T. Vitamin E. In *Fat-Soluble Vitamins, their Biochemistry and Applications;* Diplock, A. T. Ed.; Heineman: London, 1985; p. 154.

46. Leibovitz, B.; Hu, M.-L.; Tappel, A. L. *J. Nutrit.* **1990**, *120*, 97.

47. Sokol, R. J.; Devereaux, M.; Khandwala, R. A. *J. Lipid Res.* **1991**, *32*, 1349.

48. Liebler, D. C.; Baker, P. F.; Kaysen, K. L. *J. Am. Chem. Soc.* **1990**, *112*, 6995.

49. Aruoma, O. I.; Halliwell, B. *Free Radicals and Food Additives*; Aruoma, O. I.; Halliwell, B., Ed.; Taylor and Francis: London, 1991.

50. Halliwell, B. Ascorbic acid and the illuminated chloroplast. In *Ascorbic Acid: Chemistry, Metabolism, and Uses;* Tolbert, B. M. and Seib, P. A. Eds.; American Chemical Society: Washington, DC, 1982; p. 263.

51. Barclay, L. R. C.; Locke, S. J.; MacNeil, J. M. *Can J Chem* **1985**, *63*, 366.

52. Lippman, R. D. Free radical induced lipoperoxidation and aging. In *Handbook of Free Radicals and Antioxidant in Biomedicine;* Miquel, J., Quintanilha, A. T. and Weber, H. Eds.; CRC Press: Boca Raton, Florida, 1989; Vol. I; p. 187.

53. Jialal, I.; Norkus, E. P.; Cristol, L.; Grundy, S. M. *Biochim. Biophys. Acta* **1991**, *1086*, 134.

54. Samokyszyn, V. M.; Marnett, L. J. *Methods Enzymol.* **1990**, *190*, 281.

55. New, R. R. C. *Liposomes: a practical approach*; New, R. R. C., Ed.; Oxford University Press: NY, 1990.

56. Ingold, K. U. *Acc. Chem. Res.* **1969**, *2*, 1.

57. Pryor, W. A. Free Radicals in Molecular Biology, Aging, and Disease; Armstrong, D., Sohal, R. S., Cutler, R. G. and Slater, T. F. Eds.; Raven Press: New York, 1984; p. 13.

58. Pryor, W. A.; Strickland, T.; Church, D. F. *J. Am. Chem. Soc.* **1988**, *110*, 2224.

59. Pryor, W. A. Free Radicals in Autoxidation and in Aging. In *Free Radicals in Molecular Biology, Aging, and Disease;* Armstrong, D., Sohal, R. S., Cutler, R. G. and Slater, T. F. Eds.; Raven Press: New York, 1984; Vol. 27; p. 13.

60. Barclay, L. R. C.; Locke, S. J.; MacNeil, J. M. *Can J Chem* **1983**, *63*, 1288.

61. Barclay, L. R. C.; Baskin, K. A.; Locke, S. J.; Schaefer, J. D. *Can J Chem* **1987**, *65*, 2529.

62. Niki, E.; Saito, T.; Kawakami, A.; Kamiya, Y. *J. Biol. Chem.* **1984**, *259*, 4177.

63. Barclay, L. R. C.; Kong, D.; VanKessel, J. *Can J Chem* **1986**, *64*, 2103.

64. Burton, G. W.; Ingold, K. U. *J. Am. Chem. Soc.* **1981**, *103*, 6472.

65. Cosgrove, J. P.; Church, D. F.; Pryor, W. A. *Lipids* **1987**, *22*, 299.

66. Pryor, W. A.; Cornicelli, J. A.; Devall, L. J.; Tait, B.; Trivedi, B. K.; Witiak, D. T.; Wu, M. *J. Org. Chem.* **1993,** *58*(13), 3521.

67. Palozza, P.; Moualla, S.; Krinsky, N. *Free Rad. Biol. Med.* **1992**, *13*, 127.

68. Palozza, P.; Krinsky, N. *Free Rad. Biol. Med.* **1991**, *11*, 407.

69. Chan, P. H.; Yurko, M.; Fishman, R. A. *J. Neurochem.* **1982**, *38*, 525.

70. Marion, J.; Wolfe, L. S. *Biochim. Biophys. Acta* **1979**, *1979*, 25.

71. Billah, M. M.; Lapetina, E. G.; Cuatrecasas, R. *J. Biol. Chem.* **1981**, *256*, 5399.

72. Chan, P. H.; Fishman, R. A. *Brain Res.* **1982**, *248*, 151.

73. Schaeffer, B. E.; Zadunaisky, J. A. *Biochim. Biophys. Acta* **1979**, *556*, 131.

74. Cheah, A. M. *Biochim. Biophys. Acta* **1981**, *648*, 113.

75. Doberstein, C. E.; Hovda, D. A.; Becker, D. P. *Annals of Emergency Medicine* **1993**, *22*, 993.

76. Means, E. D.; Anderson, D. K. Pathophysiology of acute spinal cord injury. In *Handbook of the Spinal Cord;* Davidoff, R. A. Ed.; Marcel Dekker: New York, 1987; Vol. 4; p. 19.

77. Granger, D. N.; Hollwarth, M. E.; Parks, D. A. *Acta Physiol. Scand.* **1986**, *548*, 47.

78. Hartz, J. W.; Funakoshi, S.; Deutsch, H. F. *Clin. Chim. Acta* **1973**, *46*, 125.

79. Hall, E. D. *J. Neurosurg.* **1985**, *62*, 882.

80. Hall, E. D.; Braughler, J. M. *J. Neurosurg.* **1982**, *57*, 247.

81. Haynes, R. C.; Murad, F. *The Pharmacological Basis of Therapeutics*; 6th ed.; Macmillan: New York, 1980.

82. Braughler, J. M.; Chase, R. L.; Neff, G. L.; Yonkers, P. A.; Day, J. S.; Hall, E. D.; Sethy, V. H.; Lahti, R. A. *The Journal of Pharmacology and Experimental Therapeutics* **1988**, *244*, 423.

83. Ryan, T. P.; Petry, T. W. *Archives of Biochemistry and Biophysics* **1993**, *300*, 699.

84. Jacobsen, E. J.; McCall, J. M.; Runge, T. A. *J. Med. Chem.* **1990**, *33*, 1145.

85. Beinert, H. . In *Methods Enzymol;* Colowick, S. P. and Kaplan, N. O. Eds.; Academic Press: New York, 1978; Vol. 54; p. 435.

86. Braughler, J. M.; Burton, P. S.; Chase, R. L.; Pregenzer, J. F.; Jacobsen, E. J. *Biochem. Pharmacol.* **1988**, *37*, 3853.

87. Braughler, J. M.; Pregenzer, J. F.; Chase, R. L.; Duncan, L. A.; Jacobsen, E. J.; McCall, J. M. *J Biol Chem* **1987**, *262*, 10438.

88. Schade, A. L.; Oyama, J.; Reinhart, R. W.; Miller, J. R. *Proc. Soc. Exp. Biol. Med.* **1954**, *87*, 443.

89. Seeman, P. *Biochemical Pharmacology* **1966**, *15*, 1632.

90. Audus, K. L.; Guillot, F. L.; Braughler, J. M. *Free Rad. Biol. Med.* **1991**, *11*, 361.

91. Braughler, J. M.; Pregenzer, J. F. *Free Rad. Biol. Med.* **1989**, *7*, 125.

92. Hall, E. D.; Pazara, K. E.; Braughler, J. M. *Stroke* **1991**, *22*, 361.

93. Hall, E. *Annals of Emergency Medicine* **1993**, *22*, 1022.

94. Lunt, G. G.; Rowe, C. E. *Biochim. Biophys. Acta* **1968**, *152*, 681.

95. Bazan, N. G. *Biochim. Biophys. Acta* **1970**, *218*, 1.

96. Niki, E. *Methods Enzymol.* **1990**, *186*, 100.

97. Barclay, L. R. C.; Ingold, K. U. *JACS* **1980**, *102*, 7792.

98. Chatterjee, S. N.; Agarwal, S. *Free Rad. Biol. Med.* **1988**, *4*, 51.

99. Skoog, D. A.; West, D. M.; Holler, F. J. *Fundamentals of Analytical Chemistry*; Saunders College Publishing: New York, 1988.

100. Barclay, L. R. C.; Ingold, K. U. *J. Am. Chem. Soc.* **1981**, *103*, 6478.

101. Barclay, L. R. C. *Can. J. Chem.* **1993**, *71*, 1.

102. Barclay, L. R. C.; Baskin, K. A.; Kong, D.; Locke, S. J. *Can J Chem* **1987**, *65*, 2541.

103. Hamilton, R.; Goerke, J.; Guo, L. S. S.; Williams, M. C.; Havel, R. J. *J. Lipid Res.* **1980**, *21*, 981.

104. Hope, M. J.; Bally, M. B.; Webb, G.; Cullis, P. R. *Biochim. Biophys. Acta* **1985**, *812*, 55.

105. Lentz, B. R.; Barenholz, Y.; Thompson, T. E. *Biochemistry* **1976**, *15*, 4521.

106. Sheetz, M. P.; Chan, S. I. *Biochemistry* **1972**, *11*, 4573.

107. Spiker, R. C.; Levin, I. R. *Biochim. Biophys. Acta* **1976**, *455*, 560.

108. Suurkuusk, J.; Lentz, B. R.; Barenholz, Y.; Biltonen, R. L.; Thompson, T. E. *Biochemistry* **1976**, *15*, 1393.

109. Pryszczewska, M.; Lipiec, T. *Roczniki Chem.* **1955**, *29*, 985.

110. Tsyurupa, M. G.; Peshkova, V. M. *Vestn. Mosk. Univ., Ser. II, Khim.* **1964**, *19*, 60.

111. Crosland, S. *Diss. Abstr. Int. B.* **1989**, *49*, 5262.

112. Szoka, F.; Papahadjopoulos, D. Liposomes: Preparation and characterization. In *Liposomes: From physical structure to therapeutic applications;* Dingle, J. T. and Gordon, J. L. Eds.; Elsevier/North-Holland Biomedical Press: New York, 1981; Vol. 7; p. 51.

113. Chappell *Biochem. J.* **1964**, *90*, 225.

114. Keith, A. D.; Snipes, W. *Science* **1974**, *183*, 666.

115. Bergmann, S. P.; Nesbitt, D. M. *Biochim. Biophys. Acta* **1979**, *548*, 608.

116. Vistnes, A.; Puskin, J. S. *Biochim. Biophys. Acta* **1981**, *644*, 244.

117. Friebolin, H. *Basic One- and Two-Dimensional NMR Spectroscopy*; 2nd ed.; VCH Publishers: New York, 1993.

118. Likhtenshtein, G. I. *Spin labeling methods in molecular biology*; Wiley-Interscience: New York, 1976.

119. Knight, C. G. *Liposomes: From Physical Structure to Therapeutic Application*; Knight, C. G., Ed.; Elsevier/North-Holland: Amsterdam, 1981; Vol. 7.

120. Mabrey, S.; Sturtevant, J. M. *Biochim. Biophys. Acta* **1977**, *486*, 444.

121. Finegold, L.; Singer, M. A. *Chem. Phys. Lipids* **1991**, *58*, 169.

122. Mabrey-Gaud, S. Differential scanning calorimetry of liposomes. In *Liposomes: From Physical Structure to Therapeutic Applications;* Knight, C. G. Ed.; Elsevier/North-Holland Biomedical Press: New York, 1981.

123. Mitchell, G. V.; Grundel, E.; Jenkins, M.; Blakely, S. R. *J. Nutr.* **1990**, *120*, 1235.

124. Pacht, E. R.; Kaseki, H.; Mohammed, J. R.; Cornwell, D. G.; Davis, W. B. *J. Clin. Invest.* **1986**, *77*, 789.

125. Mitchell, G. V.; Jenkins, M. Y.; Grundel, E. *Ann. NY. Acad. Sci.* **1989**, *570*, 478.

126. Muller, D. P. R.; Sampson, M. A. G.-ì. *Ann. NY Acad. Sci.* **1989**, *570*, 146.

127. Knekt, P.; Seppanen, R.; Aaran, R. K. *Prev. Med.* **1988**, *17*, 725.

128. Cillard, J.; Cillard, P.; Cormier, M.; Girre, L. *J. Am. Oil Chem. Soc.* **1980**, 252.

129. Cillard, J.; Cillard, P.; Cormier, M. *J. Am. Oil Chem. Soc.* **1980**, 255.

130. Blume, A. *Biochim. Biophys. Acta* **1979**, *557*, 32.

131. Suzuki, Y. J.; Tsuchiya, M.; Wassall, S. R.; Choo, Y. M.; Govil, G.; Kagan, V. E.; Packer, L. *Biochemistry* **1993**, *32*, 10692.

132. Anzai, K.; Higashi, K.; Kirino, Y. *Biochim. Biophys. Acta* **1988**, *937*, 73.

133. Symons, M. *Chemical and Biochemical Aspects of Electron Spin Resonance Spectroscopy*; John Wiley & Sons, Inc: New York, 1978.

134. Ladbrooke, B. D.; Williams, R. M.; Chapman, D. *Biochim. Biophys. Acta* **1968**, *150*, 333.

135. Chapman, D.; Owens, N. F.; Walter, D. A. *Biochim. Biophys. Acta* **1966**, *120*, 148.

136. Burton, G. W.; Ingold, K. U. *Science* **1984**, *224*, 569.

137. Pryor, W. A. *Free Radicals*; McGraw-Hill: New York, 1966.

138. Stadtman, E. R. *Free Rad. Biol. Med.* **1990**, *9*, 315.

139. Bowry, V. W.; Ingold, K. U.; Stocker, R. *Biochem. J.* **1992**, *288*, 341.

140. Bowry, V. W.; Stocker, R. *J. Am. Chem. Soc.* **1993**, *115*, 6029.

141. Cao, G.; Cutler, R. G. *Arch of Gerontology and Geriatrics* **1993**, *17*, 189.

142. Ingold, K. U.; Bowry, V. W.; Stocker, R.; Walling, C. *Proc. Natl. Acad. Sci. USA* **1993**, *90*, 45.

143. Boyd, S. L.; Boyd, R. J.; Barclay, L. R. C. *J. Am. Chem. Soc.* **1990**, *112*, 5724.

144. Richter, C. *Chem. Phys. Lipids* **1987**, *44*, 175.

145. Hall, E. D. *Ann. Neurol.* **1992**, *32*, S137.

146. Francel, P. C.; Long, B. A.; Malik, J. M.; Tribble, C.; Jane, J. A.; Kron, I. L. *J. Neurosurg.* **1993**, *79*, 742.

APPENDIXES

Table A.1. Tabulated results for the effect of media on the rate of decomposition of ABAP, shown in Figure 2.2.

Media	[ABAP] (mM)	n (# observations)	Rate ± σ (μM/sec)
Phosphate buffer[a]	0.0	2	0.0016 ± 0.0000
	3.3	1	0.0036
	5.0	1	0.0079
	6.7	1	0.0061
	10.0	1	0.0080
	12.5	4	0.0114 ± 0.0008
	25.0	1	0.0181
	30.0	2	0.0207 ± 0.0036
SDS micelles[b]	0.0	2	0.0011 ± 0.0002
	0.8	1	0.0015
	1.7	2	0.0014 ± 0.0002
	2.5	1	0.0027
	3.3	2	0.0024 ± 0.0012
	4.2	1	0.0023
	5.0	2	0.0036 ± 0.0008
	6.7	1	0.0045
	8.3	1	0.0048
MLV hydrogenated PC[c]	0.0	2	0.0004 ± 0.0002
	3.6	1	0.0005
	5.2	1	0.0035
	7.0	2	0.0044 ± 0.0051
	10.5	2	0.0046 ± 0.0018
	13.9	2	0.0060 ± 0.0007
	15.3	1	0.0072
	17.2	2	0.0074 ± 0.0014
	20.2	1	0.0107
	20.6	2	0.0082 ± 0.0028
	23.8	2	0.0097 ± 0.0048
	25.0	1	0.0116
	27.2	1	0.0202
	29.7	1	0.0104
	32.0	1	0.0176

(table con'd)

ULV hydrogenated PC[d]	0.0	3	0.0021 ± 0.0012
	4.1	1	0.0022
	5.5	1	0.0019
	8.8	1	0.0063
	10.9	1	0.0040
	12.2	1	0.0077
	16.1	1	0.0120
	17.2	1	0.0087
	20.0	1	0.0143
	21.3	1	0.0097
	23.8	1	0.0157
	25.4	1	0.0120
	27.6	1	0.0127
	30.2	1	0.0146
	31.3	1	0.0150

Samples contained increasing concentrations of ABAP in the following systems: a. 50 mM phosphate, pH 7.4, 83.3 μM DTPA b. 0.5 M SDS micelles in buffer, 83.3 μM DTPA c,d. 20 mg/mL MLV or ULV hydrogenated egg PC in buffer, 83.3 μM DTPA. Data were obtained using the oxygen electrode method.

Table A.2. Tabulated data obtained for measuring the order in ABAP, shown in Figure 2.4.

Membrane Model	log[ABAP]	n (# observations)	log[Rate]
SDS micelles	-2.60	2	-7.36 ± 0.01
	-2.30	2	-7.21 ± 0.00
	-2.13	2	-7.12 ± 0.05
	-2.00	2	-7.06 ± 0.04
	-1.90	2	-7.02 ± 0.03
	-1.82	2	-6.98 ± 0.03
MLVs	-2.60	1	-8.47
	-2.30	1	-7.88
	-2.13	1	-7.81
	-2.00	1	-7.61
	-1.90	1	-7.40
	-1.82	1	-7.25
ULVs	-2.60	1	-8.37
	-2.30	2	-8.629 ± 0.45
	-2.13	2	-7.99 ± 0.25
	-2.00	1	-7.69
	-1.90	2	-7.44 ± 0.16
	-1.82	1	-7.40
	-1.76	1	-7.33

Samples contained varying concentrations of ABAP in a. 0.5 M SDS in buffer, 46.7 mM linoleic acid, 83.3 μM DTPA, b,c. 20 mg/mL MLV or ULV soy PC in buffer, 83.3 μM DTPA. Data were obtained using the oxygen electrode method.

Table A.3. Tabulated data for measuring the order in LH, shown in Figure 2.5.

Membrane Model	log[LH]	n (# observations)	log[Rate] ± σ
MLVs	-3.00	1	-7.46
	-2.60	1	-7.22
	-2.30	2	-7.17 ± 0.07
	-2.13	1	-7.02
	-2.00	2	-7.14 ± 0.08
	-1.90	1	-7.08
	-1.82	2	-6.93 ± 0.26
	-1.76	1	-7.01
	-1.70	2	-6.88 ± 0.28
ULVs	-2.60	1	-7.24
	-2.30	1	-7.32
	-2.00	1	-7.21
	-1.90	1	-7.09
	-1.82	1	-7.05
	-1.76	2	-7.13 ± 0.27
	-1.70	3	-7.14 ± 0.03

Samples contained varying concentrations of either MLV or ULV soy PC diluted with hydrogenated egg PC to control LH concentration. Samples also contained 83.3 μM DTPA and 21.2 mM ABAP. Data were obtained using the oxygen electrode method.

Table A.4. Tabulated data for measuring dependence of $[O_2]$ on the rate of oxidation in MLVs and ULVs, shown in Figure 2.6.

Membrane Model	$[O_2]$ (μM)	n (# observations)	R_{ox} ± σ (μM/sec)
MLVs	62.5	3	0.1133 ± 0.0773
	250	3	0.1108 ± 0.0790
	1250	3	0.1453 ± 0.0515
ULVs	62.5	3	0.0714 ± 0.0188
	250	3	0.0732 ± 0.0051
	1250	3	0.08173 ± 0.0277

Samples contained 20 mg/mL ULV or MLV soy PC in phosphate buffer, 83.3 μM DTPA, and 21.2 mM ABAP. Samples were bubbled with gas of varying O_2 concentrations. Data were obtained using the oxygen electrode method.

Table A.5. Tabulated data for inhibition by α-T in SDS micelles, MLVs, and ULVs, shown in Figure 3.3.

Membrane Model	[α-T] (μM)	n (# observations)	% Inhibition ± σ
SDS Micelles[a]	1.5	1	26.8
	2.0	2	63.2 ± 2.97
	2.5	3	73.2 ± 10.4
	3.0	2	83.3 ± 13.7
	5.0	5	67.3 ± 15.3
	7.5	3	83.3 ± 10.1
	10.0	4	89.5 ± 4.4
	12.5	2	85.7 ± 13.2
	15.0	4	87.2 ± 1.5
	20.0	5	63.9 ± 15.9
	25.0	3	60.6 ± 9.0
	30.0	1	69.3
MLVs[b]	5	1	18.4
	10	1	79.7
	15	1	86.0
	25	2	107.6 ± 1.8
	50	2	99.7 ± 35.6
	60	1	87.1
	75	2	82.3 ± 12.3
	90	1	80.6
	100	2	74.7 ± 1.7
	125	1	47.6
	150	2	30.8 ± 15.5
	200	2	23.4 ± 4.7
ULVs[c]	15	1	5.1
	25	1	13.8
	35	1	47.9
	50	1	96.5
	60	1	112.4
	70	3	97.6 ± 26.8
	75	2	114.5 ± 14.8
	80	3	98.5 ± 41.5
	90	4	102.8 ± 31.9
	100	3	100.9 ± 43.8
	110	1	109.4
	125	2	93.4 ± 19.3
	150	1	89.9
	200	1	55.9

Samples contained increasing concentrations of α-T in either a. 15 mM SDS micelles in buffer, 46.7 mM linoleic acid, 80 μM DTPA, and 20 mM ABAP, and b, c. 20 mg/mL MLV or ULV soy PC in buffer, 21.2 mM ABAP, and 88.3 μM DTPA. Data were obtained using the oxygen electrode method.

Table A.6. Tabulation of data measuring the inhibition of α-T with and without free fatty acids, shown in Figure 3.4.

Membrane Model	[α-T] (μM)	n (# observations)	% Inhibition ± σ
ULVs, -FFA	0	1	0
	25	1	22.5
	75	1	56.9
	100	1	74.9
	175	1	98.4
ULVs, +FFA	0	1	0
	5	2	65.9 ± 30.9
	10	1	81.9
	50	1	109.8
	100	2	88.0 ± 14.1
	150	2	97.3 ± 13.5
	200	1	111.1

System contained 5 mg/mL ULV soy PC in phosphate buffer, 100 μM DTPA, 5 mM ABAP, and 100 μM oleic acid in some samples. Data were obtained using the oxygen electrode method.

Table A.7. Tabulation of data obtained for measuring the entrapped volume of ULVs, shown in Figure 3.5.

Membrane Model	[Cr]/[T]	n (# observations)	% Intensity ± σ
Tris buffer	0	1	100
	5	1	69.0
	10	1	48.5
	20	1	19.5
	25	2	16.7
	30	1	12.3 ± 4.2
	40	1	6.1
	50	3	4.3 ± 2.0
	60	2	3.8 ± 2.7
	70	2	2.6 ± 1.1
	80	3	1.7 ± 0.6
	90	1	1.4
	100	3	1.4
	110	1	0.9
	120	1	0.9
	130	1	0

(table con'd)

ULVs	0	2	100
	10	2	26.8 ± 2.7
	30	1	17.7
	40	1	13.7
	50	3	9.1 ± 1.8
	60	2	10.2 ± 2.6
	70	4	8.2 ± 2.5
	80	4	7.7 ± 2.4
	90	2	10.0 ± 3.4
	100	2	8.8 ± 0.5
	110	2	8.5 ± 0.5
	120	2	7.9 ± 0.2
	130	2	7.1 ± 0.9
ULVs, α-T	0	1	100
	40	1	16.2
	60	1	11.3
	80	1	11.5
	90	1	2110.7
	100	1	10.6
	110	1	9.6
	120	1	9.5
	130	1	8.8
ULVs, stearic acid	0	1	100
	60	3	7.6 ± 0.5
	80	2	8.0 ± 1.7
	90	3	7.3 ± 0.3
	100	4	7.0 ± 1.3
	110	4	6.8 ± 1.2
	120	4	6.4 ± 1.4
	130	4	5.9 ± 1.4
ULVs, α-T, stearic acid,	0	1	100
	80	1	9.5
	90	1	9.5
	100	1	8.8
	110	1	8.7
	120	1	8.4
	130	1	7.8

Systems contained 60 mg/mL soy PC in Tris buffer containing 0.5 mM TEMPOL, and with and without 300 μM α-T, and 1200 μM stearic acid. Ionic strength was maintained throughout.

Table A.8. Tabulated data for measuring the inhibition by MAC-acetamide, U74389, and U74006, shown in Figure 4.2.

Antioxidant	[Antioxidant] (μM)	n (# observations)	% Inhibition ± σ
MAC-acetamide	25	1	19.1
	50	1	30.0
	100	1	44.0
	125	1	46.1
	150	1	37.7
	175	1	48.4
	200	1	56.9
U74389	25	1	26.9
	50	2	15.0 ± 4.0
	70	1	49.0
	80	1	35.9
	100	1	42.9
	125	2	66.0 ± 15.0
	150	2	39.9 ± 20.2
	175	1	57.0
	200	1	73.4
U74006	10	1	18.3
	50	1	17.4
	75	1	43.1
	100	2	51.6 ± 14.7
	150	1	56.7
	175	1	44.9
	200	1	54.5

Samples contained 21.2 mM ABAP and 83.3 μM DTPA in 20 mg/mL ULV soy PC. Data were obtained using the oxygen electrode.

VITA

Tammy Renee Dugas was born April 27, 1970, in Sulphur, Louisiana. She graduated valedictorian from Vinton High School in Vinton, Louisiana, in May of 1988. She was also named the 1988 Calcasieu Parish Student of the Year. Tammy was awarded the Chancellor's Aid Scholarship to attend Louisiana State University in the fall of 1988. There, she received her Bachelor of Science degree in biochemistry in August 1992. She continued her education by attending graduate school at Louisiana State University in January 1993, studying free radical organic chemistry under the direction of Dr. Daniel F. Church. She is currently a candidate for the degree of the Doctor of Philosophy in the Department of Chemistry. Tammy married Robert K. Gaudet on August 15, 1992. The couple has one child, Robert Jordan Gaudet, born May 23 1995.

DOCTORAL EXAMINATION AND DISSERTATION REPORT

Candidate: Tammy Renee Dugas

Major Field: Chemistry

Title of Dissertation: The Effect of Membrane Structure on Lipid Peroxidation and its Inhibition

Approved:

Mark L. McLaughlin
Major Professor and Chairman

John W. Leonard
Dean of the Graduate School

EXAMINING COMMITTEE:

Gary W. Hart

William E. Antholine

John B. Hopkins

David T. Clarke

Date of Examination:

June 17, 1996